Far-field Plume Dispersion Modelling for Backhoe Dredging Activities in the Black Rocks Harbour

J.S. van der Voorn

Delft University of Technology

Hydraulic Engineering

Rijkswaterstaat
Ministry of Infrastructure and Water Management

TU Delft

Far-field plume dispersion modelling for backhoe dredging activities in the Black Rocks harbour

To obtain the degree of Master of Science
at Delft University of Technology
To be defended publicly on 11-04-2024

J.S. van der Voorn

Student Number: 4543424
Date: 3-4-2024
Version: Final

Thesis Committee:

Prof. Dr. Ir. M. van Koningsveld	TU Delft (Chair)
Dr. Ir. J.A.A. Antolínez	TU Delft
Ir. M.N. Ruijter	Rijkswaterstaat
Ir. A.F. van der Plas	Public Entity Saba

Preface

This thesis was conducted for completion of my studies at Delft University of Technology in order to obtain the degree of Master of Science in Hydraulic Engineering. Over the last year, I dedicated my efforts to this report, which is focused on creating a representative approach to simulate the turbidity effects from dredging. This thesis was conducted in cooperation with Rijkswaterstaat and was partly carried out on Saba, a special municipality of the Netherlands.

First of all, I want to thank Michel Ruijter for introducing me to this thesis project and providing me with the opportunity to go to the Caribbean. Your guidance and critical view on the processes to consider for my report helped a lot. I also want to thank Ton van der Plas for welcoming me on Saba and providing me with valuable insight, data and advice on the harbour project. Mario Prak, thank you for advising and providing insight into the dredging operation for the harbour project. All the other people I met on Saba have made my stay an unforgettable experience.

Mark van Koningsveld, thank you for chairing my thesis committee and the advise on configuration of dredging processes in the model and on structuring my report. José Antonio Álvarez Antolínez, your feedback helped me to consider all important aspects for my model. I also thank the Deltares employees who have helped me by answering my questions on the set-up of my model.

Finally, I want to thank my family and friends for their unconditional support during my thesis.
Enjoy reading.

J.S. van der Voorn
Haarlem, March 2024

Abstract

On Saba, an island located in the Caribbean, a new harbour will be constructed. To protect coral reefs in the vicinity from light attenuation and sedimentation, it is important to monitor and predict the turbidity stresses caused by the dredging operation. In the early stages of such projects involving dredging operations, a common approach is to estimate the turbidity stresses in a simplified way. These method simplifications include the use of stationary source terms and the exclusion of important physical processes as tidal and wind-forcing by using simplified models, resulting in crude estimates on the turbidity stresses caused by the dredging operation. Better methods by Becker et al. (2015) and Tuinhof (2014) have already been developed, but have not been applied in the context of Caribbean islands. Further refinement of these methods will allow for a more suitable approach in simulating the turbidity stresses, which is favourable for the protection of corals.

This research focused on the development of a representative approach to simulate the turbidity effects from dredging activities by backhoe dredgers in the vicinity of Caribbean islands. The Black Rocks harbour project on Saba was used as a case study to test the effectiveness of the new method approach, by simulating various ways to suitably represent the turbidity stresses of the dredging process. The results of these simulations also aid in a more representative estimate on the expected turbidity stresses to protect the corals in the vicinity.

As a first step, the local physical processes, focusing on the hydrodynamic conditions and sediment characteristics, were identified and their influence on the turbidity stresses and dispersion of the sediment plumes were discussed. Insight in the wave heights and wave period should be obtained to aid in the decision for the dredging equipment to use and their workability, since exceedance of the operational limits can results in downtime. Key processes to include for a representative simulation for the dispersion of the plumes were identified to be the tidal and wind driven currents over the depth. By analysing the data over longer time periods, rare occurrences as current reversals can be captured, adding to a more representative simulation. Another local phenomenon to consider was the run-off from peak precipitation events, as this results in high background turbidity levels. Analysis of local sediment samples is required to obtain insight in the fines content, required for the estimation of the sediment flux, and the distribution of particle sizes and the particle density to determine the settling velocity.

Insight in the work method and duration of the dredging cycle provided the framework for a new methodical step to determine the temporal distribution of the source terms to suitably simulate the loss of fines over time, making a distinction for the presence of the source between day and night cycles and during relocation. The primary source term contributing to the release of fines, identified to be the bucket drip, was spatially distributed to simulate the relocation of the backhoe. An additional method step was introduced by estimating the local fines content for each source term over the dredging volume, resulting in a more representative approach for dredging volumes exhibiting a heterogeneous distribution of the fines content compared to using a single value for the fines content. The source terms were estimated using an existing method by Becker et al. (2015) and distributed over multiple sediment fractions, to include the representation of the smaller particles, affecting the far-field SSC in the model.

The effects of tidal and wind-forcing were incorporated using a 3D model, while running different hydrodynamic scenarios to test the effects for a variety of flow conditions. The grid resolution was chosen to ensure an accurate representation of the spatial distribution of the sediment concentration resulting from the bucket drip. The source terms were equally distributed over the depth to simulate the gradual loss of the fines over the depth by the bucket drip. The selection of an appropriate formulation for the settling velocity, to account for the local hydrodynamic conditions and sediment characteristics, increases the representation of the distribution of fines over time.

The model results indicated that for both a stationary and relocating source term, an accurate depiction of the average SSC values over longer time periods as days and weeks is simulated, while the relocating source tends to estimate peak concentrations more accurately, as the source location and quantity is represented more precisely. Turbidity thresholds, set for the Black Rocks project, were only exceeded on one occasion during the occurrence of a current reversal for the relocating source, but not for a stationary source. This indicates the added value of applying a more detailed approach to simulate the turbidity stresses. Following the suggested additions to the methods an updated approach to simulate the turbidity stresses by a backhoe dredger was proposed:

1. Identify and select the relevant local physical processes
2. Analyse the work method and determine temporal distribution of source terms
3. Identify the relevant source terms and distribute them spatially over the area
4. Assess and estimate the spatial variability of fines content for the source locations
5. Quantify the source terms, using the local fines content and distribute accordingly over the sediment fractions
6. Configure the relevant physical processes and source terms appropriately in the numerical model

Further research into refinement of the method, focusing on the spatial distribution of the source and appropriate spatial and vertical grid resolution, can increase the suitability of the suggested method for simulating turbidity stresses induced by a backhoe dredger.

Table of Contents

Acronyms

ADCP Acoustic Doppler Current Profiler. 5, 14, 47, 48, 52–54, 58, 77, 79, 84

BHD Backhoe Dredger. 29–37, 43, 46, 49, 50, 69, 72, 76, 80–83, 92

CSD Cutter Suction Dredger. 32

EIA Environmental Impact Assessment. 2, 6, 74, 75

NTU Nephelometric Turbidity Units. 26, 27, 51, 70

OBS Optical Backscatter. 26

PSD Particle Size Distribution. 22, 23, 42, 77, 81, 84, 97

RMSE Root Mean Square Error. 53

SD Saba Datum. 16, 17, 31, 38

SSC Suspended Sediment Concentration. iii, iv, 2, 6, 14, 15, 26–29, 36, 37, 45, 49–52, 55–58, 60–63, 65–84, 99, 109

TSHD Trailing Suction Hopper Dredger. 30, 32

1 Introduction

The island of Saba is located in the Caribbean, to the East of Puerto Rico, as can be seen in Figure 1.1, and is part of the BES islands. These three islands (Bonaire, St. Eustatius and Saba) are special municipalities within the Netherlands, referred to as public entities. The island has a steep foreshore and is made up, for a large part, by the volcano Mount Scenery. The land mass of Saba is around 13 km^2. Tourists, providing one of the most important sources of income, are attracted to the coral situated in Saba marine park and the Saba bank, which is located to the west of Saba. Many goods have to be imported to the island, which stresses the importance of a functioning harbour and airport. There are two points of entry to the island: Juancho E. Yrausquin Airport and Fort Bay Harbour.

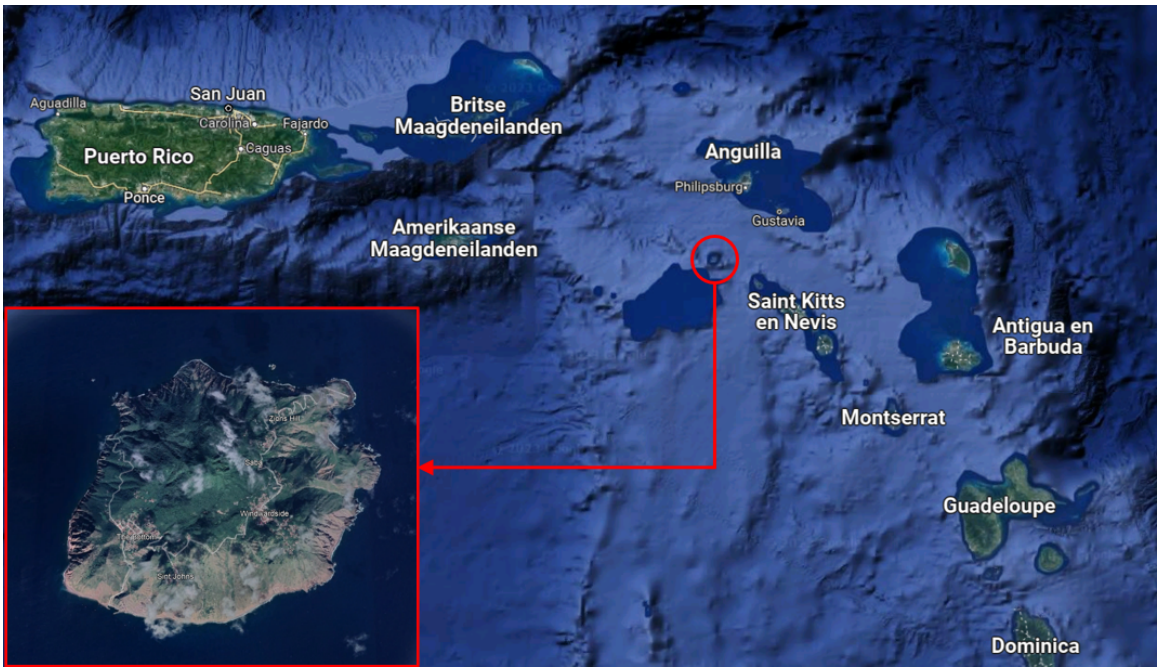

Figure 1.1: Aerial view of the island of Saba

In 2017, Saba was hit by hurricanes Irma and Maria which caused significant damage to Fort Bay Harbour. As a result, the harbour operations were partly disrupted. A plan for an upgraded and hurricane proof harbour was made, which consisted of an extension of the main breakwater into deeper water, to provide a sheltered inner harbor.
The results from physical model tests, however, showed that the extended breakwater would attract huge wave impacts during hurricanes, which would make it unstable. The investments required to guarantee the stability of the extended breakwater would be too expensive. Besides the stability issues, the limitations regarding the future expansion options at the current harbour caused the need to investigate other options for developing a hurricane and future proof harbour. Following feasibility studies, a new location eastward of the existing harbour was chosen in the area Black Rocks (see Figure 1.2). This area has a shallower foreshore, which would result in significantly smaller wave heights during hurricanes. Additionally, the terrain would provide more room to develop a future proof harbour.

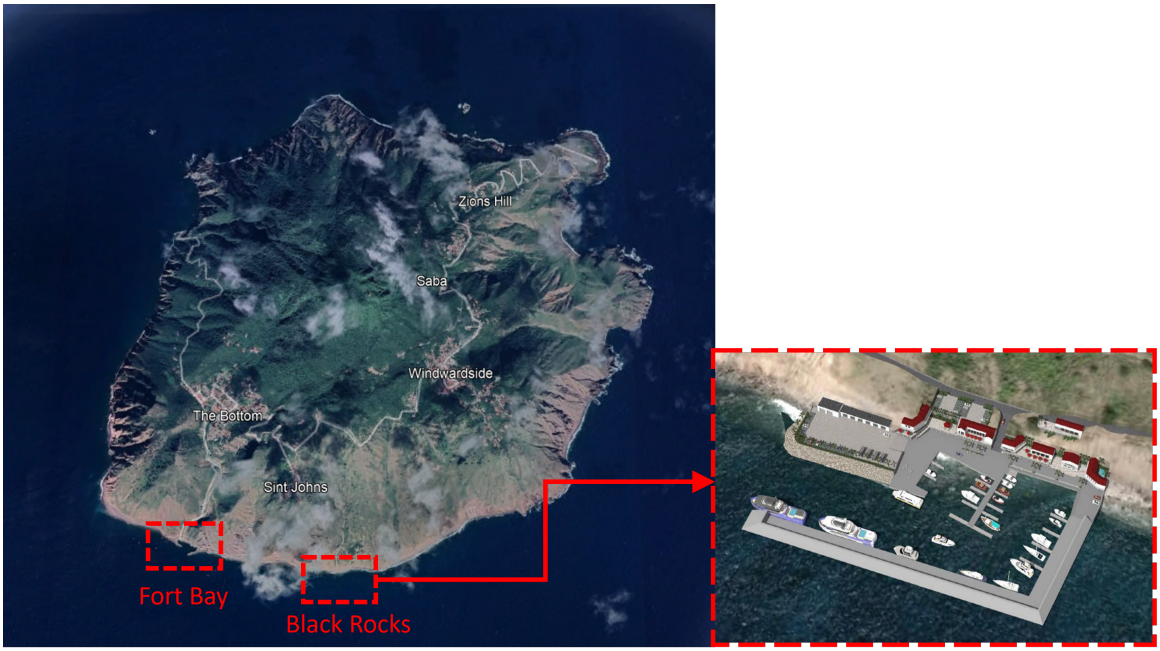

Figure 1.2: Location of the existing Fort Bay harbour and the new Black Rocks harbour

1.1 Problem description

During the construction of the harbour, turbidity in the water column is caused by dredging, rock placement and levelling, and the placement of caissons, along with other marine activities. This causes increased levels of suspended sediment loads. In the vicinity of the proposed harbour location, colonies of different coral species are present. The increased Suspended Sediment Concentration (SSC) in the water, caused by construction works and dredging, could affect the light penetration. The coral species present in the area need enough light to thrive and the created sediment plumes from dredging could endanger this process. Sedimentation of the coral reefs is another threat caused by these sediment plumes, which might result in burying of the corals and subsequently starvation.

The average coral cover around the island of Saba has already decreased from 30% to 8% in the past 25 years (Meesters et al., 2019). The exact causes of the coral starvation are unknown as this has not thoroughly been researched. Possible causes include the outbreak of diseases, pollution, run-off from land due to construction works and overgrazing by goats resulting in sedimentation and limited light transmission, global warming and a mass die-off of diadema, which prevent overgrowth of algae on the corals (Meesters et al., 2019)(van der Vlugt, 2016).

To mitigate the impact on the remaining coral colonies, it is essential to minimize the turbidity caused by the harbour construction works. Accurate estimations of turbidity levels during the dredging operation will help to assess the significance of the effects caused by dispersion of the sediment plumes. Therefore, it is important to accurately predict and monitor the turbidity levels in the proposed harbour location both before and during the harbour construction.

As part of the Environmental Impact Assessment (EIA), a depth-averaged 2D hydrodynamic model of the Black Rocks area has been set up by EcoVision. The model was used to inform the extent of the high-risk zone based on high level plume modelling. At the time, the used approach for the EIA was the best possible method. However, the model did not include some of the processes which are important when simulating a representative dredging operation in the project area. In the early stages of dredging projects, often a simplified approach is used to estimate the turbidity impact. Some hydrodynamic forcing conditions, such as tidal- and wind-forcing, important driving

factors of the dispersion of sediment plumes, are excluded from the numerical models. Additionally, continuous source terms are used as well as a depth-averaged 2D model. An approach that is too simplistic is at risk of providing unrealistic estimates of the turbidity stresses. Insight in a more detailed approach to represent the effects of the dredging operation are favourable for the protection of corals. In order to improve the quantification of the impact of the dredging operation on the environment, investigation into methods resulting in an approach which improves the estimation of dredging related turbidity stresses in the vicinity of a Caribbean island is required.

1.2 Research gap

In previous years, methods have already been developed, which provide a more suitable approach in estimating the turbidity stresses caused by the dredging operation. Examples are methods and studies by Tuinhof (2014), Becker et al. (2015) and Laboyrie et al. (2018). Research on these methods was conducted in various environments, such as Australia. While similar processes near Caribbean islands will be present as for the methods mentioned, some aspects such as local hydrodynamic processes and sediment characteristics will differ.

Insight in the specific local hydrodynamic processes near Caribbean island is required to allow for a more representative simulation of the dredging operation in this area. The impact and relevance of various metocean conditions, characteristic to the Caribbean, on the dispersion of sediment plumes must be identified. Additionally, insight in key dredging processes, which allow for a more representative simulation of the dredging operation is required. The existing methods make no clear distinction in the temporal and spatial variability of the source term during dredging. The importance of including relocation of dredging equipment, day and night cycles and the use of a stationary or relocating source are all factors influencing the estimation of the turbidity stresses.

Finally, more focus on the importance of the configuration of the processes in the numerical model will aid in developing a more representative approach of the dredging operation. By focusing on the choices regarding the use of 2D or 3D models and the input of the source in the model, the local situation can be modelled as representative as possible. To address the research gap, an analysis of the most important processes in the estimation of the turbidity impact is crucial to ensure all relevant steps that help in simulating a representative depiction of the operation are included. By applying these processes to the case of the Black Rocks harbour, various ways for a suitable approach in representing the turbidity stresses from the dredging operation can be tested.

1.3 Research objective & questions

The aim of this research is to develop a representative approach to simulate the turbidity effects of dredging activities by backhoe dredgers in the vicinity of Caribbean islands. The additions and improvement on existing methods provide a more suitable approach for estimating turbidity stresses, especially in the Caribbean. Additionally, the results of the followed approach and model, run for the Black Rocks case study, can be used to asses the possibility of the sediment concentration in the sediment plumes exceeding the turbidity thresholds. These thresholds are set to protect the sensitive receptors in the marine environment in the vicinity of the project area, ensuring no harm occurs.

The main research question is formulated as follows:

How can the turbidity impact of dredging activities by a backhoe in the Black Rocks area be simulated using a representative approach, while accounting for both local physical characteristics and dredging specific processes

The focus of the model is on the concentration and dispersion of the far-field plumes occurring from the dredging operation in the Black Rocks area. Local circumstances, including oceanographic currents, wind patterns and sediment characteristics, may differ from other cases where the effects of far-field plumes have been researched. These factors should be taken into account to ensure an accurate representation of the processes in the project area. The dynamic plume in the near-field will not be modelled as the focus is on the effects of high turbidity outside the assigned high impact zone. The coral reefs in the area will be the focus point of the sensitive receptors present in the marine environment. The corals present inside the high impact zone will be relocated and are therefore not exposed to the effects of the dynamic plume. The effects on other marine species as sea turtles and whales are not in the scope of this project. Additionally, the impact of noise and vibrations will also not be considered. The focus of the model is on the marine environment, the run-off from land is not specifically taken into account, although high precipitation events have a great impact on the turbidity levels in the water.

A number of sub questions are formulated to help in answering the main research question:

1. What relevant local hydrodynamic conditions and sediment characteristics should be considered when simulating the effects of the dredging operation?
2. What is the used work method for the dredging operation and which dredging processes should be incorporated in the model?
3. What are the relevant source terms and how should they temporally and spatially be distributed to represent the dredging operation?
4. What is the most suitable modelling approach and how should the source terms and local hydrodynamic conditions be configured and implemented for an accurate simulation of the dredging operation?
5. What is the potential intensity and duration of the turbidity stresses at the monitoring locations and on the environment resulting from the simulated dredging operation?
6. What additions to the current available methods can be suggested to improve the representation of the dredging processes?

The sub-questions serve as a foundation for answering the main research question. Each question is addressed in a separate chapter and contributes to a step-wise approach in which the main research question is answered. The final sub-question is answered in the conclusion to refer back to the suggested additions to the current methods, before the main research question is treated.

1.4 Methodology

This study aims to provide a suitable approach to simulate the effects of dredging operations by backhoe dredgers in the context of a Caribbean island. In this thesis, a case for the construction of a new harbour in the Black Rocks area on Saba is treated. In order to achieve a suitable approach, the methodology consists of four key steps in which the sub-research questions are addressed.

Step 1: Analysis of local physical characteristics
Step 1, which will answer the first sub-research question, will provide an overview of the various physical processes in the project area and the Caribbean in general and their influence on the turbidity stresses and dispersion of the sediment plumes. A comprehensive understanding of the system is of vital importance in order to determine the work method for the dredging operation and is a first step in the approach to provide a representative estimate of the turbidity stresses following the dredging operation. The approach for this step includes a combination of a literature study, data collection and analysis of both present and historically collected data to identify the relevant local conditions.

Insight in the processes is given by analysing existing reports, including the SWAN model of the Caribbean by Deltares and the design report of the harbour by Witteveen + Bos, which includes site specific data. Ongoing data collection of the metOcean conditions is performed using instruments from Obscape. This includes a tide gauge, weather station, wave buoy and turbidity sensor. Data regarding currents was collected from August 2021 to November 2021 using an ADCP mounted on a boulder next to the wave buoy. Two soil investigations have been performed by Geotron, providing essential information on the sediment characteristics in the area.

Additionally, a site visit to Saba provided a firsthand perspective of the situation and processes involved. The visit provides the opportunity to obtain valuable insights in the factors influencing the dredging operation and understanding the importance of including the various processes into the model. Finally, insight in the environmental criteria of the project area, such as identification of the location, type and number of coral species and providing the turbidity thresholds will aid in stressing the importance of developing an accurate model of the dredging operation.

Step 2: Obtain insight in the dredging operation
The second step for the methodology involves a detailed examination of the work method for the dredging operation to determine the dredging processes which should be incorporated for a representative depiction of reality. Additional focus in this step is on the identification, selection, quantification and consideration of the relevant source terms. This includes an analysis and decision for the temporal and spatial distribution of the source terms and an in depth analysis on the fines content to assign to the sources. This methodical step will help in providing the answer for sub-questions two and three.

Firstly, the dredging volume and potential equipment used is discussed, as well as the work method regarding operational hours and disposal methods. The identification of potential dredging equipment and the duration of the dredging cycle will include a persistency analysis to account for workability and possible equipment downtime. The expected duration of the dredging operation is calculated to provide insight in the temporal distribution of the source terms, which is determined next, ensuring a dynamic representation of the changing sediment flux. The different dredging processes to include for a representative representation are determined as well.

The next step involves the identification, selection and quantification of the source terms. Identification of the sources in the dredging operation contributing most to the release of fine sediment in the water column provides a next step in creating a representative model of the dredging operation. The estimation of the source terms caused by dredging is discussed and calculated through an existing method for estimating source terms for far-field dredging plume modelling developed

by Becker et al. (2015), while additions to this method for a more detailed approach are discussed as well. The spatial distribution of the source terms is determined to represent the release of fines during the dredging operation in a representative way. Additionally, an in-depth analysis on the borehole samples is performed to determine a representative fines content for the spatially varying sources. This will contribute to a more accurate representation of the source term in the model.

Step 3: Model choice and configuration
Steps 1 and 2 provide insights and input for methodical step 3, in which the most suitable numerical model is selected. After selection of the model the configuration of the dredging operation into the model to create the most representative situation must be performed. In essence, this step is a bridge between the collection of data, insight in processes and application of these processes in the model.

The chosen model must reflect the goal of the study and allow for a suitable representation of the different aspects of the dredging operation. Factors that need to be considered include representation and interaction of hydrodynamic conditions, processes influencing dispersion of the sediment plume and efficient implementation of the source terms. Inclusion of new methods regarding modelling of dredging induced plumes, such as depth layers and wind-forcing will aid provide an extension on the current methods, allowing for a suitable representation of the turbidity effects. Additionally, the computation time of the models run must be limited.

Once the numerical model is chosen, the next step is configuration of the dredging operation into the model. Data collected in step 1 and 2 must be incorporated in a way to most accurately simulate the local hydrodynamic conditions, dredging operation and the identified source terms. This involves choices regarding grid resolution and boundary conditions. The input method for the source terms is chosen with extra care to ensure a correct representation of the spillage of fines during the dredging operation.
Step 4: Analysis of model results & discussion of suggested methods
The final step consists of presenting and analysing the results of the model and discussing the suggestions for additional methodical steps to represent the dredging operation. The objective is not only to discuss the validity of the model that is created, but also to analyse if the added methods provide a more representative estimation of the SSC values during the dredging operation.

As an extra step, the results of the model are analysed with respect to the set turbidity limits in the high impact zone in the Black Rocks area. If the results indicate possible exceedance of the thresholds, recommendations will be given on possible changes to the dredging operation. The results will not serve as a concluding endpoint, but only as a guideline on the expected impact of the dredging operation.

In the discussion chapter, the uncertainties regarding the used methods and processes and their effects on the results are discussed. The created model will also be compared to the model initially created for the EIA, to compare the differences in methods and processes modelled. Finally, the suggested additions to the existing methods and their impact on creating a suitable approach in simulation the turbidity effects from dredging are analysed in the conclusion.
An overview of the most important steps regarding the explained methodical steps is given in the schematic in Figure 1.3.

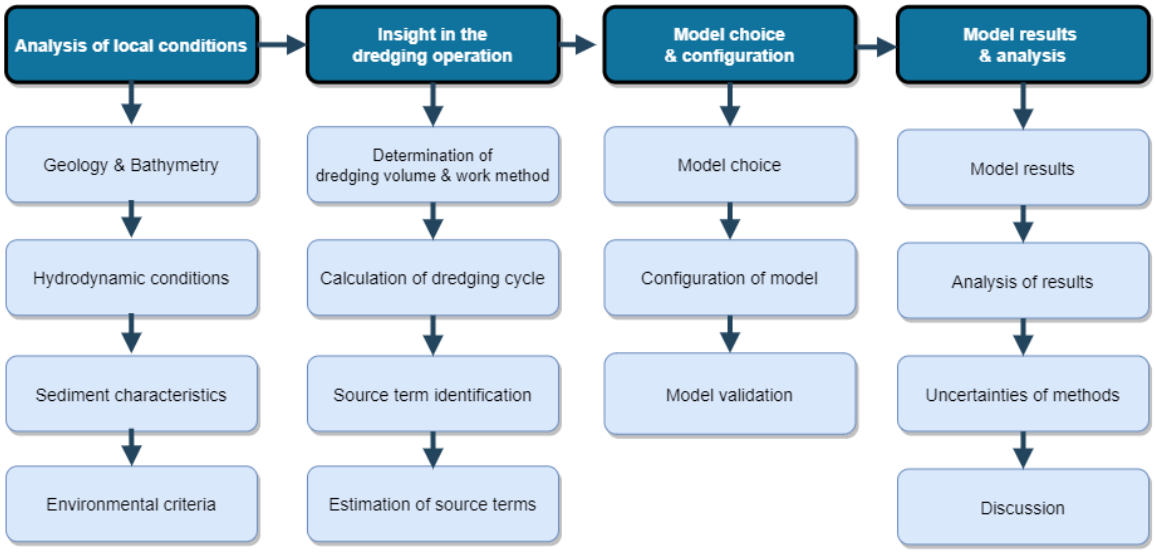

Figure 1.3: Schematization of the methodological steps taken in this thesis report

1.5 Thesis outline

The report is outlined as follows: the area study, in which the Black Rocks area is studied and data on the hydrodynamic conditions and sediment characteristics is collected, is presented in Chapter 2. In Chapter 3 the dredging operation is discussed including the dredging volume, equipment, workability and cycle duration. Chapter 4 identifies the relevant source terms in the dredging operation and provides an estimate of the sources, which can be used as input for the model. Additionally an in-depth analysis on the sediment samples is provided. The model choice and configuration of the dredging cycle in the model is reported in Chapter 5. The results of the model are discussed and analysed in Chapter 6. Finally Chapter 7 contains the discussion in which the uncertainties of the used methods is analysed. Discussion of the results and limitations of the research are discussed in this chapter as well. The conclusion and recommendations for further research and improved results are presented in Chapter 8. A schematic of the thesis outline, including indications in which chapters the research questions and methodical steps are discussed can be seen in Figure 1.4:

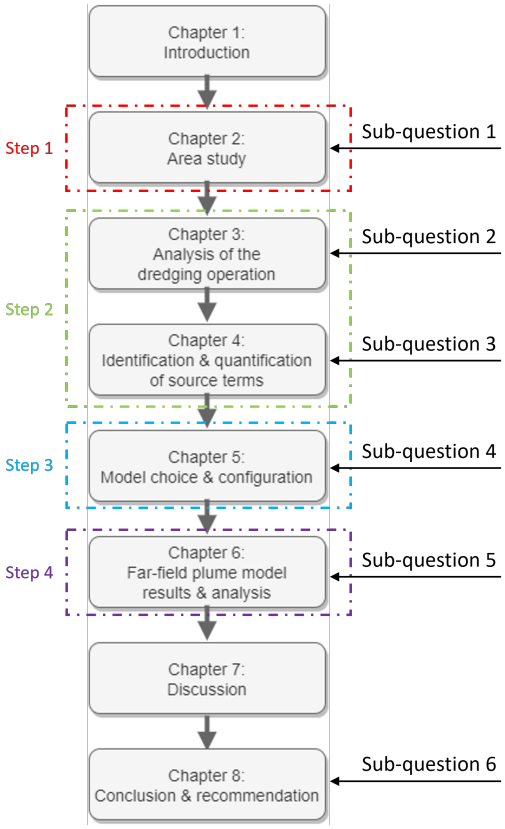

Figure 1.4: Schematic of the thesis outline indicating in which chapters the research questions and methodical steps are discussed

2 Black Rocks area study: Analysis of the physical processes

Understanding of the natural system is of vital importance when creating a representative model of the project area. This chapter focuses on the various physical processes in the area and their influence on the turbidity stresses and dispersion of the sediment plumes. An area study is conducted on the Black Rocks area to obtain a better understanding on the area itself, including the bathymetry, hydrodynamic conditions, sediment characteristics and environmental criteria. Many physical processes near Saba occur at other Caribbean islands, such that the described processes and their effects on the turbidity stresses can be used for other dredging related projects in the area.

The chapter starts with a brief overview of the areas of interest for the Black Rocks project. Through a combination of a site visit, literature study and data collection an examination regarding the bathymetry, metocean conditions, sediment characteristics and environmental criteria, such as present coral species and turbidity thresholds is conducted. This will provide a more complete overview of the processes that should be included in the model for a representative simulation, discussed in Chapter 5, while input for validation of the model is collected simultaneously. Finally, an overview of all the relevant physical processes to consider for a representative simulation of the dredging operation in the context of a Caribbean island is given in a separate section.
In this chapter the first sub-research question is answered:

What relevant local hydrodynamic conditions and sediment characteristics should be considered when simulating the effects of the dredging operation?

2.1 Areas of interest on Saba

The main focus for this area study is on the area Black Rocks, as the new harbour will be constructed here. A high impact zone, outside which several coral patch reefs are located, will be used as reference for placing observation points for the model at a later stage. Other areas of interest are the current harbour and the assigned dumping location located to the north-west of Saba. An overview of the areas of interest is given in Figure 2.1.

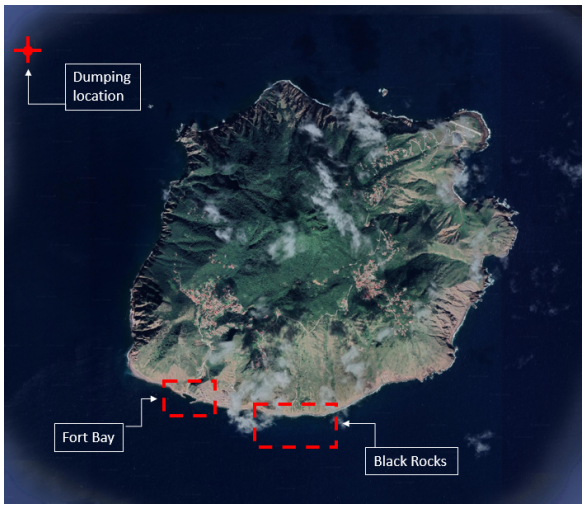

Figure 2.1: Overview of areas of interest for the Black Rocks harbour project

Situated on the south side of the island, the Black Rocks area has a much more favourable topography compared to many other parts on Saba. The relatively flat nature of the surrounding area provides a suitable environment for construction of restaurants, offices and other amenities due to the absence of (relatively) steep cliffs. One issue to take into account for the harbour construction is the presence of two large gullies. During heavy rain water flows via these gullies towards the ocean. Due to the

lack of trees in the area, erosion rates are expected to be high. Consequently, eroded sediment is transported through the gully, resulting in run-off that can induce temporary peaks in background turbidity values.

2.2 Bathymetry

The collection of bathymetric data is not only essential for accurately depicting the hydrodynamics in the model, but also for determining the work method for the dredging operation based on depth for navigation and identification of the presence of boulders. Both single-beam and multi-beam echo sounders are used for data collection. While single-beam sounders only map directly below the vessel, multi-beam sounders transmit an array of beams, resulting in a higher resolution profile (Breman, 2010).

Bathymetry data is available from a single-beam survey performed in 2019 and a multi-beam survey performed by Geotron in June 2023 in the Black Rocks area. Two older datasets from surveys performed by the Royal Netherlands Navy in 2006 and 2018 for the western and eastern part of Saba are used, together with manually added points from Navionics to create a more complete overview. The available data from the multi-beam survey stretches from 1 m depth near the coastline to a depth of 25 m at a distance of 350 m offshore. The results of the multi-beam survey can be seen in Figure 2.2.

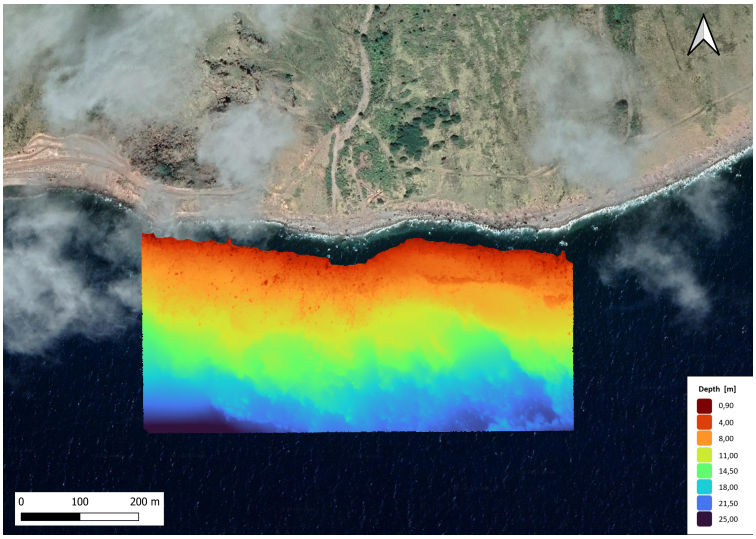

Figure 2.2: Results from the multi-beam bathymetry survey in the Black Rocks area

Noticeable are the large boulders present in the Black Rocks area. Theses boulders, as well as the more gentle slope in the Black Rocks area creates a more difficult working environment for dredging and construction of the harbour. Not only must these large boulders be removed for the port to be constructed, but also to be able to get close enough to shore for the dredging vessels. Some boulders in the area have a diameter up to 5 metres and can weigh up to 15 tonnes. An example of the boulders present at the new harbour location can be seen in Figure 2.3.

Figure 2.3: Overview of large boulders present in the Black Rocks area

The results of the single-beam surveys in the project area and near Fort Bay harbour as well as a comparison between the single and multi-beam survey at the project area are reported in Appendix A.1.

The final dataset used for the bathymetry consists a domain from the GEBCO 2023 bathymetry dataset, refined with the multi- and single-beam surveys, datasets from the royal dutch navy and points obtained from Navionics. Through interpolation using the triangulation method a complete overview of the bathymetry around Saba has been created, which can be seen in Figure 2.4.

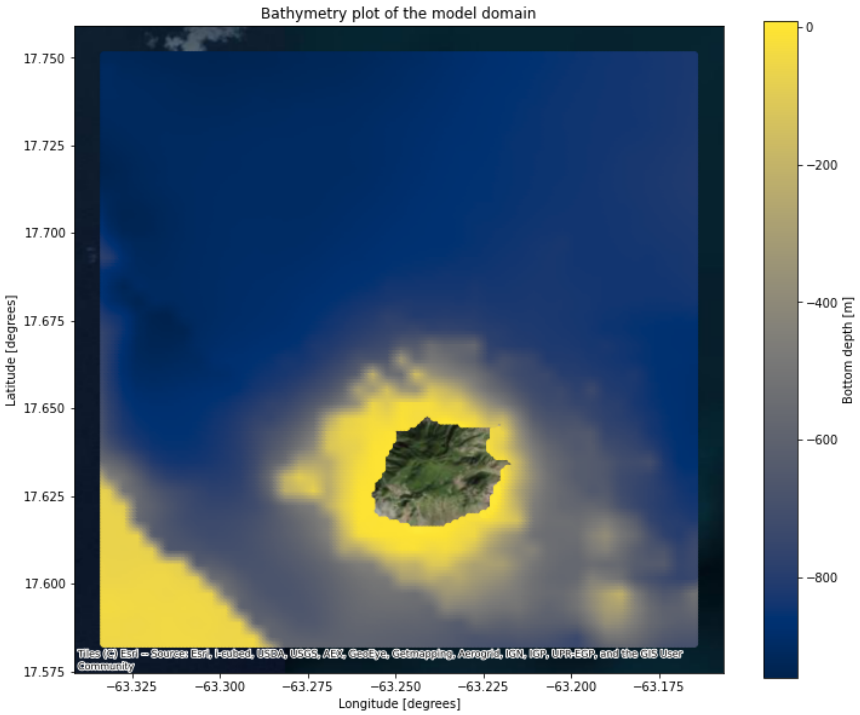

Figure 2.4: Complete bathymetry overview around the island of Saba

2.3 Hydrodynamic conditions

The hydrodynamic and atmospheric conditions on which data collection is performed include waves, currents, tide, wind and precipitation. Analysis of the data will help to identify key processes, which must be included in the model for a more suitable representation of the conditions during dredging. For each of the processes, their influence on the dredging operation and the dispersion and the quantity of the turbidity stresses is discussed.

Waves
A study on the wave conditions is mainly conducted to obtain a better understanding of the possible working conditions during the dredging operation. Large wave heights and long wave periods may result in downtime as these conditions hinder the workability of the dredging equipment.

Offshore from the new harbour location a wave buoy has been deployed. This buoy is continuously measuring the wave height, wave period and direction every 30 minutes, providing valuable and accurate data. During a measuring period from 13-10-2022 to 21-09-2023 it was found that, on average, the significant wave height $H_s = 0.78$ m while the average peak and mean wave period are $T_p = 6.5$ s and $T_m = 4.1$ s respectively. The peak period ranges from 4 s to 13 s depending on the incoming swell direction. Occasional swells approach the Black Rocks area from the South-West, as they come from the North and diffract around the island. The mean wave direction is 144 °N. An increase in wave height generally occurs during the hurricane season, which spans yearly from June to November. A wave rose plot of the data can be seen in Figure 2.5, while Figure 2.6 shows the daily averaged significant wave height over a full year.

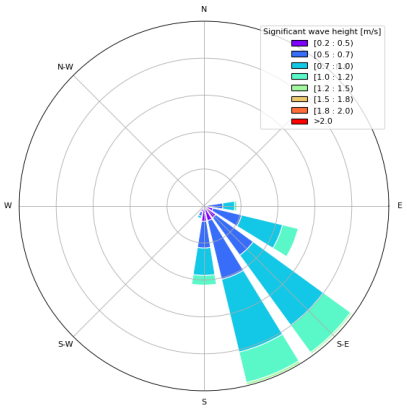

Figure 2.5: Wave rose of the yearly measured significant wave height in the Black Rocks area

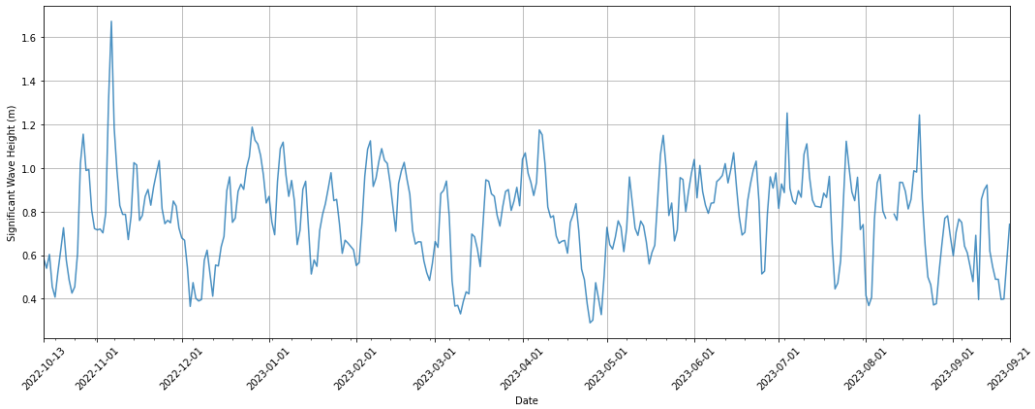

Figure 2.6: Overview of the daily averaged significant wave height measurements between 13-10-2022 and 21-09-2023 in the Black Rocks area

The measurements of the daily averaged peak wave period measured over a year can be seen in Figure 2.7. The different swell periods during which large wave periods occur are clearly visible. These originate from (tropical) storms and hurricanes in the area.

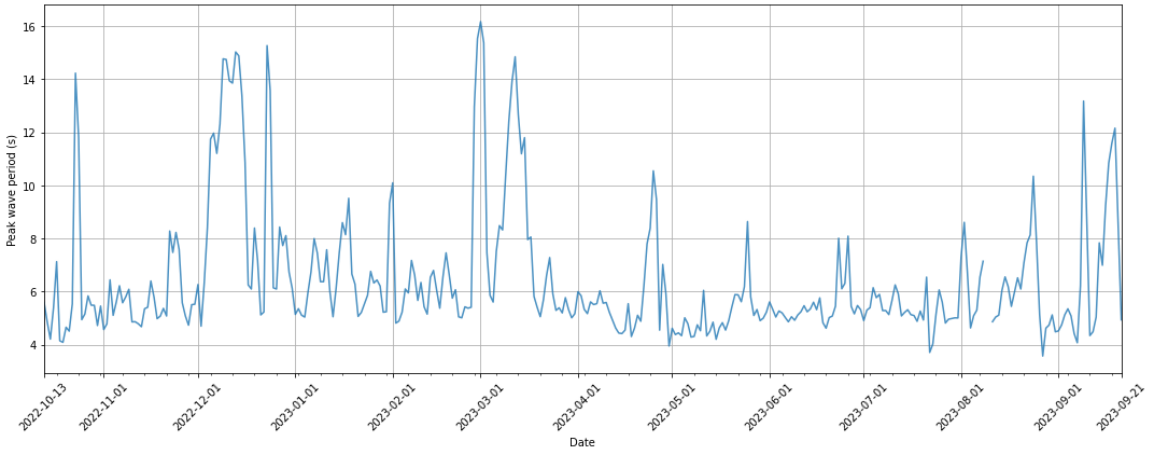

Figure 2.7: Measurements of the daily averaged peak wave period from 13-10-2022 to 21-09-2023 in the Black Rocks area

During the hurricane season in the Caribbean, which spans from June to November, the significant wave height can be considerably different. When a hurricane or tropical storm passes by northwards of the island, a calm situation with a low wind speed and low wave height occurs. When a hurricane passes southwards of the island, large swell waves can occur on the south side of the island, while a hurricane passing over the island will naturally cause high wind speeds and large waves.
In addition to the available data from the wave buoy, a study has been performed by Deltares, in which a SWAN model has been set up in the Caribbean focusing on the island of St. Eustatius, but also including Saba in the model. In the SWAN model both hurricanes Irma and Maria were modelled, while also setting up a hindcast of 42 years of data from 1980 to 2021. During hurricane Irma, a maximum significant wave height near Saba of Hs = 6 m was obtained. The SWAN results have shown that during hurricane Maria a Hs of 11 m occurred at different parts in the Caribbean, meaning that the significant wave height near Saba could have turned out to be much greater in case of a different path for hurricane Maria. This was one of the findings that let to the design of a new harbour. The SWAN model showed, however, an average bias in the significant wave height of 29%, overestimating the wave height. An overview of the 42 year hindcast data of the significant

wave height computed using the SWAN model can be seen in Figure 2.8

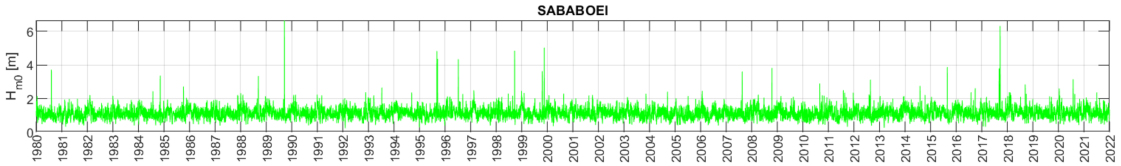

Figure 2.8: Overview of 42 year hindcast data of the H_s near Saba

In addition to workability, the resuspension of fine sediment induced by waves is a process affecting the SSC. Waves can play a crucial role in mixing of the water column and transport of the sediment plumes. Resuspension of the settled sediment in the nearshore region increases the SSC in the nearshore plume. The extend of the increased concentration depends on the amount of fines settled nearshore, which is influenced by the wave and current direction.

Currents
Understanding the current direction and velocity magnitude is a crucial step in modelling the effects of the dredging operation as they significantly influence the dispersion of the sediment plumes. Fluctuations in the current direction and magnitude over time and over the depth must be investigated to obtain a clear overview of the local conditions.

The current direction and velocity in the project area has been measured by use of an Acoustic Doppler Current Profiler (ADCP) in the period of September to November 2021. The ADCP was mounted on a rock at a height of 0.7 m from the seabed. The depth averaged current measured during this time period was 0.13 m/s, where the current velocity ranged from 0 to 0.6 m/s throughout the water column. The ADCP has been measuring the current velocity and direction every 0.5 m from the boulder on which the equipment was mounted on towards the surface. The current velocity and direction has been plotted for three locations: at 0.7 m, 3.2 m and 6.7 m from the seabed. All three figures show the measurements for a two day stretch between 27-10-2021 and 29-10-2021.
Figure 2.9 shows the current velocity and direction at 0.7 m above the seabed, Figure 2.10 at the middle depth and Figure 2.11 at the surface. These figures are used to illustrate the fluctuations in current speed and direction over the depth.

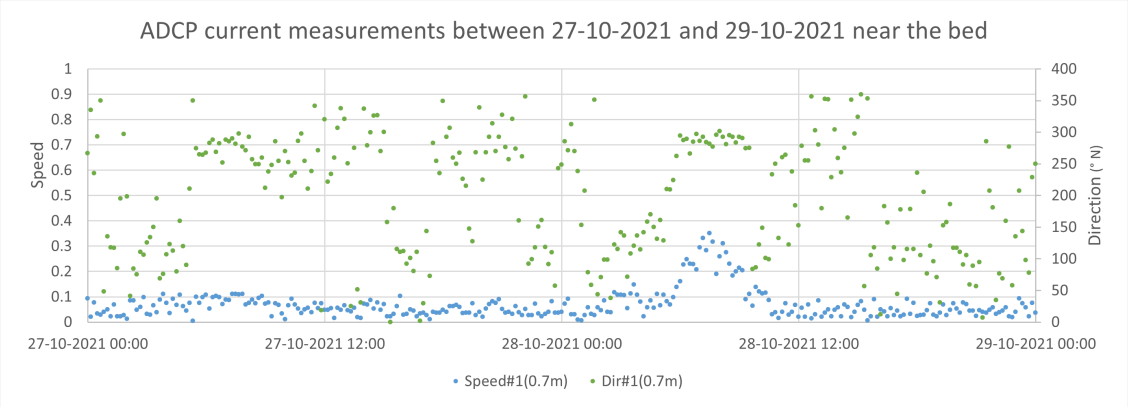

Figure 2.9: Current velocity and direction near the seabed in the Black Rocks area

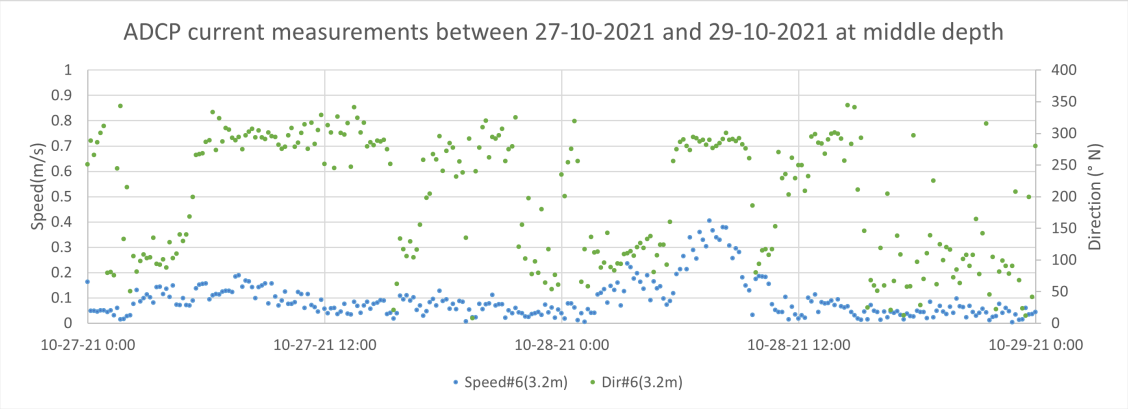

Figure 2.10: Current velocity and direction at 3.2 m from the seabed in the Black Rocks area

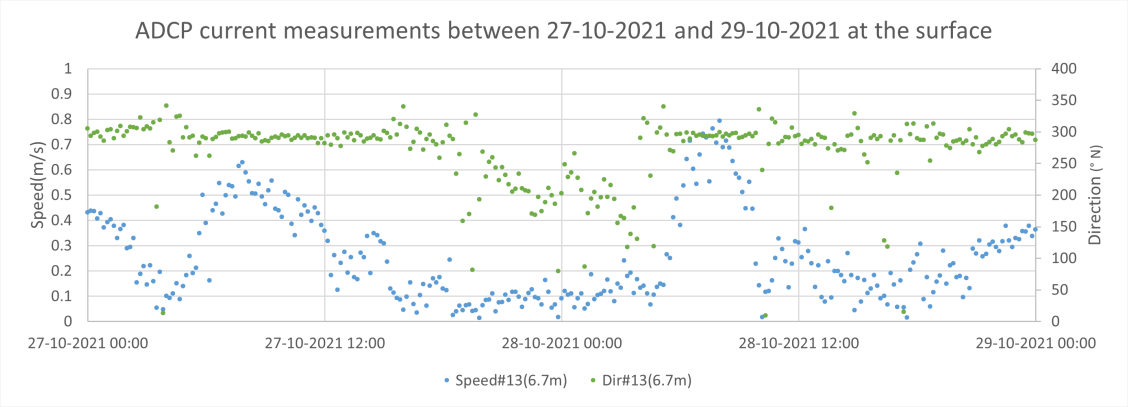

Figure 2.11: Current velocity and direction near the surface in the Black Rocks area

Near the seabed, current velocities are low on average. Noticeable are the current reversals near the bottom, which are caused by the tidal influence. Halfway of the water column the tidal influences are still noticeable, with velocities slightly higher than those near the bed. Both near the seabed and at middle depth the main current direction is 300 °N, which corresponds to a westward alongshore current.

At the surface, the influence of the tide is less visible. Here, the current direction is almost consistently around 300 °N with a high current velocity varying between 0 and 0.6 m/s. These high current velocities can be related to surface stresses caused by wind on the top layer of the water column. Occasionally, current reversals occur over the entire depth, in which the main current direction is directed towards the east for a limited time. These reversals are rare and are only present once or twice a month. Large ocean circulations moving through the Caribbean can have influence on the current directions in the project area as well.

The difference in the velocity magnitude over the depth and the fluctuations in the current direction are factors which influence the dispersion of sediment particles and consequently, the SSC in lateral and vertical direction. Due to tidal-induced current reversals, particles near the bed can move in opposite direction compared to the particles in the wind-driven upper layer. As an effect, differences in the sediment concentrations between the different layers can be observed, stressing the need of a 3D model. Simulating various time-periods is another important factor to consider for a suitable approach in simulating the dredging operation, as the occasional eastward current reversals can be captured as well to provide a complete overview of the local processes.

Tide

As discussed in the section on currents, tidal influences play a role in the dispersion of the sediment plumes due to the tidal-influenced current reversals near the bed. The tide near Saba can be characterized as diurnal, where the tidal amplitude is maximum 0.45 - 0.5 m during spring tide and around 0.25 - 0.3 m during neap tide. The reference point of the tide gauge is at Saba datum (SD), which is at 8.6 cm above MSL. The tide gauge is installed in Fort Bay harbour near the end of the breakwater. An overview of the measured hourly averaged water levels in September 2023 can be seen in Figure 2.12.

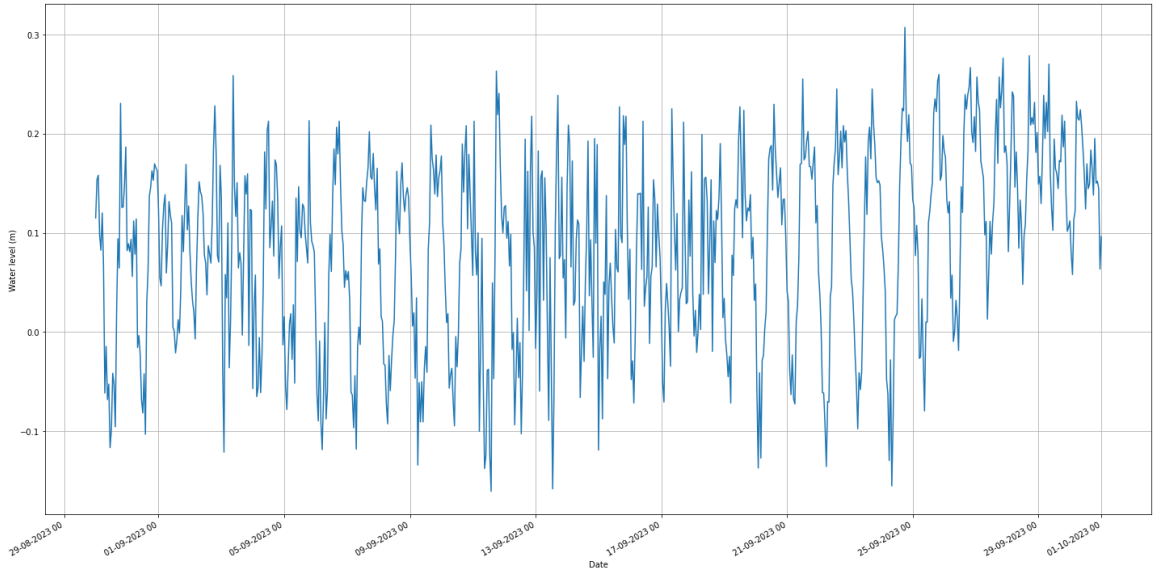

Figure 2.12: Tide plot of the hourly averaged measured water level elevation in the Fort Bay harbour in September 2023

Historical data on the tidal amplitude has also been obtained from a pressure sensor which was installed on the outer edge of the breakwater. The pressure sensor has been collecting data from 01-02-2019 to 16-02-2023, providing a second set of data. A snapshot showing a comparison between the hourly averaged tidal amplitude at Fort Bay and the amplitude from the TPXO8 global tide model for the month of September in 2021 can be seen in Figure 2.13.

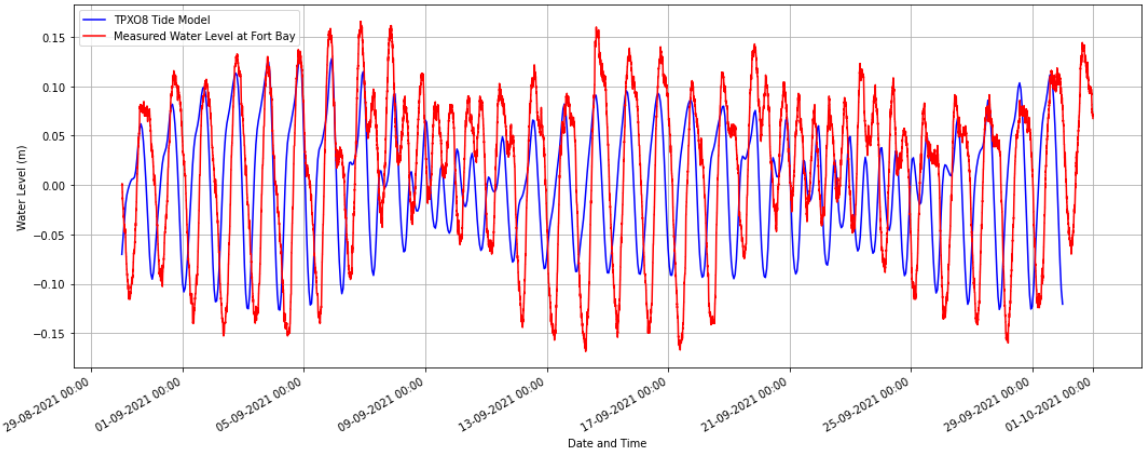

Figure 2.13: Comparison between the TPXO8 tidal amplitude and the hourly averaged measured tide in the Fort Bay harbour in September 2021

Wind

As visible in the measurements of the top layer in the ADCP data, wind is one of the driving factors for the current direction and speed in the area. Surface stresses caused by wind act on the surface layer contributing significantly to the current velocity in this layer. In order to accurately reflect the current velocities in the model, incorporation of wind forcing will be of vital importance.

A weather station has been deployed on land next to the proposed harbour location at a height of around 15 m SD to measure the wind speed in the area. This instrument collects measurements of both the wind speed and direction.

The average wind speed is 4.3 m/s with a mean direction of 79 °N measured over a one year period from 21-09-2022 to 21-09-2023. The main variance in wind direction is between 30 and 130°N. This shows that the main wind direction is coming from the east, resulting in an additional current orientated towards the west. As mentioned in the section on waves, during the period from June to November, the wind speed can change considerably due to passing hurricanes in the Caribbean. This will not only have an effect on the wave height, but also directly on the workability of the dredging vessels. The results are visualised in a wind rose plot in Figure 2.14. Figure 2.15 shows the yearly data of the measured wind speed.

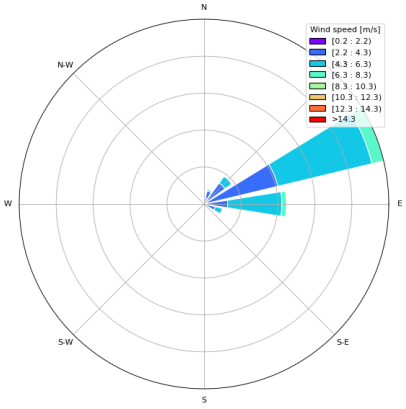

Figure 2.14: Wind rose of measurements of the wind speed and direction between 21-09-2022 and 21-09-2023

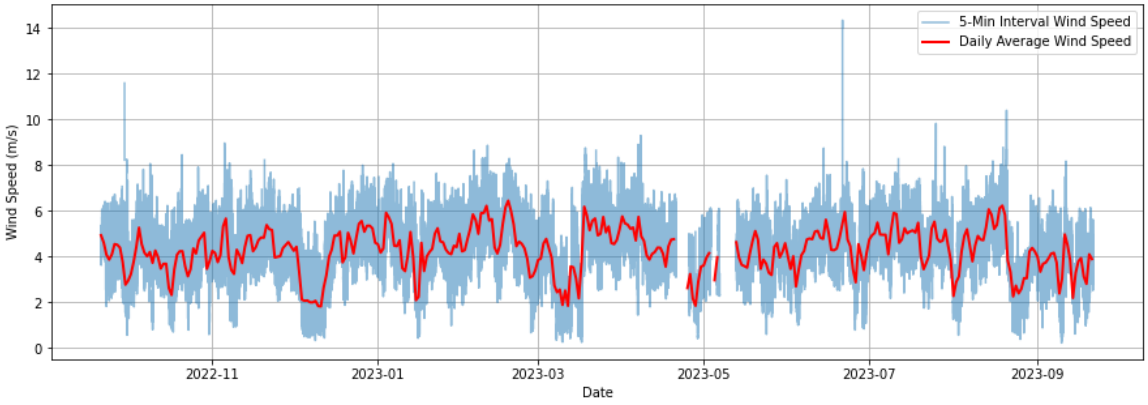

Figure 2.15: Wind speed measurements between 21-09-2022 and 21-09-2023 in the Black Rocks area. A daily mean of the wind speed is added as shown in red.

As the weather station in the Black Rocks area is placed at a sheltered location, the wind speeds at sea are expected to be higher than the measured wind speed on land. From the ERA5 atmospheric dataset wind speed data is obtained at a height of 10 m. The difference between the ERA5 and the measured wind speed is visualised in Figure 2.16 for September 2021. This comparison confirms the expectation of a lower wind speed measured by the weather station, as a difference of 1 m/s can be observed. Figure 2.17 shows the comparison between the wind direction from both datasets, which indicate a good correlation. In Figure 2.17 a change in wind direction can be observed on 21-09-2021. In the available ADCP data a current reversal towards is observed at this moment in time, correlating the change in wind direction to the occurrence of the current reversal.

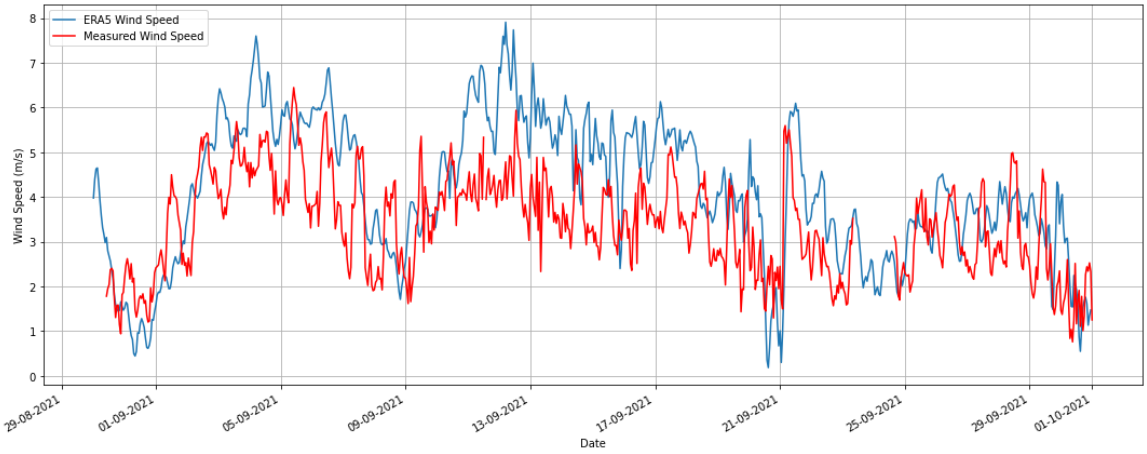

Figure 2.16: Comparison of the modeled wind speed from the ERA5 dataset to the measured wind speed at the Black Rocks area

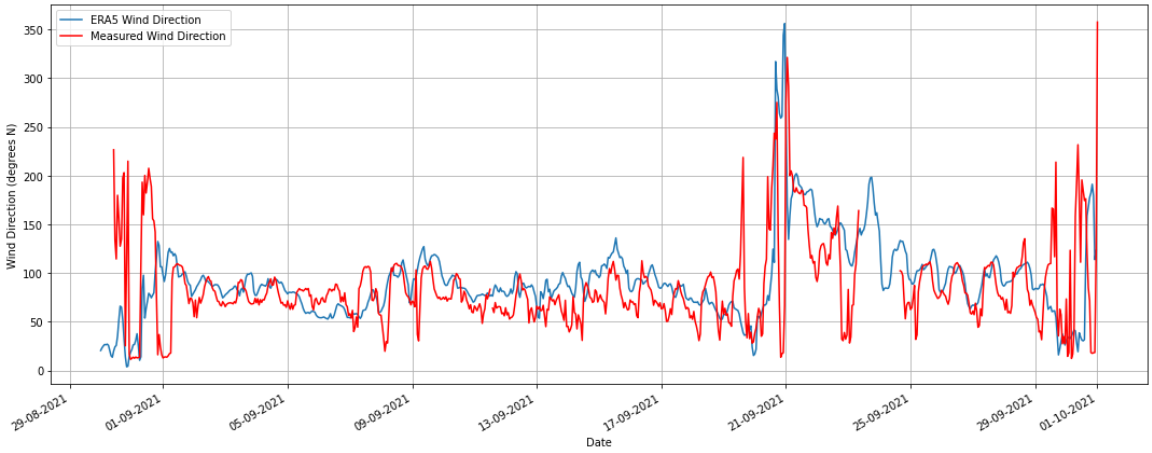

Figure 2.17: Comparison of the modeled wind direction from the ERA5 dataset to the measured wind direction at the Black Rocks area

Precipitation
Precipitation rates in the project area are examined to show events of heavy rainfall. As erosion rates at the Dutch Caribbean islands are high (Meesters et al., 2019), high run-off rates can be expected following peak precipitation events, which cause increased turbidity levels. While the impact of high precipitation events is acknowledge for this study, it is not included in the model due to data limitations regarding the magnitude of the sediment concentration in the run-off. However, the run-off caused by these extreme precipitation events is believed to cause significantly higher turbidity levels compared to the dredging operation.

The precipitation rates in the Black Rocks area between 01-01-2023 and 01-01-2024 can be seen in Figure 2.18. Figure a) represents the precipitation rate over a one hour interval, while Figure b) present the total daily precipitation rates.

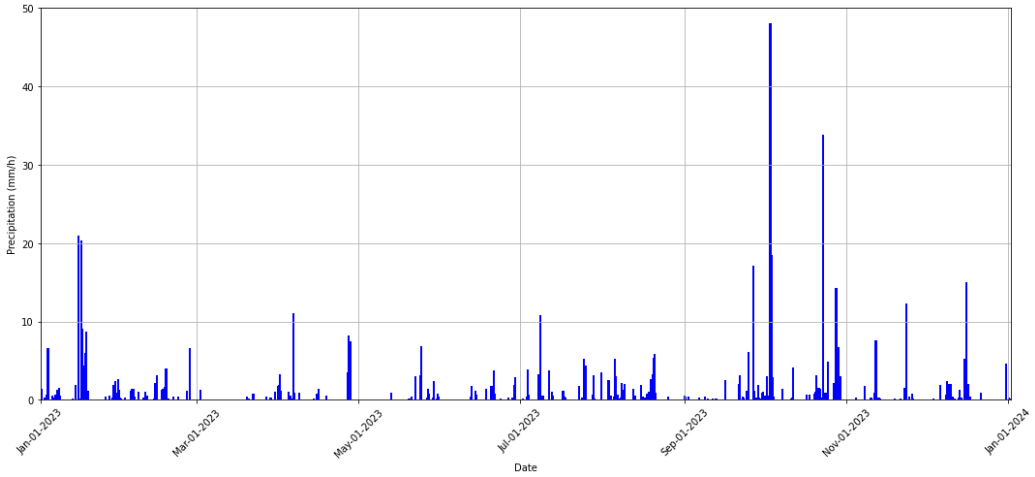

(a) Precipitation rate in mm per hour in the Black Rocks area in 2023

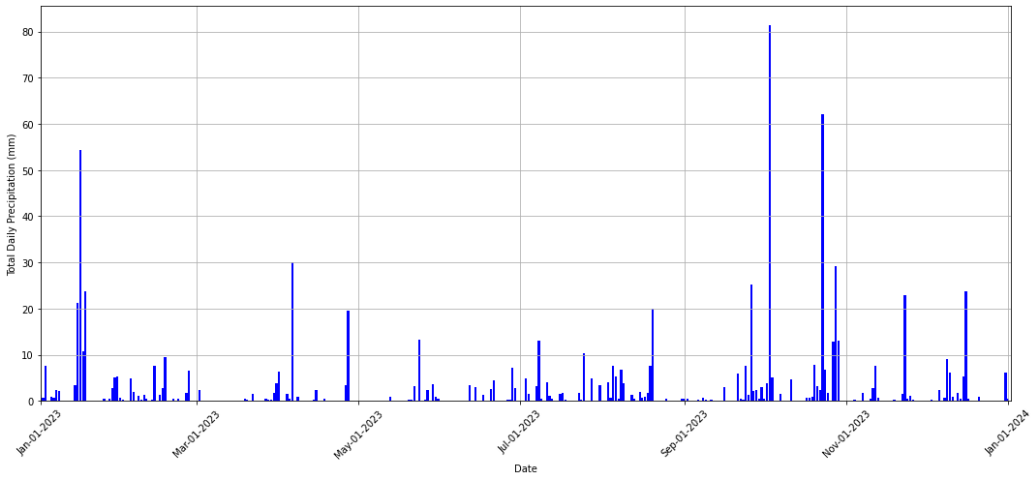

(b) Daily total precipitation rate in the Black Rocks area in 2023

Figure 2.18: Bar charts of the precipitation rates for an hourly interval (a) and the total daily precipitation rate (b) in the Black Rocks area in 2023

The highest recorded precipitation rate for the hourly interval during this period is 48 mm/h, observed in September, while a rate of 34 mm/h is recorded in October. A total daily precipitation rate of around 80 and 60 mm is recorded on the day of these peak precipitation events. This

indicates that the highest precipitation rates occurred on peak moments, rather than being evenly distributed throughout the day. Higher rates during these months can be related to the hurricane season. Throughout the year multiple events of rainfall with a rate between 10 and 20 mm/h have been recorded, which shows that heavy rainfall is not only a seasonal occurrence.

2.4 Sediment characteristics

The collection and analysis of local data on the sediment characteristics is essential to identify the properties of the sediment in the dredging volume. The amount of fines in the dredging volume and the distribution of the various particle sizes determine the concentration of the plume and the settling velocity. First, a general description on the geology of Saba is given, which highlights some key properties on the soil layers. The data collected in the two soil investigations is discussed next to identify the local sediment characteristics. This data serves as a basis for the in-depth analysis to determine the specific fines content in the dredging volume in Section 4.3.

2.4.1 Geology of Saba

Saba is a relatively young volcanic island with an age of less than a million years old, dominated by a single volcano called Mt Scenery (Sab, 2017). Due to its volcanic formation, the island is characterized by steep slopes on all sides. The island overlies a fault line which results in seismic activity and the risk of seismic events.
Due to its volcanic nature, the large boulders scattered around the island are mostly made up volcanic rocks as basalt and andesite with andesite being the predominant type (75%) (Lindsay, 2005). Due to Saba being a young volcanic island, a small amount of fines in the soil samples can be expected. The impact from past volcanic eruptions is visible in the cliffs of Well's bay, located on the North-West side of the island. Figure 2.19 shows the presence of (large) andesite boulders, pebbles, gravel and sand distributed throughout the entire cliff. The soil layers exhibit a heterogeneous pattern, referring to the inconsistent build-up of the different layers. For instance, at location A, large andesite boulders and some gravel can be found, while these features may be absent at location B just metres apart from the first location.

Figure 2.19: Cliffs at Wells bay, located on the western side of Saba, showing the different sediment types and soil layers

The heterogeneity of the soil is visible when four borehole logs originating from the 2023 soil investigation in the Black Rocks area are examined, see Figure 2.20. The four boreholes are all situated along the coastline of the Black Rocks area. All four borehole logs show the presence of gravel, boulders and sand. The layers, however, show variations in the soil composition at each location.

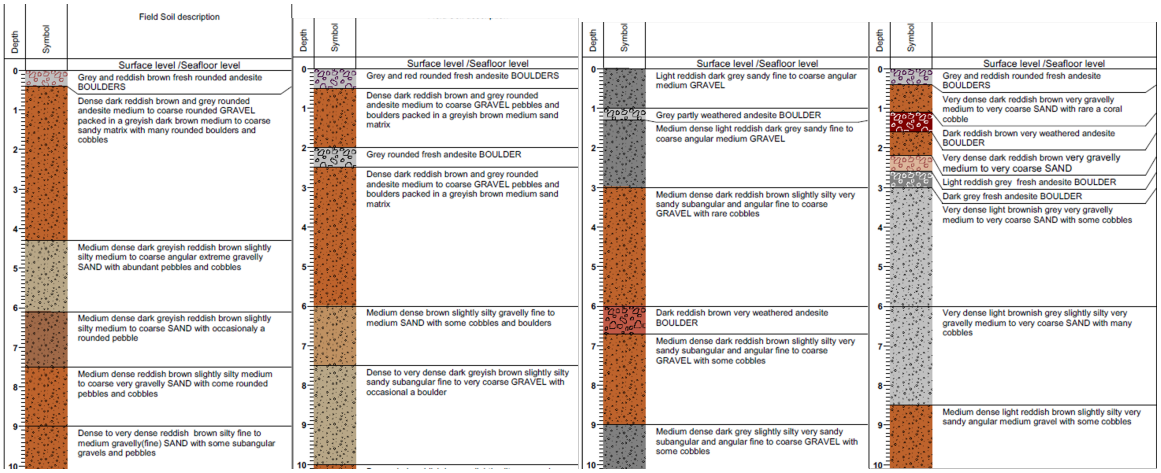

Figure 2.20: Overview of the boreholes logs of BH1 to BH4 in the Black Rocks area

2.4.2 Local sediment composition and properties

The local sediment characteristics can be investigated by analysing the data from two soil investigations, conducted on two separate occasions in the Black Rocks area in 2020 and 2023. The geotechnical investigation in 2020 included tests at 17 different borehole locations in the project area, covering both onshore and offshore locations. For the 2020 survey, the maximum depth of the boreholes depends on the depth at which the borehole collapsed. The 2023 investigations consisted of 6 boreholes onshore and 3 offshore. For this survey, each of these boreholes has a depth of 20 m measured from the bed level at each location. The locations of the boreholes can be seen in Figure 2.21. The jack-up barge used to mount the drill for the offshore boreholes can be seen in Figure 2.22.

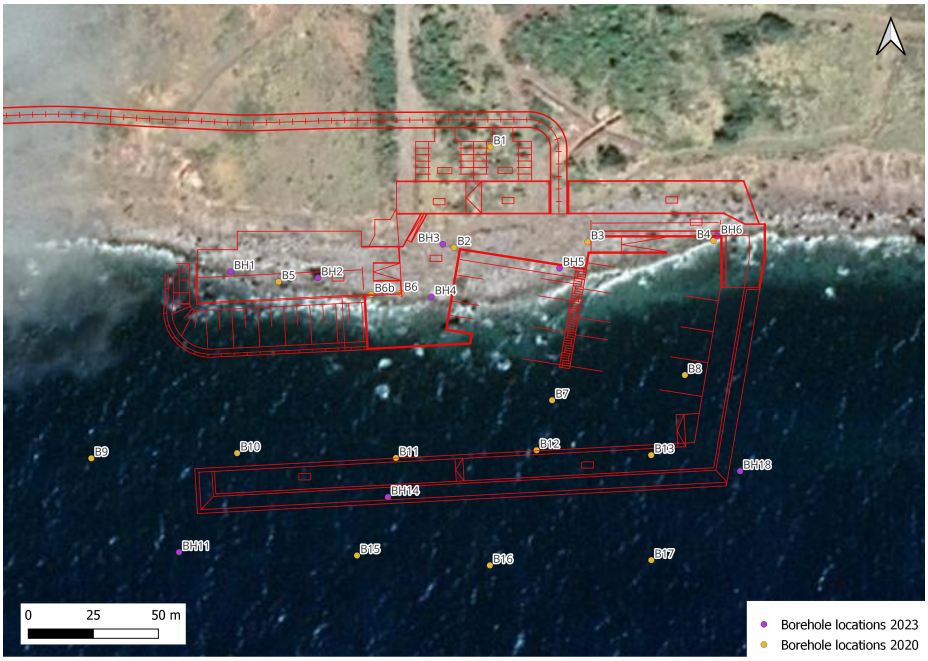

Figure 2.21: Overview of the different borehole locations on land and at sea in the Black Rocks area for the geotechnical surveys in 2020 and 2023.

Figure 2.22: The drilling platform located at the Black Rocks area for the soil investigation in August 2023

At several borehole locations, samples have been collected for lab testing. The laboratory tests include Particle Size Distributions (PSD's), pycnometer tests (to determine the specific gravity of the soil samples), carbonate and organic content, minimum and maximum density, chemical analyses and Unconfined Compression Tests (UCS) and Brazilian Tensile Strength tests (BTS).

The samples taken in the Black Rocks area consist of a mixture of sand, some silt, gravel, pebbles, coral limestone and larger boulders. These boulders consist predominantly of andesite rock. The interest for this study is on the fines content in the soil, since these smaller particles can remain in suspension for longer periods of time. The figures containing the PSD's for the average of all samples can be found in Appendix D.1, while a complete overview of the fines content in each sample taken at the boreholes is listed in Appendix D.2.

The laboratory results on the samples of the two geotechnical surveys show a limited variation in the fines content. The average PSD for the samples from the 2020 survey, excluding some outliers, show an average fines content (<63 μm) of 4%, sand 91% and gravel 4%. The samples of the 2023 survey are categorized into onshore and offshore boreholes. The average PSD on the onshore samples shows an average fines content of 6.4%, sand 39.3% and gravel 54.3%. Offshore the fines content was slightly higher at 8% while the sand content was 42.5% and gravel 49.5%.

The fines content in the 2023 samples is generally higher than for the samples of the 2020 survey. Multiple factors could have influenced the results obtained in both surveys. First, the heterogeneity of the soil and the fact that the borehole from the two surveys were not taken at the exact same location provide the possibility for a varying fines content in the samples. Another possible reason can be related to the diameter of the drill used to obtain samples. In 2020 the drill had a diameter of 40 mm, while during the 2023 survey a drill with a diameter of 62 mm was used.

The effects resulting from sediment being brought in suspension is visible in Figure 2.23. This figure, taken during the 2023 soil investigation, indicates the limited presence of fine sediment in the boreholes. Most of the sediment particles in the plume, which was caused by leakage of sediment originating from the boreholes into the ocean, had settled around 20 m from the source.

Figure 2.23: Sediment plume caused by leakage of sediment during drilling from the borehole samples into the ocean during the 2023 soil investigation

Next to the fines content, other sediment characteristics such as the organic content, carbonate content and dry and particle density should be investigated to obtain a complete overview. If a large organic content is present in the soil, processes as flocculation become important to consider. The lab results indicated a low organic content of less than 1% for all samples, except for one outlier. Therefore, the organic content is not further considered in this report. Regarding the carbonate content, different values are observed in the samples from the two soil investigations. From the 2020 survey, the carbonate content on land exhibited values of less than 0.1%, while in samples from

offshore boreholes percentages around 10 % where found with two outliers at 24 and 27%. The samples taken in the 2023 survey exhibited a more generalised carbonate content of 9,8% with a coefficient of variation of 2% for both the onshore and offshore samples. The high carbonate content in some samples can be related to the presence of coral reefs in the area. Since carbonate minerals are easily erodible, it can be expected that a large portion of the carbonate content found in the soil samples is present as fines in the dredging volume. For the sand samples taken at B7, the maximum and minimum dry density of the sand were determined. The mean maximum dry density was 1500 kg/m3 and the mean minimum dry density 1160 kg/m3. For calculations the maximum value of the dry density reported will be used. The average particle density for the sand grains is 2620 kg/m3.

Due to the heterogeneity of the soil layers and the disparities between the fines content in the samples taken alongshore in the 2020 and 2023 soil investigation, an in-depth analysis of the borehole samples will be performed in Chapter 4 to find a representative value for the fines content at different locations alongshore.

2.5 Environmental criteria

The need for modelling the effects of the dredging operation arises from the presence of coral colonies in the area, which must be protected. Therefore, it is important to map the location of the coral colonies to obtain knowledge on the areas in the model which must be observed. Additionally the turbidity thresholds, which cannot be exceeded during the dredging operation will be given. The turbidity thresholds for the Black Rocks case are based on the environmental permit related to the construction works of the harbour.

Coral
The sediment plumes caused by the dredging works are a risk to sensitive receivers in the surrounding area. The term 'sensitive receiver' refers to different flora and fauna which can be exposed to risks caused by dredging or other ecological risks (Bray, 2008). Corals are the main sensitive receiver on which the focus is for the harbour project in this report. This section provides an overview of the coral species and location in the project area. An insight into the characteristics of corals and the several coral stressors can be found in Appendix B.

The Black Rocks area contains different patch reefs. The most abundant protected coral species present in the area are the Acropora Palmata, Orbicella annularis and the Orbicella faveolata. Some colonies of Acropora cervicornis, Dendogyra Cylindrus and Montastrea Cavernosa are also present. The location of each colony of these species with respect to the future harbour location can be seen in Figure 2.24.

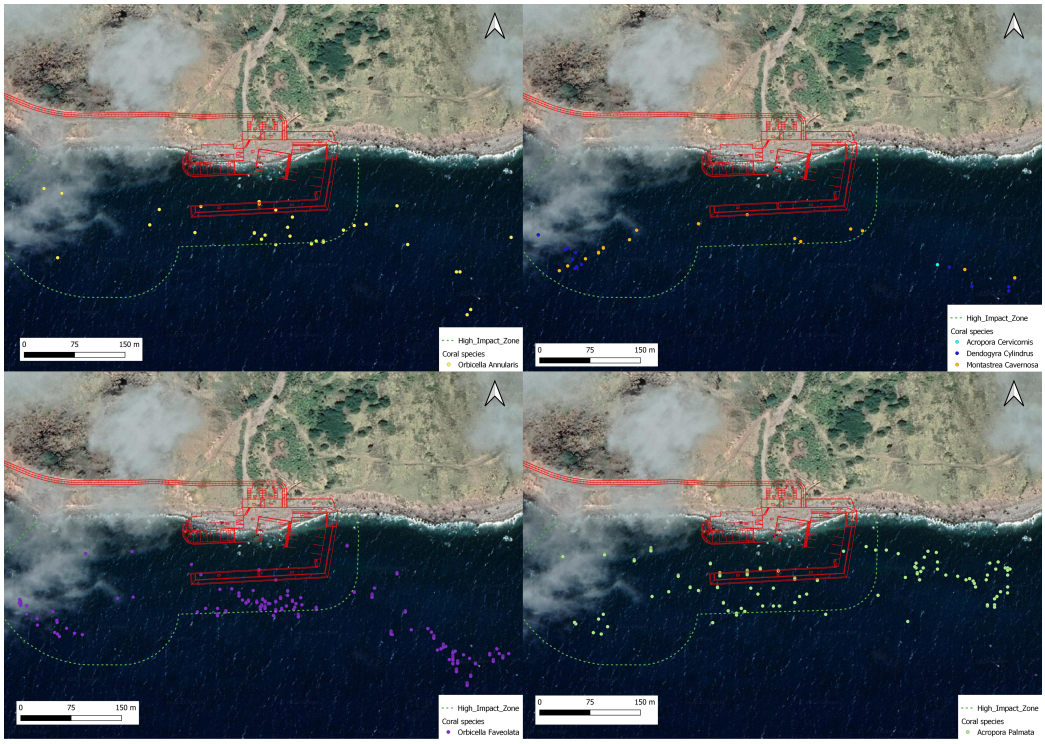

Figure 2.24: Overview of different coral colonies present in the Black Rocks area

The Acropora palmata, which can be seen in Figure B.1, is regarded as the most endangered species. About 40% of the coral in the area consists of colonies of Acorpora Palmata.
Before construction and dredging operations commence, the present coral colonies will be relocated to a different area. Only the colonies in the direct vicinity of the new harbour will be relocated. As coral colonies are located around the whole island, the dispersion length and direction of the sediment plumes should still be checked to see if any other corals will possibly be damaged.

The coral colonies present in the project area will be relocated as they can be exposed to different stress levels due to sedimentation and light attenuation in the water column as an effect of dredging. Dependent on the type of stressor, an increased duration of the coral to these stressors can have an increasingly negative effect (Erftemeijer et al., 2012). A relationship between the intensity of an impactful event and the duration can be seen in Figure 2.25.

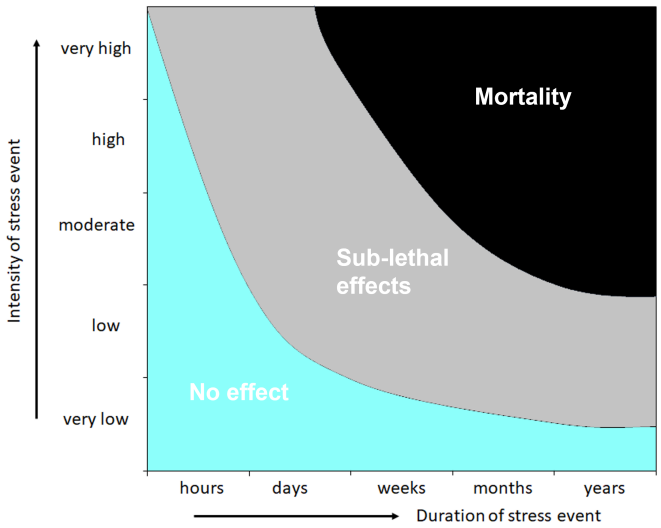

Figure 2.25: Relationship between the intensity of a stress factor and duration of a stress event on corals and risk of the (lethal) effects. Figure after Erftemeijer et al. (2012).

The intensity of the stress event, in this case the suspended sediment caused by dredging, depends on the SSC in the plumes. High values for the SSC can result in sub-lethal effects on the corals if these concentrations are present for a couple of hours, while lower sediment concentrations are only likely to affect the corals if these are present for longer periods of time, such as days or weeks. These insights should be taken into account when interpreting the estimated concentrations following the model results for this case study in the Black Rocks area in Chapter 6.

Turbidity
An important term regarding the SSC is turbidity, which causes light attenuation, reflection and scattering instead of light transmission in straight lines (Ziegler, 2002). If the turbidity in a fluid is high, light penetration is reduced causing aquatic organisms and plants to be less exposed to the light. Certain organisms, such as corals, need enough light exposure to thrive.
Turbidity can be measured in Nephelometric Turbidity Units (NTU). To measure the turbidity in NTU, a device is used which monitors the scattered and absorbed light from suspended particles at an angle of 90°with respect to the incident beam (Toh, 2012). A higher NTU value means more scattering of the light, which is caused by more suspended particles in the water column. NTU can be measured by an optical backscatter (OBS), which detects infrared light reflected from suspended particles in the water column (Ridd et al., 2001).

In order to protect the marine environment, in which the focus is on the coral colonies, a threshold for the turbidity values must be set to take into account during the dredging operations and construction of the harbour. One method, which could be used to determine these thresholds for the coral species, is the method described by McArthur et al. (2003). Here, measurements of the SSC are taken over a longer period of time to accurately determine the background values and the turbidity levels occurring during storms. Using these values, the thresholds for turbidity under which the coral species are able to survive can be known and used as threshold for the dredging works.

The threshold values for turbidity during construction and dredging operations are chosen as follows:

- The average hourly value per day cannot exceed a value of 10 NTU
- The average value per day cannot exceed a value of 3 NTU
- The average value per week cannot exceed a value of 2 NTU

The thresholds apply to the high impact zone, which is an area around the new harbour that is expected to suffer the highest impact of the dredging operation. In case any of the above mentioned threshold values are exceeded, any dredging or construction activities should be halted immediately. Background turbidity values will be added to the threshold mentioned above, if they exceed a value of 0 NTU. A measuring campaign for a period of 12 months is set-up to determine the average background turbidity values in the area. An In Situ turbidity sensor is used to collect the data. The sensor is located 2 m below the water surface, measuring the turbidity in NTU continuously every 30 minutes. The sensor is located at 17°36.79 N, 63°14.55 W (UTM Zone 20N: X = 474272, Y = 1947427). During construction of the harbour the turbidity sensor will be located at the same location as during the measuring campaign to obtain data on the background turbidity. Before deployment the sensor has been calibrated by use of a calibration fluid. The location of the high impact zone, together with the turbidity sensor can be seen in Figure 2.26.

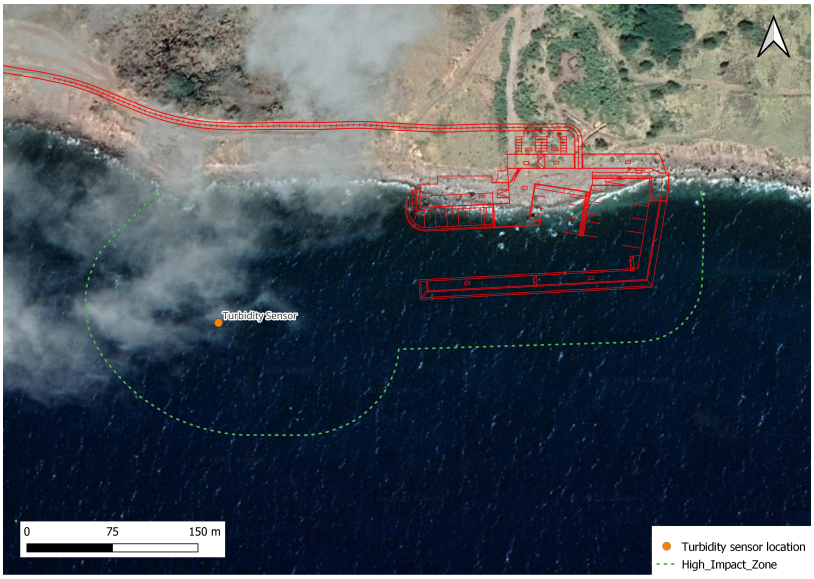

Figure 2.26: Overview on the location of the turbidity sensor and the assigned high impact zone in the Black Rocks area

While the turbidity sensor measures in NTU units and the thresholds are given in NTU as well, the results from the numerical model are normally given in mg/l. There is no standard correlation between measurements of suspended sediment in mg/L and NTU (Henley et al., 2000). Therefore extra tests for calibration to convert from one unit to the other have to be performed for each area specific sample. A turbidity sensor can be used to measure the turbidity of the water in the tank in NTU. This experiment can be repeated several times for different SSC to obtain a relationship between the NTU and mg/l values. An experiment as described was not performed for the sediment samples taken on site and the turbidity sensor installed. Values from literature will therefore be used to translate the threshold values given in NTU to a value in mg/l. Several values have been reported in mg/l to equal 1 NTU: 6 mg/l, 2 mg/l, 0.9 mg/l to 0.5 mg/l ((Wenger and McCormick, 2013), (Cartwright et al., 2022), (Ellison et al., 2014), (Hossain et al., 2004)). As 6 mg/l is seen as an outlier, this value is not taken into account to determine an average from the literature values. It is chosen that a value of 1 mg/l is to be equal to 1 NTU.

2.6 Overview of relevant physical processes in the Caribbean

In this section a concise overview is provided of the physical processes that are considered to be relevant when simulating the effects of the dredging operation in the context of a Caribbean island. Each process and their relevance and significance in the dispersion of sediment plumes and the turbidity stresses on the sensitive receptors is discussed. A distinction is made between the hydrodynamic processes and sediment characteristics. While many of the physical processes mentioned in this section occur in numerous locations across the Caribbean, each area has its own distinct processes and these must therefore be investigated for each project separately.

Hydrodynamic processes
First of all, studying the wave climate in the project area is important to obtain a better understanding of the possible working conditions during the dredging operation. The wave climate affects both the choice for the selection of the dredging equipment and determination of the workability to estimate the duration of the dredging operation. The characteristic significant and maximum wave height as well as the wave period determine the operational limits of the dredging equipment. Extreme conditions in the area can be caused by swells and tropical storms during the hurricane season in the Caribbean, which spans from June to November. Additionally, wave-induced resuspension can affect the SSC as particles are kept in suspension for longer periods of time. Fines, which have settled nearshore can be brought in suspension again by breaking waves. While for this case study the impact of resuspension by waves is considered to be limited, the significance of the effect of wave-induced resuspension must be assessed for each project separately.

Investigating the current velocities and direction will provide insight in the dispersion direction of the sediment plumes and the distribution of the sediment concentration over the depth. When discussing currents, the influence of the tide and wind becomes important as these can influence the flow velocities and direction over the depth. Surface stresses caused by wind can result in higher flow velocities in the top part of the water column, while tidal-induced current reversals can occur near the bed. These factors provide the possibility of varying flow velocities and current direction over the depth, stressing the need of using 3D models for a representative approach in simulating the dispersion of the sediment plumes from dredging. Varying wind directions and large ocean circulations moving through the Caribbean can result in current reversals. While the occurrence of such an event may be rare during the dredging operation, the negative effects on sensitive receptors present in the opposing direction of the main current direction should be kept in mind. Therefore, it is advised to run simulations during varying flow conditions.

Finally, if the location of the considered project area has problems regarding erodibility, the effects from run-off on the turbidity should be kept in mind. If high precipitation events are likely to occur, a significant increase in the background turbidity can be expected caused by the run-off. This might result in downtime for the dredging operation in order to oblige to the set turbidity thresholds.

Sediment characteristics
The fines content in the soil is an important concept for the estimation of the turbidity stress caused by dredging in the far-field. Accurate data on the fines content in the area is essential for a representative approach. The build-up of the soil layers must be observed to determine if the soil composition is heterogeneous or homogeneous. If the layers exhibit a varying composition, spatial variability of the fines content in the dredging volume must be taken into account. In case of a large difference over the dredging volume, the source at the dredging locations can be simulated using a location specific fines content, aiding in a representative approach. Knowledge on the distribution of the smaller particles in the soil is crucial as well, as the size and density of the particles has a large influence on the settling velocity and, consequently, the concentration of the plumes. Additionally, insight must be obtained in the organic content to decide if flocculation is important to consider.

3 Analysis of the dredging process: Equipment selection and cycle duration

The second step in simulating the turbidity effects of the dredging operation using a representative approach is to determine the work method. This includes providing a brief introduction on the behaviour of dredging plumes originating from the dredging operation and an introduction into existing methods, which are used as a starting point. Additionally, insight is obtained in the dredging volume, appropriate dredging equipment is selected and their workability is determined. This will be based on the data collected in Chapter 2. The selected equipment and work method are used to determine which dredging processes should be included in the model. Subsequently, the dredging time for the entire operation is calculated. This calculation not only determines the duration of the dredging operation, but aids in the determination of the temporal distribution of the source terms, discussed at the end of this chapter.

By focusing on these different aspects, a more comprehensive understanding of the work method is obtained and therefore a more accurate approach can be followed in representing the dredging activities. This chapter answers the second sub-research question and partially research question three:

2: What is the used work method for the dredging operation and which dredging processes should be incorporated in the model?

3: What are the relevant source terms and how should they temporally and spatially be distributed to represent the dredging operation?

3.1 Dredging plumes and existing methods

The focus in this study is on the turbidity effects in the far-field. To obtain a better understanding of the difference between the near-field and the far-field regarding dredging plumes, a short description on the different processes involved is provided. Additionally, an introduction and explanation on the approach used by existing methods to simulate the effects from dredging in a representative way is given. These methods will form a basis for a more detailed representative approach, specifically focused on Backhoe Dredgers (BHD).

3.1.1 Dredging plumes

A distinction between a dynamic and a passive plume can be made in the plumes created as a result of dredging. The spill caused by dredging can either mix directly in the water column or behave as a density current when reaching the seafloor (Winterwerp, 2002). The plumes mixing directly with the water are the passive plumes and the dynamic plumes are the ones behaving as a density current. Both type of plumes have a different impact on the surrounding area. This study will only focus on the effects of the passive dredging plume. The reason for this is that the interest is on the effects on the sensitive receptors far from the source. Due to their ability to travel farther than dynamic plumes, the passive plumes are of more importance when assessing the impact on sensitive receptors further from the source.

Advection and diffusion are the two dominant processes in a passive plume as these influence the dispersion of the finer particles (Becker, 2011). The passive plume is caused by sediment mixing directly with the water column. Processes as stripping and entrainment cause the formation of this passive plume (Dankers, 2002). The passive plume will therefore contain the finer particles removed from the dynamic plume. The SSC in the passive plume will therefore be low compared to the dynamic plume. Due to the low settling velocity of the sediment particles in the passive plume, these particles can stay in suspension for long time and spatial scales (Tuinhof, 2014).

3.1.2 Introduction to existing methods

As mentioned, a number of existing methods providing an approach to simulate the turbidity stresses from the dredging operation have already been developed. The methods by Becker et al. (2015) and Tuinhof (2014) will be used as a starting point for developing a more representative approach in simulating the turbidity effects. For both methods the focus points are discussed as well as the simplifications.

The method developed by Becker et al. (2015) will be used as a starting point, since the focus of the suggested approach was on the far-field, focusing on the effects of the passive plume. The main focus point of the method is to estimate the source terms caused by dredging. Source terms for dredging refer to the sediment flux, which is released during the dredging operation (Tuinhof, 2014). The source term relates to the amount of fine suspended sediment available for dispersion following the dredging operation. These source terms can be used as input for a numerical model of the dispersion of dredging plumes (Becker et al., 2015). This method will be used to estimate the source terms for the Black Rocks case study in Chapter 4. For both hydraulic and mechanical dredging methods for quantifying source terms have been developed by Becker et al. (2015). Only the mechanical method is focused on due to the use of a BHD. A general approach for quantifying source terms, consisting of four steps, is proposed in the method to follow for any equipment used:

1. Analyse the work method for plume sources
2. Assess the total amount of available fines
3. Distribute available fines over work method elements, applying source term fractions to derive far field model source terms
4. Ensure appropriate application of source terms on the computational grid

In the first step, the used work method is analysed, including the duration of various aspects in the dredging cycle, such as filling of barges and sailing time. In step two, the total available amount of fines in the dredging volume available to be brought in suspension is determined for which a number of equations is provided. Step 3 involves the determination of the amount of fines lost by applying empirical source term fractions to the work method elements. This provides a numerical value for the sediment flux over time for input into the used numerical model, which is the fourth step. Special attention is given to the chosen grid cell size, as a too large grid cell can result in a diluted concentration of the initial sediment flux.

The research of Tuinhof (2014) focused both on the near-field and far-field and the transition between the two. Experiments for both 2D and 3D models were performed for stationary, uniform flow in which different sized grid cells were tested. The tests, which involved distribution of the source in both lateral and vertical direction, were run using a continuous source and a single grain size of 63 μm. The results were compared to field data collected from dredging plumes originating from a Trailing Suction Hopper Dredger (TSHD) and indicated that the grid size influences the far-field fluxes in a similar way as described by Becker et al. (2015).

A number of limitations in the two methods give room for developing a more representative approach to simulate the dredging operation. In both methods, no specific attention is given to the consideration of varying flow velocities and other metocean conditions to include in the simulation, which was focused on in Chapter 2. Only limited attention is given to the temporal distribution of the source. While the Becker method notes to choose the time-step for the sediment flux with care, no specific information is provided to when the source must be present. In both methods, the focus is on the fraction smaller than 63 μm, but the effects and importance of modelling multiple sediment fractions have not been researched. Additionally, while the possibility of an inhomogeneous dredging volume is mentioned, the use of a spatially varying source quantity has not been considered.

Finally, both methods have not specifically been developed for the use of BHD's, resulting in no specific description in the distribution of the source term over the vertical.

Each of the limitations mentioned will be addressed in this study in order to develop a more representative approach in simulating the dredging operation for a BHD.

3.2 Dredging volume

To identify the work method and estimate the total source term originating from the dredging operation, the total volume of sediment to be dredged must be known. The material that will have to be dredged at the project location consists of both large boulders and a sediment mixture of mainly gravel and sand, including some silt. The total dredging volume given in this section will only consist of the loose sediment, excluding the volume of the boulders.

The total dredging volume remains an estimate due to uncertainty about the exact size and number of boulders under the seabed. A single-beam sonar was used during the mapping survey of the area to create a sub-bottom profile of the Black Rocks area. No clear conclusion could be drawn from these results regarding the amount and position of the large boulders beneath the bottom surface. The harbour is assumed to be built using caissons for this case study, therefore the total dredging volume contains both the dredging of the inner basin and approach channel, but also the dredging required to create a trench for placement of the caissons. The harbour construction tender is be split into two separate packages. Package A (main dredging works) and package B (package A + additional dredging):

- Package A: Dredging approach channel & construction breakwater. 33.400 m^3 dredging.
- Package B: Package A + Finger pier construction and dredging of inner basin. 10.881 m^3 additional dredging.

The dredging operation for Package A is split up in two parts: dredging for placement of the caissons accounting for 15.450 m^3 of the total dredging volume and dredging for the harbour basin accounting for 17.950 m^3 of the dredging volume. From the total 33.400 m^3 to be dredged, 11.251 m^3 will be dumped at the disposal site, while the remaining sediment is used for filling of the caissons.

For Package B the dredging for caisson placement equals the amount for package A. In the harbour basin a volume of 28.831 m^3 now has to be dredged as the inner basin dredging volume is now included. The total dredged volume for package B is 44.281 m^3. The total amount of sediment that will be transported to the disposal site therefore increases to 22.132 m^3.

The harbour is divided into two separate areas each with a different dredging depth. The inner basin, which is Area I will be dredged to a depth of -2.75 m SD. The outer basin and the approach channel are labelled as area II and are dredged to a depth of -5.25 m SD. An overview of the different dredging depths can be seen in Figure 3.1.

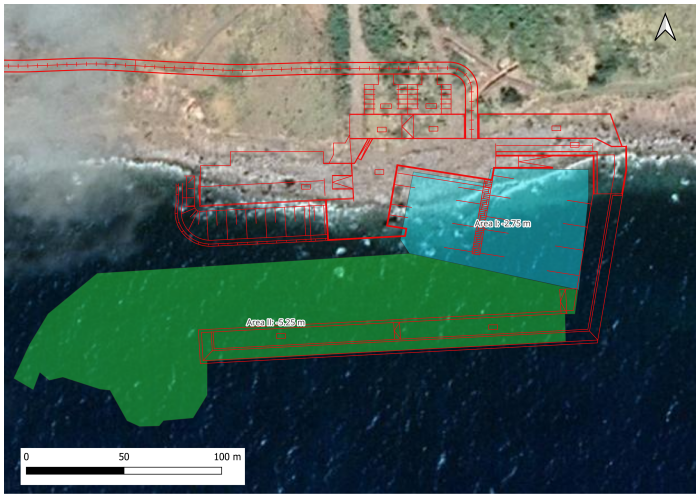

Figure 3.1: Overview of the different areas to be dredged in the Black Rocks area including their final depths

3.3 Dredging equipment & work method

An overview of the dredging equipment needed for the dredging operation is required to determine the sequence and duration of the dredging cycle. Knowledge on the work method is used to identify the relevant source terms from the dredging operation in Chapter 4.

In the model, the dredging operation will be executed entirely by use of a BHD with barges. The use of a TSHD is not feasible as the draught for these vessels is much larger than for the BHD. This could pose a challenge due to the large boulders present in the area and the relatively shallow waters closer to shore. A Cutter Suction Dredger (CSD) is considered to be impractical for this operation due to the relatively small dredging volume and the fact that a CSD would be considerably more expensive than a BHD. Another positive effect of the BHD usage, besides the cost efficiency, is that the noise produced is less than for a hydraulic excavator.

When determining the duration of the dredging cycle, workability of the BHD is an important factor to consider. Workability of the BHD depends on factors such as its pontoon size, site conditions, bucket volume and reliability, therefore the size of the equipment must be decided upon. As at the moment of writing the exact equipment used for the dredging operation is unknown, an estimate is made on the BHD size, number of barges and barge capacity used for the project. Following consultations with experts in the dredging field, a BHD with a bucket volume of 10 m^3 was decided to be feasible. The associated draught for the pontoon supporting the backhoe is around 2 m. The choice to not use a larger pontoon is based on multiple reasons. Navigational constraints, caused by the shallow dredging depth and the presence of numerous large boulders, influence the pontoon size. Additionally, the higher cost of a larger BHD and the limited dredging volume and depth make selecting a relatively small BHD a logical choice.

Two barges will be used for the operation, which will transport the excavated sediment towards either the dumping site, the existing Fort Bay harbour for temporary storage or directly to the caissons for filling on site. However, the final option is not considered for this research as the details on how this operation would be executed and the amount of released fines during this process are unknown, making it unsuitable for the simulation purposes in this report. Therefore, the choice is made to transport all of the dredged sediment in the simulations to the dump site by the barges. A dumping site has been appointed at a location northwest of Saba (see Figure 2.1 in Chapter 2). The disposal site is located at 17°39.125 N, 63°16.194 W (UTM Zone 20N: X = 4713722, Y = 1951880).

In addition to dredging sediment, the BHD can be equipped to handle the removal and crushing of large boulders. For the boulder extraction process, only the generation of fines is taken into account as an extra small percentage for the bucket drip, which will be discussed in more detail in Chapter 4.

3.4 Workability

Before calculating the duration of the dredging operation, workability limits need to be considered for the estimation of downtime of the BHD. A persistency analysis must be performed to calculate the possible operational hours based on the site conditions. If the wave height is too large the BHD will not be able to manoeuvre, while a too large wave period will cause instability of the pontoon, risking both crew safety and equipment damage. Therefore, the BHD will be limited by restrictions on H_s, H_{max} and T_p.

A pontoon is chosen based on its expected operability in maximum significant wave heights of 0.9 m, maximum wave heights of 1.5 m and peak wave period of 10 s. The datasets containing measurements collected by a wave buoy in the Black Rocks area between August 2020 and October 2023 on all three parameters are subjected to an analysis in which the number of workable days per time period is calculated for each day between 5:00 and 19:00. During the project, it is anticipated that dredging is possible for 84 operational hours per week, accounting for unforeseen circumstances, maintenance and refuelling. For a week with 84 operational hours, this gives 12 working hours per day for dredging with two extra hours per day for sailing to and from site. This provides knowledge on the possibility to relocate equipment to a safe location before weather conditions are expected to change, which is especially important in hurricane prone areas as the Caribbean. The complete analysis can be seen in Appendix C. Following the analysis the conclusion can be drawn that H_{max} is the critical parameter in the analysis as for the 2021 period this only gives 97 workings days. For the period in 2023 this was 119 single days. The measurements for the period in 2022 were omitted as they were deemed to be unreliable. An overview of number of workable days for 2021 and 2023 according to the critical parameters can be seen in Table 3.1.

Year	Parameter	Days in dataset	Number of days
2023	Hs	342	169
2023	Hmax	342	119
2023	Tp	342	268
2021	Hs	348	149
2021	Hmax	348	97
2021	Tp	348	303

Table 3.1: Overview of the number of workable days for 2021 and 2023 related to the selected parameters

The graphs on the wave parameters shown in Appendix C indicate a seasonal influence of the maximum wave height. From the graphs it can be seen that the most favourable conditions occur around March and April, but no guarantee on the exact workable days can be given. It can be concluded that for the chosen BHD downtime due to rough weather conditions is likely to occur, but difficult to predict. Because of the unpredictable nature of the environmental conditions, downtime is not included in the duration of the dredging cycle. This is regarded as a limitation in the representation of the dredging cycle, as no occurrence of downtime during the dredging operation is an unrealistic expectation. The potential difference that a standstill of the dredging operation has on the turbidity levels is not observed using this approach and must therefore be taken into account when the results are discussed.

3.5 Dredging cycle duration and temporal distribution

Following the determination of the work method, the calculation for the duration of the dredging operation can be made. Consequently, the temporal distribution of the source terms for the simulation is determined to provide a representative time-step for the presence of the sediment flux.

3.5.1 Calculation of dredging duration

A single dredging cycle for filling and emptying the bucket of a BHD consists of the following movements: digging, lifting/swinging, dumping, swinging and lowering, and positioning. While the dredging depth is limited to 5.25 m, reducing the cycle time, the boulders in the area could hinder and slow down the process, leading to a cycle time between 1.5 and 2 minutes. This results in 30 to 40 cycles per hour. With a bucket of 10 m^3, the maximum production rate, at which the Backhoe will be working when there is no downtime, is estimated around 400 m^3/oh.
To transport the dredged sediment towards the dump location, two split-barges with a volume of approximately 1000 m^3 each will be used, ensuring minimal to no downtime for the BHD. It is assumed that a filled barge sails at a speed of 8 knots and has an empty sailing speed of 10 knots.

The calculation for the duration of the dredging operation is executed using a Python script, incorporating all parameters mentioned in this chapter. This includes the total volume to be dredged, BHD and barge specific parameters and the sequence of the cycle described. The script considers a limit of 84 operational hours per week, restricting dredging at night. This translates to 12 operational hours per day. The two barges are incorporated in the script such that an alternating filling process is ensured. In case both barges are sailing to or from the dumping site, dredging is halted. The downtime during relocation is added to the total dredging time as well as the hours at night when no dredging takes place to ensure a complete overview of the duration of the dredging cycle. The sailing path to the dumping location is calculated by providing three locations where the starting point is the dredging area. An intermediate location is added to ensure a correct sailing distance. The distance is calculated using the Haversine formula. At the dumping location, a dumping time of 10 minutes is added to empty the split-hopper barges before the hoppers can sail back to the dredging area.

Taking into account the parameters mentioned, the whole dredging operation will take around 9.6 days to be completed. This is excluding downtime due to rough weather conditions and not taking into account the removal of boulders.

3.5.2 Temporal distribution of the source terms

One important aspect to take into account for a representative simulation is that the dredging process is a cycle and exhibits a temporal and spatial signal. An additional step in the methods, discussed in Section 3.1.2, is therefore to determine the temporal and spatial distribution of the source terms. A more representative approach in simulating the turbidity stresses from dredging activities can be obtained by creating a distinctive overview of the moments and locations at which the source should be present in the model. The focus in this section is on the temporal distribution.

The exposure to sensitive receptors from the sediment plumes can vary throughout the dredging cycle. The turbidity values can be classified as constant, peak and pulsed exposure. A schematic by Dupuits (2012) is shown in Figure 3.2.

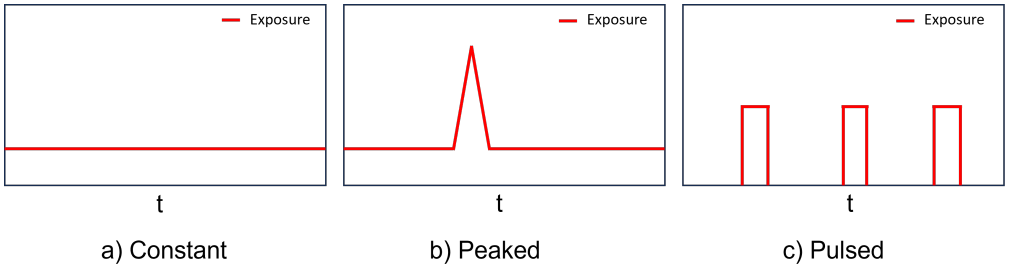

Figure 3.2: Schematization of a constant, peak and pulsing exposure pattern based on (Dupuits, 2012). a) represents a constant exposure pattern, b) represents a peaked exposure pattern and c) shows a pulsed exposure pattern

As shown in Figure 2.25 by Erftemeijer et al. (2012), the intensity and duration of the sediment flux is important when focusing on the turbidity stresses affecting corals. The temporal distribution of the source can range from longer time-frames as the day and night cycle all the way up to individual lifting cycles of the bucket. It is essential to make a decision on the required level of detail, depending on the applied methods.

Following the work method analysis in this chapter, it was decided that dredging will occur for 12 hours each day and therefore commences at 6:00 and ends at 18:00 each day. The BHD will dredge continuously throughout the day, such that the source term will have a constant value during this time-frame. At night, the sediment flux will be 0 kg/s as no dredging takes place. When the BHD is relocating, which is assumed to take two hours for this project, no source term is present as no dredging takes place.

The decision to use a constant source term throughout the dredging period, rather than a more detailed approach in which a distinction is made between bucket lifting periods, is supported by the findings during development of the Becker method. The focus in this study is on the turbidity effects in the far-field. For the used method, extensive testing was conducted focusing on the correlation between the estimated production of fines in the near field to the measured fluxes in the far field. The results indicated a difference in fluxes when dredging was halted for longer periods of time, but no difference for pulsed behaviour of the source on short time scales, which would occur if distinctions were made between bucket lifting periods. Therefore, it was determined that variations in the source term during short time intervals do not significantly impact the far-field concentrations. This implies that using a constant source between dredging periods serves as a suitable approach in representing the sediment flux from the dredging operation when applying the Becker method.

4 Identification, distribution & quantification of source terms

The identification, distribution and quantification of source terms from dredging are vital aspects to consider for accurately simulating the effects of the dredging operation. This chapter focuses on these source terms, which refer to factors and mechanisms that contribute to the release of fine sediment. First, the source terms are identified based on the knowledge obtained on the work method in Chapter 3 and a selection is made on which sources are included in the simulation. Subsequently, a decision on the spatial distribution of the source terms is made. As part of this methodical step, an in-depth analysis on the spatial variability of the fines content in the dredging volume is conducted to provide an estimate on the spatially varying fines content for a more locally representative source. This provides essential information to quantify the source terms, which are estimated using the method developed by Becker et al. (2015).
Each step contributes to the answer to the third research question:

What are the relevant source terms and how should they temporally and spatially be distributed to represent the dredging operation?

4.1 Identification of source terms

Before the distribution and magnitude of the sources can be estimated accurately, an overview has to be created of the possible source terms occurring during the dredging operation. Building upon the defined work method outlined in Chapter 3, this section lists the possible source terms for the dredging operation using a BHD and explains whether they will be included in the model or not. Each source term plays a role in sediment release during the operation, and the decision to include them in the model depends not only on their significance, but also on feasibility of quantification. Mistakes regarding over- or underestimation of the source terms can occur if insufficient data is available for an accurate quantification. The work method is divided in three parts to identify the source terms: excavation by the backhoe, sailing and dumping and back-filling of caissons.

The bulk of the source term is caused by the bucket drip of the BHD, which occurs during lifting of the bucket after sediment excavation. While some overflow may occur when the bucket is emptied into the barge, this should be prevented at all times in order to comply with contractual obligations. Therefore, it is expected that the amount of fine sediment released in the water column due to an overflowing barge is negligible in comparison to the bucket drip. Consequently, the source term caused by overflow of sediment is not taken into account as a separate term, but included in the percentage of the bucket drip by taking the upper limit of the empirical source term fraction determined by Becker et al. (2015). Another source of fine sediment generation occurs during the removal of boulders. It is anticipated that a portion of the boulders will have to be crushed because their size or weight exceeds the BHD's design limits. The amount of fines released when crushing the boulders is unknown, as no tests have been carried out to obtain relevant data. However, as it is inevitable that some fine material is suspended, a small percentage is included for the source term of the bucket drip.

Concerning the split-barges, leakage of the bottom doors is a potential source term. If a leak were to be present, increased suspended sediment loads during loading and sailing of the barge are expected. This factor is, however, not considered in the model, as the contractor is obliged to certify the split barges, minimizing the likelihood of a leak near the bottom doors. For this reason, the expected source term arising from a potential leak is assumed to be 0. When reaching the disposal location, the bottom doors of the barge are opened to dump the excavated sediment. This results in a rapid increase in the SSC at the disposal location, which is located in deep water. The suspended sediment can be transported far from the disposal location, depending on the settling velocity of the fines and the current velocity and direction in the area. Nevertheless, the effects that the dumped sediment can have on the area surrounding the disposal location, are out of scope for this study, and therefore, not considered further.

Finally, source terms are present during emptying of the barges and back-filling of the caissons. The exact process and location for back-filling of the caissons is unknown for the project. The caissons can either be directly filled at the new harbour, limiting the area where sediment can be spilled or the barges can be emptied at Fort Bay harbour. The second option potentially creates a new sediment pollution zone, which will need to be monitored. The contractor is obliged to minimize the loss of sediment. Due to the uncertainty of the working method of the caisson-filling process and its potential impact, the potential source term caused by filling of the caisson is out of scope for this research.

The impact of the source terms is expressed as a percentage of the fraction of fines lost from the total volume of fines available. According to Becker et al. (2015), a reasonable range for the bucket drip is from 0 to 0.04. As mentioned, the upper limit of 0.04 is chosen to avoid underestimating the amount of fines released during the dredging operation by accounting for possible overflow of the barge. The source term related to extraction and crushing of boulders is estimated to account for an additional factor of 0.005 of the total fines available. Since no experiments have been performed, this remains a rough estimation, meaning that a large overestimation is possible. However, it is decided that an overestimation of the total amount of fines is a better choice for this study than an underestimation, as the results can be used to assess the potential impact on the sensitive receptors. While the fines released during this process do not originate from the total mass of fines present in the sediment to be dredged (as the boulders were excluded from the total dredging volume), the extra percentage is decided to be a suitable estimate of the extra fine sediment fraction released.

As mentioned, the source terms caused by leakage during sailing, dumping at the disposal site and back-filling of the caissons are out of scope. The two source terms that are included give a total source of 0.045, meaning 4.5% of the total available amount of fines in the dredged sediment is estimated to be lost in the water column.

4.2 Spatial distribution of source terms

Now that the relevant source terms for representing the dredging operation have been identified, the next step is to determine how these sources are distributed spatially. While the source originating from a BHD can be classified as stationary, the backhoe will need to relocate to be able to complete the dredging works. The research by Tuinhof (2014) indicated that the lateral distribution of the source influences the far-field plume concentrations. As this will influence the intensity of the turbidity stress on the corals over time, simulating the source at different locations throughout the basin will allow for a more representative approach. Two different scenarios will be considered in order to assess the difference in SSC between a stationary and relocating source in combination with varying hydrodynamic conditions, providing both a simplified and more detailed approach.

The stationary scenario consists of a single source, placed in the middle of the harbour throughout the entire dredging operation, therefore representing the fines released from the entire dredging volume. This simplified approach requires the calculation of only one sediment flux, making the process efficient and quick. As the dredging volume for this study is relatively small, it is chosen to model the source at three different locations located 80 metres apart in the harbour basin for the relocating scenario: west near the breakwater edge, in the middle of the harbour and on the eastern side, which is the shallower part of the basin. The dredging area is divided into three sections with equal dredging volume assumed, such that dredging at each of the three locations take equally as long. The different areas, as well as the locations at which the BHD will dredge, can be seen in Figure 4.1.

4.3 Spatial estimation of fines content for source terms

Before the source terms can be quantified, it is essential to analyse the area-specific sediment characteristics to determine the total mass of fines in the volume to be dredged. Only the sediment fraction smaller than 63 μm is considered as "fines" in the method by Becker et al. (2015). The existing methods do not take the effects of a spatially varying fines content over the dredging volume into account. Use of the approach of the current methods can therefore lead to an over or underestimation of the source term at varying locations in the project area. An addition to the method proposed by Becker et al. (2015) is suggested to estimate the spatial variability of the fines content in the dredging volume from representative borehole samples, which results in a more representative approach in estimating the available fines at each source location. If the soil samples taken from the dredging volume do not exhibit a spatial variation in the fines distribution, this step is not required and the normal procedure can be followed to use an average percentage of fines for the entire dredging volume.

In the analysis of the physical processes for this case study, a spatially varying content of the fines alongshore was noticed, which can be linked to the heterogeneous nature of the soil layers around Saba. Therefore, an analysis is made to assess which samples from the two soil investigations are most representative to give an estimate on the spatial distribution of the fines content in the dredging volume. A borehole sample is deemed to be representative if the depth at which the sample is taken does not exceed the maximum dredging depth at that location. Additionally, the proximity of the sample to the considered source must be taken into account, as using a sample taken on the eastern side of the basin should not be used for the estimation of the fines content on the western side.

Each of the samples taken at the boreholes introduced in Section 2.4 will be analysed. For the stationary source an average fines content using all representative samples is determined, while for the relocating source the proximity of the samples is taken into account as well. Both the location and sample depth will be compared to the final dredging depth for the new harbour to classify the importance of each borehole. Samples taken from a depth of 10 m will be less representative for the sediment characteristics in the dredging volume than samples taken at a depth of 4 m due to the relatively shallow dredging depth, with a maximum of 5.25 m. It is decided that borehole samples taken at a depth of more than 5.5 m relative to SD on land will not be taken into account to determine the average fines content of the dredging volume due to the maximum dredging depth of 2.75 m SD nearshore. For the offshore boreholes the maximum depth at which collected samples are assumed to be representative is around 8.5 m SD. A relatively large depth range is taken for the determination of the fines content due to the limited number of samples available at shallow depths. Figure 4.1 provides an overview to illustrate the proximity of each borehole to the final dredging depths.

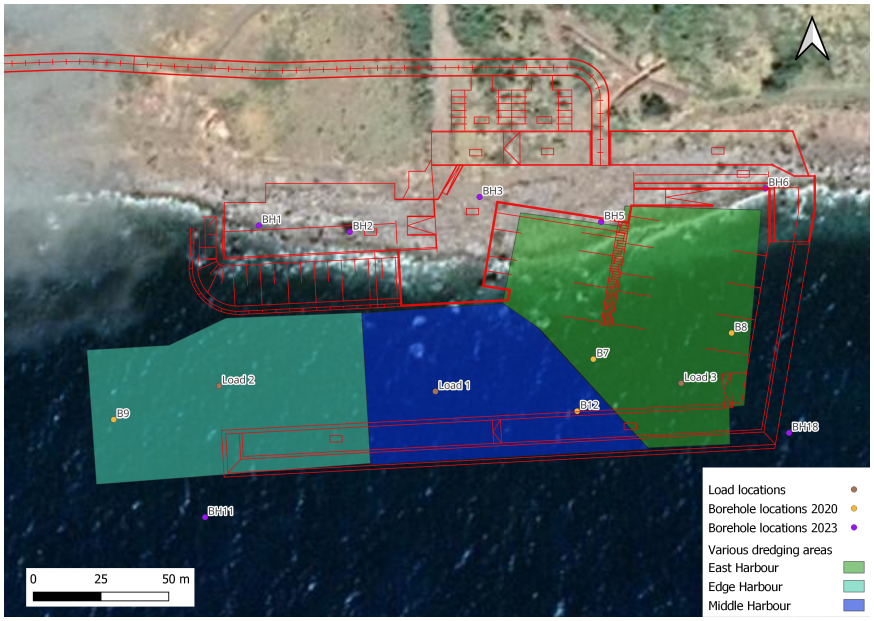

Figure 4.1: Location of the different borehole locations on land and at sea in the Black Rocks area that are considered to be representative for the dredging volume. The load locations have been included as a reference.

The samples, including their fines content, that are used to estimate the fines content at the source locations are listed in Table 4.1:

Borehole	**Depth relative to SD [m]**	**Fines content [%]**
B7	6.00 - 6.45	4
B8	7.50 - 9.50	3
B9	6.60 - 6.75	3
B12	8.30 - 8.80	1
BH1	3.44 - 3.89	6
BH1	4.94 - 5.39	12
BH2	5.02 - 5.47	8
BH3	(+) 2.17 - (+) 1.82	4
BH3	(+) 0.67 - (+) 0.22	5
BH3	0.83 - 1.28	5
BH3	3.83 - 4.28	4
BH3	5.33 - 5.78	7
BH5	1.90 - 2.35	6
BH5	4.90 - 5.35	7
BH6	3.88 - 4.33	6
BH6	5.38 - 5.83	8
BH11	8.78 - 9.23	5
BH18	7.07 - 7.52	3
BH18	8.57 - 9.02	7

Table 4.1: Overview of the fines content in the representative borehole samples taken during the two geotechnical surveys in the Black Rocks area

From the depth analysis it can be concluded that only 12 samples taken at boreholes on land and 7 samples taken at boreholes offshore are deemed to be representative. For the onshore boreholes

an average fines content in the samples of 6.5% is found, while offshore this was only 3.7%. When taking the average of all samples an average fines content of 5.5% is found. This average, which represents the fines content of the total dredging volume, will be used to characterize the stationary source.

It must be noted that these are estimates from the limited number of samples available. The heterogeneity of the soil and the inconsistent depths at which the samples are taken are all uncertainties that should be taken into account. An example is the sample taken at B3, which showed an average fines content of 33%, while at a similar location for BH5, only metres apart, a fines content of 7% was found. While B3 was identified as an outlier, the possibility of multiple pockets containing a large amount of fines cannot be excluded. For this report the calculations will, however, be made using the average fines content obtained from Table 4.1. This example stresses the importance of analysing the borehole samples as taking the average fines content of all samples would not have given a representative value of the fines content due to such outliers.

Next a distinction between the location of the samples along the coastline is made to determine the representative boreholes and subsequently the fines content for each of the three sources illustrated in Figure 4.1. Starting from the area at the outer edge of the breakwater, only samples of boreholes B9, B10, BH2 and BH11 are taken into account due to the deeper location, while BH2 is included to take one of the samples closest to shore into account. The average fines content for this area, considering these samples, is 5.3%. For the middle part of the harbour the samples from boreholes B6, B6b, B7, B11, B12, BH4 and BH14 are used, which gives a fines content of only 4.3%. Finally, the area located on the eastern side of the harbour takes into account the samples of boreholes B3, B4, B7, 8, B13 and BH6. The fines content from the actual sample taken at borehole B3 of 33% is not used. Instead, a higher value of 10%, which is slightly higher than the fines content of 7% found at BH5, is used. This gives an average fines content in this area of 6.5%. An overview of the different fines contents that have been given in this section can be found in Table 4.2.

Load	**Fines content** [%]
Stationary (Load 1)	5.5
West side harbour (Load 2)	5.3
Middle of the harbour (Load 1)	4.3
East side harbour (Load 3)	6.5

Table 4.2: Overview of the fines content for the two scenarios in the different sections defined in the harbour

4.4 Quantification of source terms

With all the relevant data collected on sediment characteristics and fines content in the dredging volume, the source terms can be quantified. The calculated sediment flux is implemented in the numerical model to simulate the spilled sediment. The sources terms are calculated using the method for estimation of source terms by Becker et al. (2015). As stated in Section 3.1.2, the method does not specify the number of sediment fractions to include in the model for a representative simulation. Considerations in the number of fractions to include are an addition to the method and is elaborated upon at the end of this section. First, an overview of the calculation steps is given followed by the quantification of the source terms at the load locations for the two scenarios considered for the case study.

To quantify the source terms, the total available amount of fines must be calculated, starting with the total in situ volume to be dredged. From this the total amount of fine material ($< 63\ \mu m$) can be calculated using the following formulae:

$$\rho_d = (1 - n)\rho_s \tag{1}$$

$$\rho_{situ} = \rho_d + n \cdot S_r \cdot \rho_w \tag{2}$$

$$m_t = \rho_d \cdot V_{situ} \cdot f_{<63\mu m} \tag{3}$$

The dry density is used to calculate the mass of the solids in the total material using the porosity n and the grain density ρ_s. Depending on the available data, the dry density, ρ_d, can be calculated using the second equation with the in situ density. Here, S_r is the degree of saturation. The final equation is then used to calculate the total mass of fines m_t.
If the estimated situ production rate P_{situ} is known, the total production of fines per cycle can be calculated:

$$m_{tcycle} = \rho_d \cdot f_{<63\mu m} \int_{t_0}^{t_2} P_{situ} dt \tag{4}$$

Here t_0 and t_2 refer to the dredging time until the barge is filled.
Calculation of the amount of fines dispersed in the far-field by the bucket drip is performed by using the following equation:

$$m_b = m_t \cdot \sigma_b \tag{5}$$

Here, σ_b is the empirical fraction used to calculate the amount of fines released by bucket drip. With these values the total suspended sediment flux and the total mass of fines can be calculated. By dividing the mass of fines lost per cycle by the loading time, a value in kg/s is obtained, which can be used as input for a numerical model.

The final step involves correct application of the source term to the far-field model. Both the computational time step and number and dimension of grid cells have to be chosen carefully. Choosing a wrong time step may result in too high 's during certain times. Choosing a too large or too small grid cell size may result in artificial diffusion or too high local 's. Application of the sources in the model are discussed in Chapter 5.

Source term calculations
Following the steps outlined in the method for estimating source terms, the sediment fluxes for the identified source terms are calculated. Four distinct sediment fluxes need to be calculated: one for the stationary averaged source term and three for the area specific sources. These can be used to model the situation and effects for a stationary backhoe throughout the operation and for a backhoe relocating to different areas.

To start the calculations, a number of constant values regarding the sediment characteristics, dredging operation and source term fractions must be defined. The values are reported in Table 4.3.

Constant	Symbol	Amount	Unit
Seawater density	ρ_w	1025	kg/m3
Grain density	ρ_s	2620	kg/m3
Dry sediment density	ρ_d	1500	kg/m3
Porosity	n	0.42	kg/m3
Loading time per barge	-	9000	s
Total dredging volume	V_{situ}	44,281	m^3
Operational hours per week	-	84	oh
Total source term fraction	σ_b	0.045	-

Table 4.3: Overview of the constant values used in the calculation for the estimation of source terms

The sediment fluxes can now be computed. For each load, the location, fines content, source duration and intermediate calculation steps are provided. In the case of the average, stationary load in the middle of the harbour, the total dredging volume is used to calculate the total available mass of fines. For the other loads only one-third of the total volume is available. The results of the calculations are presented in Table 4.4 below. Here, m_t presents the total available mass of fines in the dredging volume, $m_h cycle$ refers to the mass of fines lost in the water column per cycle and the duration refers to the total dredging time at each location.

Load	**Fines content [%]**	m_t **[kg]**	$m_h cycle$ **[kg]**	**Duration [days]**	**Sediment flux [kg/s]**
Stationary average	5.5	3,653,188	5,069	9.6	0.56
West harbour	5.3	1,173,448	5,083	3.07	0.56
Middle harbour	4.3	952,043	4,124	3.07	0.46
East harbour	6.5	1,439,135	6,234	3.07	0.69

Table 4.4: Overview of the intermediate calculation steps for the different source terms

Sediment fraction considerations
For an accurate representation of the dispersion of fines brought into suspension during the dredging operation, the calculated sediment fluxes should not only be represented by a fraction with a diameter of 63 μm, but also by smaller fractions that remain in suspension for a longer period due to their lower settling velocities. However, as the minimum sieve size used for both soil investigations was 63 μm, no representative data for the smaller fractions is available for this study.

Multiple methods can be used to obtain an estimate of the distribution for the smaller fines fraction. One approach is to extrapolate the available PSD curves to obtain an estimate on the distribution of the smaller fractions. Another method involves using grading curves from similar surveys in the Caribbean to obtain a broader insight in the likely distribution of fines below 63 μm. A more accurate extrapolation on the available sieve data can be performed by using the distribution of these surveys. As grading curves from samples taken at similar areas in the Caribbean are not available at the moment of writing, extrapolation of the PSD curves is chosen as the best available method.

Due to the uncertainty in this method, only two different fractions are considered: 63 μm and a smaller fraction of 30 μm. From the three available PSD's (see Appendix D) it can be concluded that the average distribution of the two different fractions in the fines is around 40% for 63 μm and 60% for 30 μm. The corresponding sediment flux per fraction for each load is given in Table 4.5.

Load	**Sediment flux 63** μm **[kg/s]**	**Sediment flux 30** μm **[kg/s]**
Stationary average (Load 1)	0.22	0.34
West harbour (Load 2)	0.22	0.34
Middle harbour (Load 1)	0.18	0.28
East harbour (Load 3)	0.28	0.41

Table 4.5: Overview of the sediment fluxes for the two sediment fractions

5 Modelling of the dredging operation: model choice and configuration

Having collected comprehensive data on the local hydrodynamics, sediment characteristics, work method and source terms, the translation step to the model can be made. This chapter focuses on the selection and configuration of the numerical model. These steps are critical to ensure a correct representation of the turbidity impacts from dredging activities by a BHD. The model choice and approach is discussed first, which is crucial as it determines which aspects of the operation can be simulated. Subsequently, the configuration of the source terms and hydrodynamic conditions into the model is determined. This step aims to encompass all important aspects of the operation for a representative simulation.
The following sub-research question is answered in this chapter:

What is the most suitable modelling approach and how should the source terms and local hydrodynamic conditions be configured and implemented for an accurate simulation of the dredging operation?

5.1 Model choice

The selected model should include the necessary specifications, capabilities and flexibility to represent all relevant processes, boundary conditions and time and spatial scales. Understanding the limitations is important to ensure that these limitations do not compromise an accurate reflection of the hydrodynamic and sediment dispersion processes.

The first step is to determine the level of detail required regarding the simulation of the physical processes. Different options are available to simulate the physical processes such as detailed Computational Fluid Dynamics (CFD) models, which often have a spatial resolution ranging from millimetres to metres, and more global models as Delft3D, MIKE21 and FINEL for which the spatial resolution is in the range from metres to kilometres. The focus for this method is on the simulation of the far-field plume and not on the dynamic plume near the source. Advection and diffusion are processes more important for dispersion of the far-field plume, while for the near-field plume dispersion is highly dynamic and therefore turbulence becomes important (Tuinhof, 2014). CFD models are often to used for a more detailed simulation at a higher resolution and smaller spatial scale to include processes as turbulence and heat transfer, while the global Delft3D, MIKE21 and FINEL models are used to solve hydrodynamic processes on a much larger scale. The global models are chosen for this method as the level of detail together with the computational efficiency is considered to be sufficient for modelling the far-field plume dispersion.

Taking into account considerations regarding licenses and modelling support, the software Delft3D was chosen to use for this study. Both the older and more stable version, Delft3D-4, and the newer Delft3D Flexible Mesh (FM) are viable options. Delft3D FM makes use of unstructured grids, where Delft3D-4 uses structured grids. Delft3D FM is chosen to use, as it provides the possibility of locally refining the grid without the need of coupling separate grids. This can greatly reduce the calculation time of the model.

Delft3D FM consists of different modules such as D-Flow, D-Morphology and D-Water Quality, each designed to simulate various processes such as tides, wind and wave-driven flow and different processes regarding sediment transport, morphology and water quality. For the hydrodynamics, the D-Flow module is used in which choices must be made for which processes to include. The user manual (Deltares, 2023a) explains that the unsteady shallow water equations are solved in either 2D or 3D by the model. The flow can be forced by the tide at the open boundaries, while D-Flow also allows modelling of flow caused by wind stress at the surface. The effects on the flow caused by pressure gradients (barotropic or baroclinic) can be included as well. When solving the model in 3D, the water column can be divided in discrete layers, so-called z-layers, which results in layers

with a standard depth. At shallow depths this will result in the use of less layers than at deeper locations. The other option is to use σ-layers, which each have a specific depth. The σ grid does not consist of straight horizontal lines over the depth, but follow the contours of the bottom profile and the free surface more closely. This causes the vertical grid to be divided into an equal number of layers consisting of an equal fraction of the water depth across the entire modelling domain. For this reason σ layers will be used for the vertical grid. D-Flow FM can also be coupled to D-Waves (SWAN) to include the influence of waves on the hydrodynamics. It is chosen to not include wave forcing for this project as the impact on the dispersion of the plumes is thought to be limited, while omitting waves also reduces the complexity of the model.

When the hydrodynamics using the D-Flow FM suite has been modelled, the transport of the suspended sediment can be modelled. Two different options are available: D-Morphology and D-Water Quality. A choice has to be made based on the dispersion and settling of the different sediment fractions. From the D-Morphology user manual (Deltares, 2023b) it follows that a distinction is made between the transport of cohesive and non-cohesive sediment. For non-cohesive sediment, including sand and gravel, the settling velocity is calculated using equations from the method of Van Rijn 1993. Three different equations for the settling velocity are specified based on different ranges for the sediment diameter.

For cohesive sediments, which include finer fractions as silt and clay, different equations can be used to account for processes such as flocculation. The option for the user to directly input the settling velocity per sediment fraction is also available. For the exact equations on the settling velocity for cohesive and non-cohesive sediments it is advised to consult the D-Morphology user manual. As the D-Morphology suite is run simultaneously as the D-Flow model, the computation time may increase significantly when running different scenarios for the input of suspended sediment in the model.

In D-Water Quality, various water quality processes can be simulated such as dispersion of sediment, transport of nutrients and simulation of biological processes. The user manual of D-Water Quality (Deltares, 2023c) states that for inorganic matter (suspended sediment) the settling velocity must be specified per sediment fraction by the user. The settling velocity of different grain sizes must therefore first be calculated manually. D-Water Quality is a separate module that requires a hydrodynamics (.hyd) file as input, which is obtained by running a D-Flow model. Once the sediment characteristics and input location has been specified, D-Water Quality only has to solve the advection diffusion equations, greatly reducing computation time compared to the D-Morphology suite.

The D-Water Quality module is chosen as the software to use for modelling the suspended sediment. Use of the D-Water Quality module will limit computational time, as the D-Flow FM module only has to be run once. When the same hydrodynamics are utilized, but the location and quantity of the sediment concentration varies, using the D-Water Quality module becomes more beneficial in a time-dependent context. Another reason to use D-Water Quality is that D-Morphology is more suited for situations in which a morphology change has an effect on the hydrodynamics. As this is not the case for the limited changes due to dredging, D-Morphology is less suitable for this study. Additionally, the use of cohesive sediment in D-Morphology has not been fully tested yet, therefore using the D-Water Quality module prevents the occurrence of unforeseen calculation errors, while the limitations resulting from using a user-specified settling velocity remain known. A schematization showing how the data structure and input and output files of the hydrodynamic and water quality model are linked is shown in Figure 5.1.

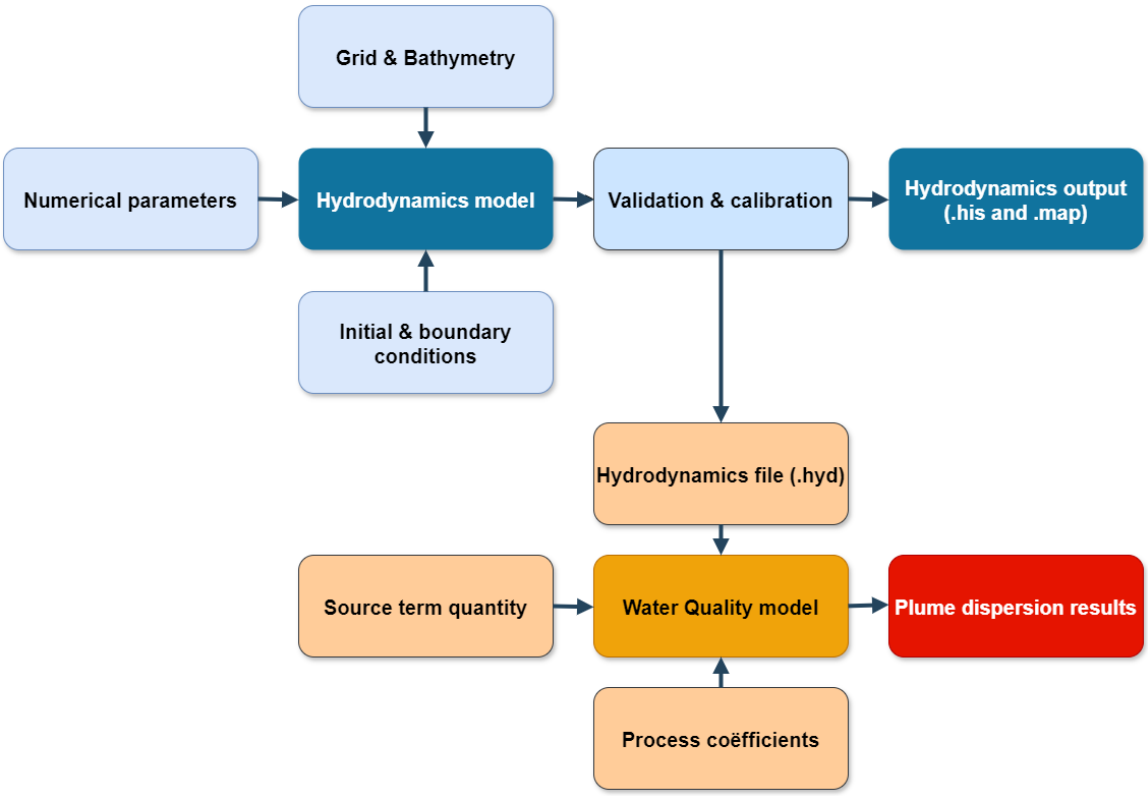

Figure 5.1: Schematization of the model structure for D-Flow FM and D-Water Quality

5.2 D-Flow model configuration

Now that the modules to be used have been selected, the configuration of the flow and water quality modules is next. The hydrodynamics from the D-Flow module is required as input for the D-Water Quality module in which the source terms will be added. The processes modelled, datasets used and configuration of these into the model are discussed in this section. The set-up of the D-Flow and D-Water Quality modules are discussed in separate sections, starting with the hydrodynamic model.

The set-up of the hydrodynamics model D-Flow FM is divided into four main components: Computational grid, bathymetry, initial & boundary conditions and numerical parameters. Each of these components is essential as input for the model and contributes to the accuracy of the model results.

Computational grid

The grid resolution of the model should be chosen with care. A too large grid size can results in a diluted SSC of the initial sediment flux, while grid cells that are too small can result in artificially high concentrations, as discussed by Becker et al. (2015) and Tuinhof (2014). To simulate the bucket drip of a backhoe, it is recommended to choose the smallest grid cell size in the range of the bucket dimensions.

The computational grid created used for both the hydrodynamic and water quality model around Saba is illustrated in Figure 5.2. The domain spans an area ranging from x = 63.333 ° W, y = 17.583 ° N to x = -63.165 ° W, y = 17.750 ° N. The large model domain around the island is chosen in order for the boundaries to match the grid resolution of the Copernicus Marine Service. The data portal will be used to extract data used for the boundary conditions.

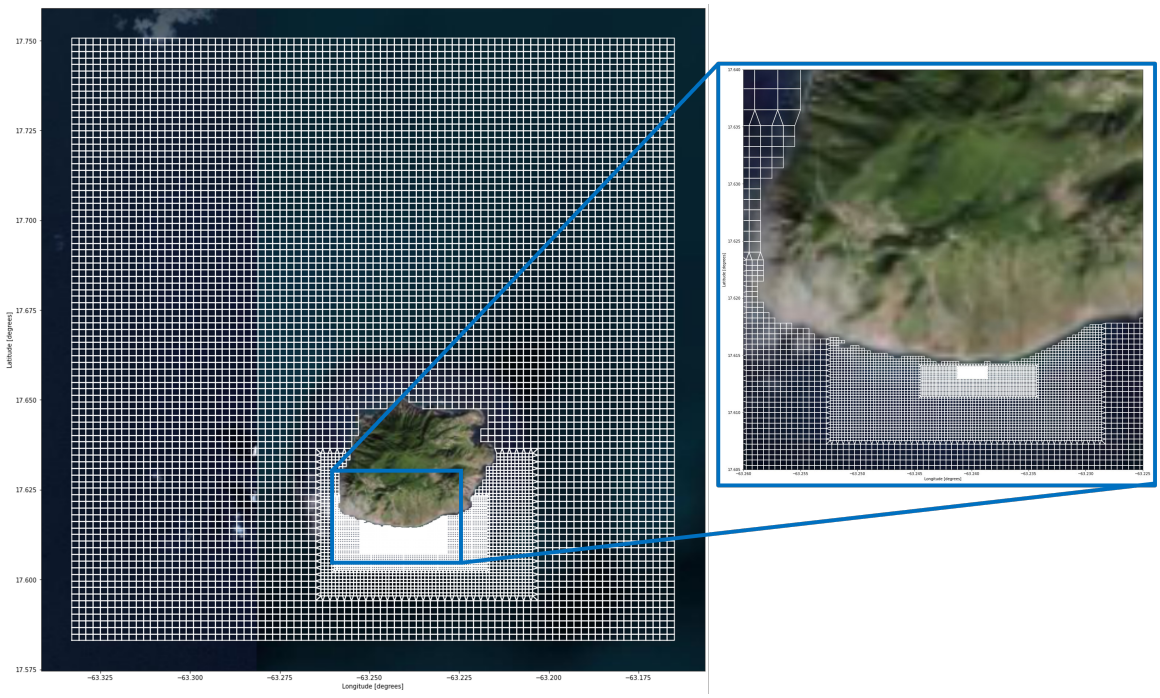

Figure 5.2: Computational grid used for the hydrodynamic and water quality model. The local refinement of the grid is seen on the right

The grid maintains a resolution of 212 m in both x and y direction at the boundaries and is refined a total of six times. Each refinement step halves the size of the grid cells, creating areas with grid cells of around 106, 53, 26, 13, 6.6 and 3.3 m. It is chosen to not include the complete boundary of the island (excluding the northern side) in the refinement of the grid to limit the computation time. However, occasional swells coming from the North and diffracting around the island may not be accurately captured in the model using this approach. As this phenomenon rarely occurs, it is regarded as a limitation to consider when discussing the results. At the south side of the island to eventually have a minimum resolution of 3.3 m in the area where dredging will take place. This fine resolution is chosen to accurately represent the surface area directly affected by the bucket drip of the BHD. In the surrounding area, which stretches from x = -63.244452 ° W, y = 17.611408 ° N to x = -63.234328 ° W, y = 17.614056 ° N, the grid has a resolution of 6.6 m. The high-impact zone, which has to be monitored extensively, is located within this area.

In the vertical direction, the grid has been divided into 5 uniform σ layers. The use of different depth layers allows for capturing the varying flow conditions over the vertical. The layers are distributed equally over the depth, such that each layer represents 20% of the water depth. No grid refinement over the vertical is introduced to reduce the computation time. It is believed that the flow, including currents induced by wind and dispersion of fine sediment over the depth is accurately modelled using an equal layer distribution. A visual representation of the vertical grid created for the model can be seen in Figure 5.3.

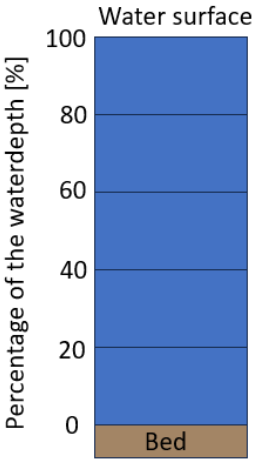

Figure 5.3: Schematization of the vertical grid showing the different sigma-layers.

Bathymetry
The bathymetry used for the model is obtained from the GEBCO 2023 dataset, where data points from the bathymetric datasets displayed in section 2.2 have been interpolated. The bathymetry is visualised in Figure 2.4 in Chapter 2. The dataset has been interpolated directly on the model grid. The rapidly decreasing depth contours are visible around the island, while some elevated areas around the island can be recognised, such as a famous dive site on the west side of the island. The elevated area at the south-west is the Saba bank.

Boundary conditions
To accurately reflect the hydrodynamic processes in the model, the relevant processes discussed in Section 2.6 must be imposed as boundary conditions. To reduce the complexity of the model and allow for computational efficiency, only the most processes of most influence on the plume dispersion can be selected.

The model domain for this study consists of four open boundaries on the north, east, south and west side of the island. A polygon file was created on the edge of the grid domain with 224 separate points. At each location the boundary conditions have been defined per time step.

The boundary conditions considered for the model include water level elevation, currents and tidal and wind forcing. The site visit and data collection discussed in Chapter 2 emphasize the importance of including both tidal and wind forcing to accurately simulate the dispersion of the sediment plumes during the dredging operation. Excluding wind forcing results in significantly lower current velocities at the top layer compared to the currents measured here using the ADCP. Additionally, more frequent current reversals at the top layer are simulated when only tidal forcing is imposed in the model.

For this study, no salinity and temperature are included as the expectation is that the influence of these parameters is small and therefore including these parameters would only increase the computation time and complexity of the model. As already mentioned, wave forcing is not included in the model either. Even though waves could play an important role in the re-suspension of sediments, the model would become too complex for this study if waves were included too.

The boundary conditions have been extracted from global databases. For the tide, tidal components from the global database TPXO8 are used. The tidal elevation plot obtained from the dataset of this database is compared to the observed tide at Fort Bay and can be seen in Figure 2.13 in Chapter 2. The maximum observed difference between the measured and modelled tidal amplitude

is 5 cm.

The water levels and flow velocities are forced at the open boundaries by data extracted from Copernicus Marine Services. All boundary conditions have been downloaded for the period 30-08-2021 to 30-09-2021 to facilitate a month of data to be modelled. For this time period ADCP data is also available such that the model results can be validated.

Wind forcing data is obtained from the ERA5 dataset. The wind speed obtained from the ERA5 dataset is the wind speed observed at a height of 10 m and has a temporal distribution of one hour. A comparison of the modelled and measured wind speed, shown in Figure 2.16 in Chapter 2, illustrates that the modelled wind speed is almost consistently 1 m/s higher than the the wind speed measured at the weather station. As explained, this is likely due to the sheltered location of the weather station at the project site. Figure 2.17 compares the wind direction, which does illustrate a good correlation between the two datasets.

Other parameters regarding horizontal eddy viscosity and diffusivity have not been changed. For the horizontal eddy viscosity and diffusivity the values were kept at 0.1 m^2/s. For the bed friction the Manning's formula is used with a uniform friction coefficient of 0.040.

Time-step & Numerical parameters
As mentioned for the boundary conditions, the model time-frame spans from 30-08-2021 to 30-09-2021. A time-step of 10 min is chosen for the simulation. For the hydrodynamics file, which will be used as input for the water quality model, an interval of 10 min is chosen. Regarding the numerical parameters no changes have been made to the standard input of the D-Flow FM model.

The model will be calibrated using the data collected with the ADCP in the Black Rocks area. Both the water level and flow velocities will be calibrated and verified by comparing the modelled to the measured ADCP data. Additionally, the flow directions are verified as well. The calibration results of the hydrodynamics module are presented in Chapter 6. This serves as input for the water quality module, of which the configuration is discussed next.

5.3 D-Water Quality model configuration

When configuring the water quality model, it is important to input source terms in a manner that closely resembles the process of fines released by the BHD during the dredging operation. As discussed in Section 3.1.2, existing methods have not specifically been developed for simulating dredging by a BHD. Consequently, a clear description of the distribution of the source term of the bucket drip over the vertical is currently unavailable. Furthermore, the importance of selecting a suitable formulation to calculate the settling velocity has not been stressed, despite its significant impact on the settling velocity and, consequently, the SSC in the far-field. This section will address these additions to the existing methods.

The processes involved and their coefficients are specified first, after which the location of the source term loads and observation points in the model are discussed. Subsequently, the input of the source terms, which involves the specification of the sediment flux per fraction over time and location, is specified. Two different scenarios are modelled as mentioned in Chapter 4: a stationary backhoe with an average fines content and a backhoe which relocates, changing the source term.

Process coefficients & settling velocity
The first step is to select the processes which represent the source terms caused by dredging. As discussed, only suspended sediment is modelled due to the negligible fraction of organic matter. Suspended sediment is referred to as inorganic matter in D-Water Quality. Two different sediment fractions are modelled, which are 0.063 mm and 0.030 mm (see Section 4.4). No larger fractions are modelled as the focus on the estimation of source terms is on fractions of 0.063 mm and smaller. In D-Water Quality, the coefficients for the processes need to be defined manually. Both sedimentation and re-suspension of the sediment can be modelled. The focus is on the dispersion of the particles initially brought in suspension due to the dredging operation, therefore the re-suspension of these particles is not considered.

The settling velocity of the particles must be defined by the user in Delft3D. The settling velocity of a sediment particle is influenced by its shape, size and density (Hawley, 1982). Larger particles will generally have a higher settling velocity, as well as particles with a higher density. The turbulence of the fluid and the properties of the ambient fluid, such as viscosity and salinity, also play a role (Cuthbertson et al., 2008). Based on the hydrodynamic conditions and local sediment characteristics, a suitable formulation for the settling velocity must be selected. The use of a method developed for laminar flow will be less suitable compared to a method applicable for turbulent flow when simulating the dispersion of sediment in a coastal environment.

Multiple options are available to calculate the settling velocity, with each their own range of applicability and their limitations. For this study the settling velocity relations of Stokes and Van Rijn are considered.

The Stokes formula is generally applicable for situations in which the Reynolds number is low ($Re < 0.5$) (Hawley, 1982). As in the marine environment the flow can be considered as turbulent, the Stokes formula is considered too simple to apply in this study.

The method proposed by van Rijn (1993) for calculating the settling velocity was developed to be applicable in the marine environment. This method provides three different formulations applicable for various ranges in particle size. The smallest range is applicable for fractions with a diameter between 0.065 mm and 0.1 mm, while the focus is on fractions smaller than 0.063 mm. This is regarded as a limitation in the used methods and must be considered when discussing the results.

To calculate the settling velocity of both sediment fractions, the Van Rijn settling velocity can be used (van Rijn, 1993):

$$w_s = \frac{(\frac{\rho_s}{\rho_w} - 1)gD^2}{18\nu} \tag{6}$$

Here, w_s is the settling velocity in m/s, ρ_s and ρ_w are the density of the particle and fluid, D refers to the diameter of the particle and ν is the kinematic viscosity of the fluid.
A kinematic viscosity for seawater of 0.000001 m^2/s is used, while the density of the particle and the seawater are respectively $\rho_s = 2620\ kg/m^3$ and $\rho_w = 1025\ kg/m^3$. This gives the following settling velocities for the different fractions:

- $w_{s(0.063)} = 0.0034\ m/s$
- $w_{s(0.030)} = 0.00076\ m/s$

The units required as input for the D-Water Quality module is in metres per day (m/day), which gives an input value of $w_{s(0.063)} = 291\ m/day$ and $w_{s(0.030)} = 66\ m/day$. The large difference in settling velocity between the two sediment fractions indicates the importance of including multiple fractions in the model simulation.

Source term distribution
The suspended sediment from the source terms will be released at different load locations in the model. The three different load locations have been illustrated in Figure **??** in Chapter 4. The stationary load corresponds to Load 1 in the middle of the harbour, while Load 2 represents the western dredging location and Load 3 the eastern part. Computing two different simulations provides the opportunity to compare the significance of varying the dredging location on the SSC.

A correct representation of the source distributed over the vertical will allow for a more representative simulation. The distribution over the vertical should therefore be considered as an addition to the existing methods. While the exact distribution is unknown, spreading the bucket drip equally over the depth, instead of concentrating the sediment flux at the bottom or surface, is considered to be a representative approach. Each load considered for this study is spread equally across the 5 depth layers, as sediment is lost continuously throughout the water column when lifting the bucket. In the middle of each layer, 20% of the total source term per fraction is added to account for an equal distribution. The source terms computed for the two sediment fractions at each location in Section 4.4 are used to calculate the source quantity per layer. The new source terms per layer for each fraction in each load are specified in Table 5.1.

Load	**Sediment flux 63 μm [kg/s] per layer**	**Sediment flux 30 μm [kg/s] per layer**
Stationary average	0.044	0.068
West harbour	0.044	0.068
Middle harbour	0.036	0.056
East harbour	0.056	0.082

Table 5.1: Overview of the source terms per fraction added to each depth layer in the model

The temporal and spatial distribution for the source terms was determined in Chapter 3 and 4. The exact data and time-steps appointed to the loads must be defined. The time-steps for the sediment flux are obtained from the dredging script used to calculate the full dredging cycle. It is decided to start the dredging operation 3 days after the start of the model run to take the spin-up of the hydrodynamic model into account. As discussed in Chapter 4, dredging occurs daily from 06:00 to 18:00 with a constant source. The temporal distribution for the two modelled scenarios is similar, while the source location and quantity varies. The source input starts at 02-09-2021 6:00 and ends when the dredging operation has finished, which is around 9 days later at 11-09-2021 16:00. As the dredging operation is halted at night, the source term from 18:00 to 6:00 is set at 0 kg/s. Relocation of the BHD is simulated at two moments: 05-09-2021 08:00 and 08-09-2021 12:00. Relocation takes

two hours, meaning that the sediment flux is 0 kg/s for two hours from the moment relocation starts. The scenario simulating the relocating source changes the quantity of its source after relocation has finished. The simulation for this scenario starts on the western side of the basin (Load 2) and ends on the eastern side (Load 3). In order to simulate periods with varying hydrodynamic conditions, the operation is run again starting on 14-09-2021 06:00. The relocation periods for the second run occur at 17-09-2021 08:00 and 20-09-2021 12:00.

No additional boundary conditions or initial conditions regarding the background turbidity will be specified. As the preliminary results of the turbidity sensor showed values close to 0 NTU, pointing at negligible amounts of suspended sediment in the water column before dredging commences, the initial SSC value is kept at 0 $kg/m3$.

Observation points

A number of observation points are added to the model to accurately monitor the values of the SSC in the vicinity of the dredging location. The locations are chosen to enable monitoring both near and further away from the source, covering locations close-by and all around the border of the high-impact zone to monitor if the turbidity thresholds are exceeded. Additionally, observation points are placed at all load locations to validate the source input. At these load locations, the SSC is expected to be significantly higher than further away from the source location.
For every location, two observation points are placed. One calculates the average of all the layers, while the other reports a separate value per layer. This facilitates the opportunity to monitor the total SSC value over the depth, but also visualises the difference in suspended matter in the different layers. The location of the observation points is shown in Figure 5.4.

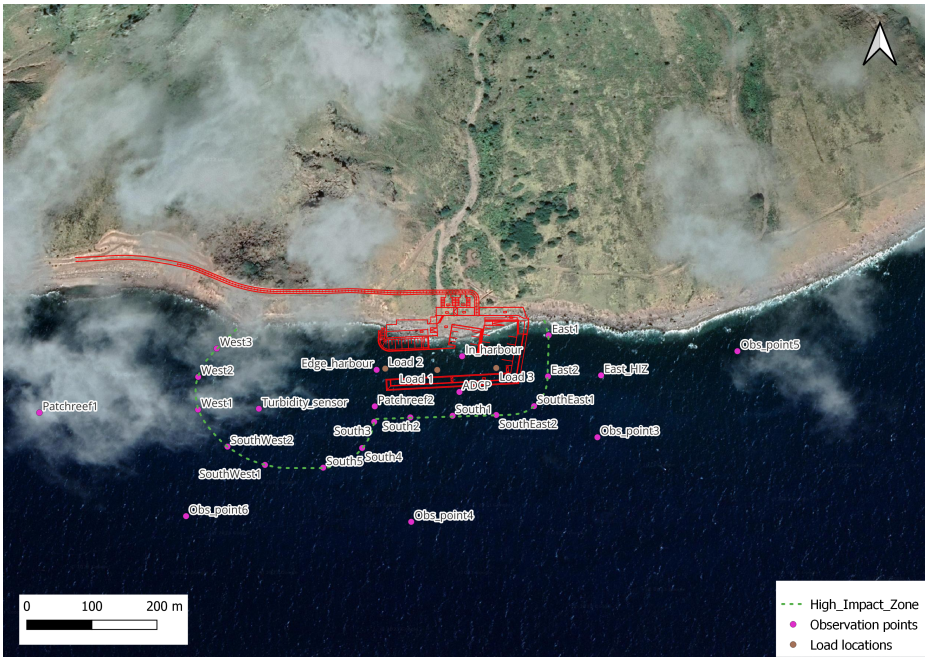

Figure 5.4: Overview of the location of all observation points added to the water quality model

6 Far-field plume model results

In this chapter, the results of the far-field sediment plume dispersion models are reported and analysed. First, the calibration and verification steps for the D-Flow model are presented. Secondly, for both scenarios run in the water quality model, the results regarding the SSC are reported at a select number of observation points over different time periods. Additionally, an overview of the area showing the dispersion direction of the sediment plumes will be given to analyse the dispersion length and the sediment concentration in the plumes further from the source. Finally, the results of both scenarios are compared, while the results concerning the turbidity thresholds are reported and discussed as well.
This chapter addresses the fifth sub-research question:

What is the potential intensity and duration of the turbidity stresses at the monitoring locations and on the environment resulting from the simulated dredging operation?

6.1 D-Flow calibration & verification

A crucial step before the results of the hydrodynamic model can be used as input for the water quality model is validation of the model. By validating the model, the reliability of the model result is improved, ensuring an accurate representation of the hydrodynamic conditions in the area. The ADCP was placed at x = -63.239796 ° W and y = 17.6135427 ° N, close to the location of the wave buoy. The modelled current velocity near the surface was compared to the measurements near the surface and near the bed of the ADCP. The location at the top of the water column was chosen to compare the influence of the wind in the model to the measured current velocity. Additionally, the model is calibrated using the water levels. Both the modelled water level and the measured data from the ADCP have a temporal distribution of 10 minutes. It is chosen to present the hourly averaged data for both datasets in the graphs. The validation of the water level can be seen in Figure 6.1, while the validation of the current velocity is illustrated in Figure 6.2. The red line shows the ADCP data and the blue line the modelled data for the current velocity and water levels.

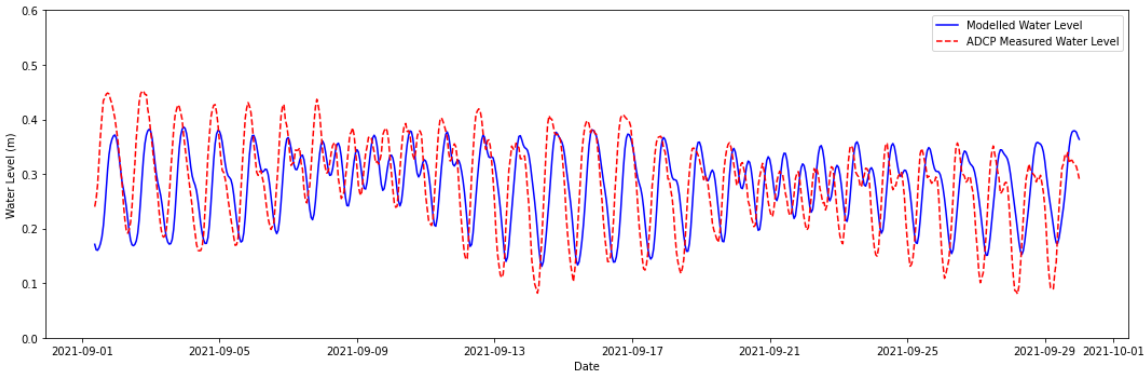

Figure 6.1: Validation of the water level comparing the hourly modelled water levels to the hourly measured ADCP data.

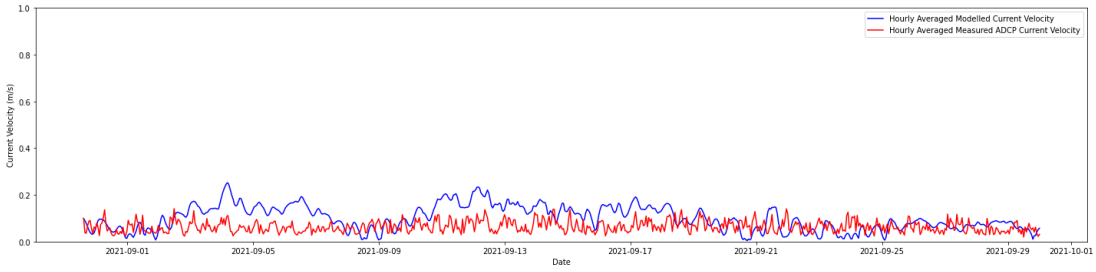

(a) Validation of the current velocity at the bed

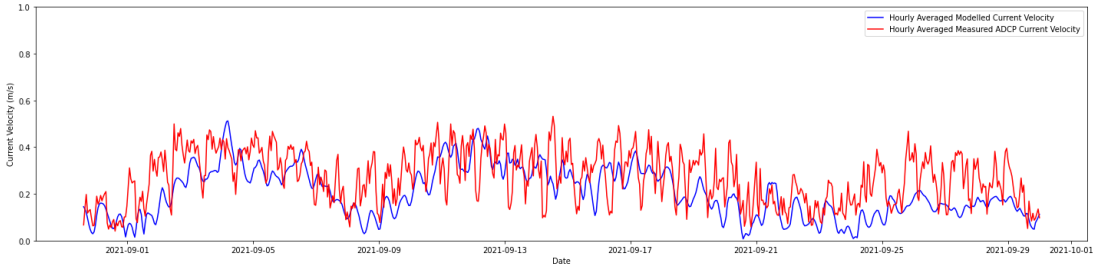

(b) Validation of the current velocity near the surface

Figure 6.2: Validation of the model results for the comparison of the hourly averaged modelled current velocity (blue) at the bottom (Figure a) and near the surface (Figure b) to the hourly averaged ADCP data (red)

The two datasets have also been compared by computing their Root Mean Square Error (RMSE). This is a measure of the difference between the values of the two datasets. A lower value for the RMSE relates to a better correlation of the two datasets.

For the comparison of the water levels the RMSE is 0.08, representing a fairly good correlation. At the start and near the end of the simulation a difference of 0.05 m can be observed in the water level. The RMSE value calculated for the current velocity near the surface is 0.12, which corresponds to an intermediate good correlation of the two datasets. The ADCP data exhibits more fluctuations, while the model data slightly underestimates the current velocity. Finally, for the current velocity at the bottom the RMSE is 0.065, representing a better fit compared to the velocities in the top layer. Overall, the model shows a good representation of the hydrodynamics in the area. As the ADCP was only placed at one location, no other points in the model can be validated as no data is available for these locations.

Additionally, the hourly averaged modelled current direction at the surface and at the bottom is compared to the hourly averaged measured current direction by the ADCP. The site visit and data collection in Chapter 2 indicate that the model results should show a main current direction towards the west, with the possibility of some current reversals. Near the seabed, the ADCP data showed the reversal of the current direction due to tidal influences. The results are illustrated in Figure 6.3.

(a) Comparison of the hourly averaged modeled current direction vs the hourly averaged measured current direction at the ADCP location near the surface

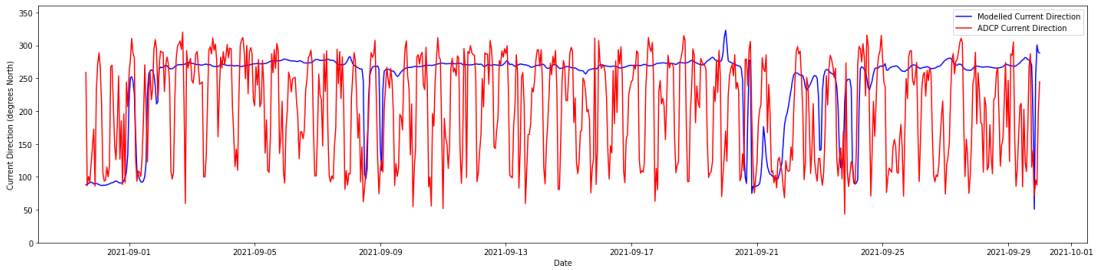

(b) Comparison of the hourly averaged modeled current direction vs the hourly averaged measured current direction at the ADCP location near the bed

Figure 6.3: Verification of the model results for the comparison of the hourly averaged modelled current direction (blue) near the surface (Figure a) and at the bed (Figure b) to the hourly averaged ADCP data (red)

The comparison of the current direction at the top layer shows a reasonably good agreement between the measured and model results. The main current direction is approximately 280 °N, while a current reversal towards the east has been successfully captured by the model as well. However, the data from the ADCP does exhibit more fluctuations over short time periods compared to the modelled current direction. From Figure 6.3b, it becomes clear that the model does not capture the tidal influence on the current direction near the seabed well. The model captures the reversal of the current direction around 09-09-2021 and during the current reversal starting on 21-09-2021, but fails to do so consistently at other times. This inconsistency in the current direction at the bed between the model and the ADCP data at other moments in time is regarded as a limitation that must be considered when interpreting the model results.

6.2 Results water quality model

Having analysed the results of the hydrodynamics model, the results of the water quality model can be discussed. Two different scenarios have been run containing a stationary and a relocating source. For both scenarios, the dredging operation is run twice to simulate the effects during normal flow conditions and during the current reversal occurring on 21-09-2021. For each scenario, the depth averaged SSC is reported first, followed by the concentration in both the top and bottom layer at each observation point to compare the difference in concentration over the depth. Finally, an overview is given on the dispersion direction and length of the plume. The results for the SSC are reported separately for the observation points located to the east and west side of the harbour, in order to provide a clear overview in the graphs. Only at a select number of monitoring stations the results are reported. The chosen observation points, illustrated in Figure 6.4, represent the most representative and significant results.

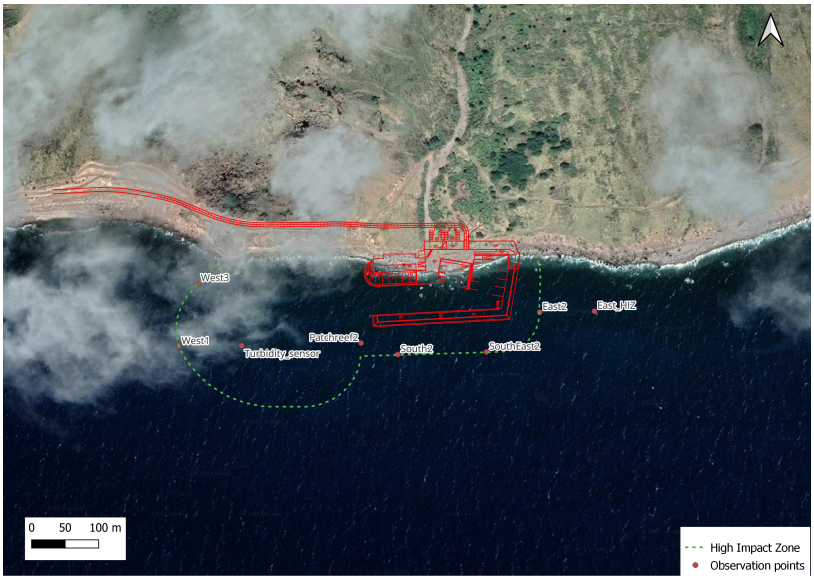

Figure 6.4: Overview of the location of the used observation points for the model results

6.2.1 Stationary source scenario

The results for the stationary source are reported and analysed first, starting with the depth averaged SSC for the western and eastern observation points illustrated in Figure 6.5. The temporal distribution of the water quality model results for the SSC is 10 minutes for each scenario which is discussed.

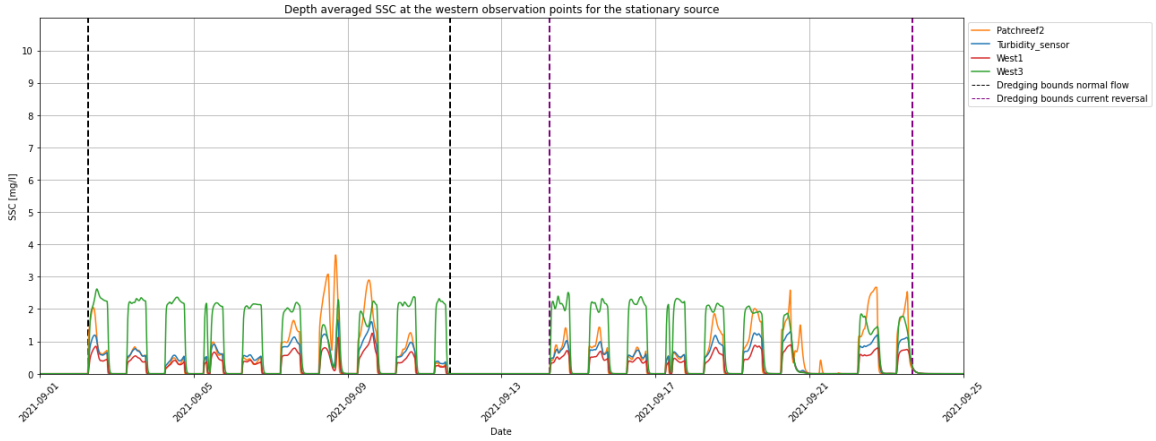

(a) Modelled depth averaged SSC for the specified observation stations west of the harbour

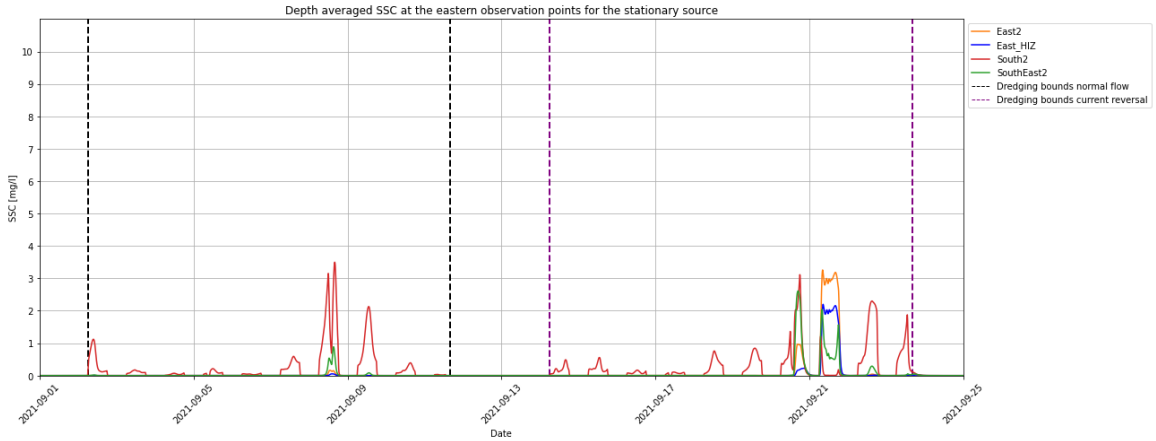

(b) Modelled depth averaged SSC for the specified observation stations east of the harbour

Figure 6.5: Modelled depth averaged SSC values at the observation points west (a) and east (b) of the harbour. The results shown are for the stationary dredging scenario in which the source term was released at one location.

The results indicate a clear difference in the SSC between the western and eastern sides of the harbour for both modelled time-frames. Higher concentrations are observed on the western side, which is expected due to the predominantly westward current direction. During the current reversal on 21-09-2021, the concentrations drop to zero at the western locations.

On average, the highest concentrations are recorded at observation point West3, situated nearshore to the west of the harbour, with an SSC of around 2.2 mg/l during dredging for the first run and around 1.6 mg/l for the run including the current reversal. This suggests that the sediment plume tends to remain nearshore while dispersing towards the west. At observation point West1, located further away from shore, reports considerably lower values compared to West3. This confirms that the plume is more concentrated nearshore, while dispersing towards the west.

At the turbidity sensor, the average concentration remains below 1 mg/l, while a peak value of 1.75 mg/l is reported. The difference in concentration between the turbidity sensor and observation point West1, located on the same latitude but 100 m apart, indicates the settling of the particles in the plume. The highest recorded concentration on the western side, 3.7 mg/l, occurs at Patchreef2 on 08-09-2021 during a period with low flow velocities and a tide-induced current reversal near the bed. This caused the suspended sediment to remain close to the source.

At the eastern observation points, lower average SSC values are observed. The highest average and peak concentrations are reported at South2, located most towards the west from these four observation points. The peak concentration of 3.5 mg/l occurs at the same moment as the peak at Patchreef2. The peaks at South2 during 22-09-2021 and 23-09-2021 can be related to two current reversals for a short time period.

During the entire first run the concentrations at East2, SouthEast2 and East-HIZ (East of the High Impact Zone) are negligible. However, during the current reversal in the second run, higher concentrations are reported, such as at SouthEast2 with a concentration peak at 2 mg/l just before and after the current reversal. The highest concentration during the reversal is reported at East2 at 3 mg/l for the entire duration of the reversal. While observation point East1, located closer to shore (see Figure 5.4), was not included, similar values are observed here as for East2. At East-HIZ, 80 metres to the east, the concentration has dropped to 2 mg/l, suggesting a similar behaviour of the plume remaining close to shore as for the dominant westward current.

The impact of halting the dredging operation at night can be observed at all observation points, with concentrations dropping to 0 mg/l during this period. Downtime due to relocation of the backhoe indicates a positive effect in reducing the SSC, which is especially visible at Patchreef2 and South2 on 08-09-2021, as the peak concentrations drop due to the short period in which no sediment flux is present. To put the concentrations at the observation points, located at some distance from the source, into perspective, the results of the depth averaged SSC at the load location is provided in Appendix E.1.

Now the concentrations in the top and bottom layers are analysed and compared. First the results at the western observation points illustrated in Figure 6.6 are discussed.

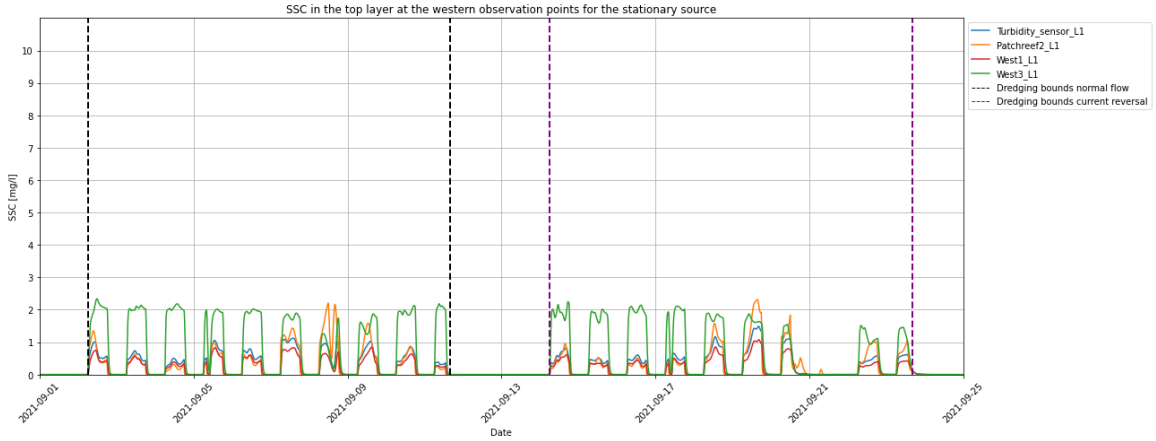

(a) SSC at the top layer for the specified observation stations west of the harbour

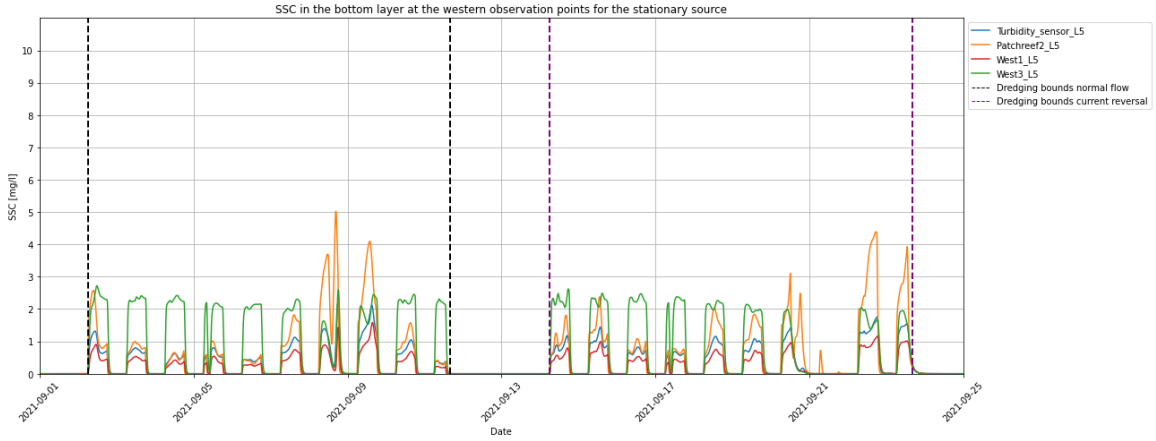

(b) SSC at the bottom layer for the specified observation stations west of the harbour

Figure 6.6: Modelled SSC at the top (a) and bottom (b) layer at the western observation points. The results shown are for the stationary dredging scenario in which the source term was released at one location.

In both the surface and bottom layer similar patterns are observed as for the depth-averaged results. Overall, concentrations are higher in the bottom layer compared to the top layer, but the difference is generally limited to 0.5 mg/l. The difference between the upper and bottom layer is expected, as sediment is released equally across the depth at the source. Further from the source, the concentration in the top layers will generally be lower, as larger particles will have already settled.

Clear differences are visible when observing the current reversal at the bed on 08-09-2021. At Patchreef2, concentrations near the bed are twice as high as those near the surface at this moment. From Figure 6.3 it becomes clear that the disparity in SSC is due to the reversal being only present near the bed. Similar situations occur on 09-09-2021 and at the end of the second run for the dredging operation. As discussed in the analysis of the results for the hydrodynamics, the model fails to capture the current reversal at the bed induced by the tide consistently. Taking into account the measurements of the ADCP, it is expected that the higher peak concentrations near the bed will not only occur at the instances mentioned previously, but consistently during the dredging operation. As Patchreef2 is located closest to Load2, which is the source for the stationary scenario, the

most significant differences are observed at this observation point. On 21-09-2021, when the current reverses over the entire depth, no significant differences are reported.

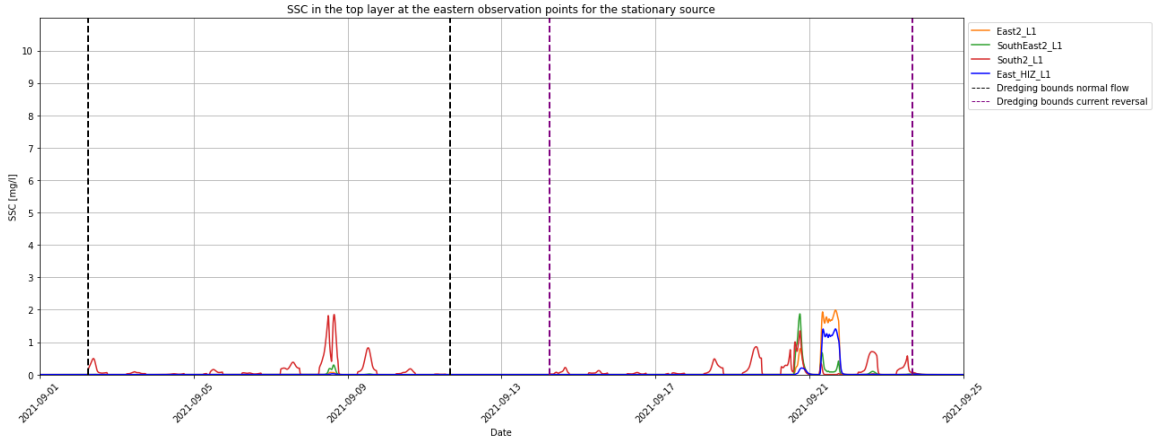

(a) SSC at the top layer for the specified observation stations east of the harbour

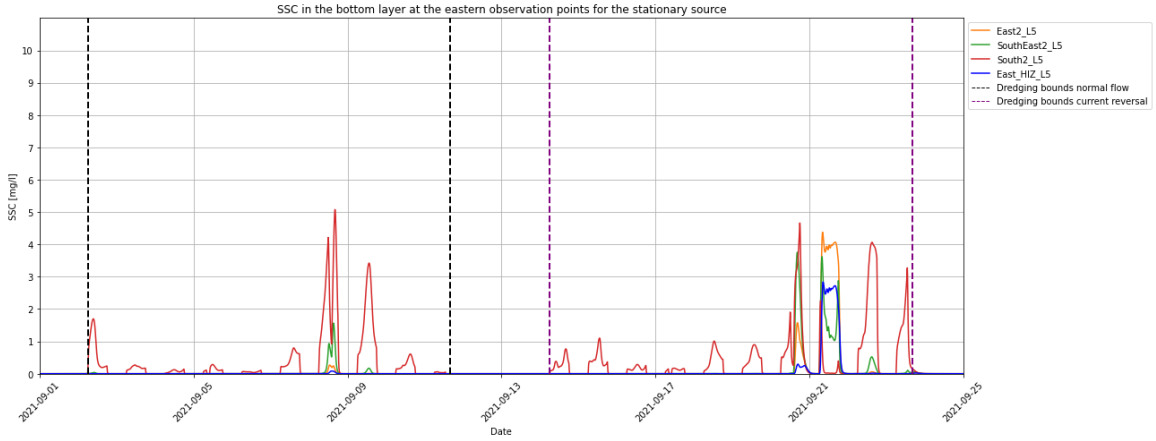

(b) SSC at the bottom layer for the specified observation stations east of the harbour

Figure 6.7: Modelled SSC at the top (a) and bottom (b) layer at the eastern observation points. The results shown are for the stationary dredging scenario in which the source term was released at one location.

At the eastern observation points, the difference in concentration between the surface and the bed is generally low during normal flow conditions, as the concentrations are already negligible at these moments. However, during periods when the current reversal is only present at the bed, similar patterns as for Patchreef2 are observed at South2 and to a lesser extent at SouthEast2. Near South2, concentrations at the bed are two to three times higher than near the surface. This larger concentration difference, compared to Patchreef2, can be linked to the closer proximity of observation point South2 to the source location. At the moment of the main current reversal, concentrations at the bed are observed to be twice as high compared to the surface for observation points SouthEast2, East2 and East-HIZ.

Before providing an overview of the dispersal direction and length of the plumes in the project area, the locations in which an hourly averaged concentration of 10 mg/l or higher was reported are presented first. The turbidity thresholds, as outlined in Section 2.5, indicate that an average concentration of 10 mg/l per hour cannot be exceeded, as exceeding this threshold could have a high impact on sensitive receptors in the area. Figure 6.8 illustrates the locations at which an hourly average SSC value of 10 mg/l or higher was reported over the entire modelled time-frame. It can be seen that the high concentrations are confined within the high-impact zone and are concentrated around the load location. Figures illustrating the locations at which the daily and weekly thresholds are exceeded for the stationary source are reported in Appendix E.1. This overview helps to put the concentrations, which will be reported in the plume figures, in perspective.

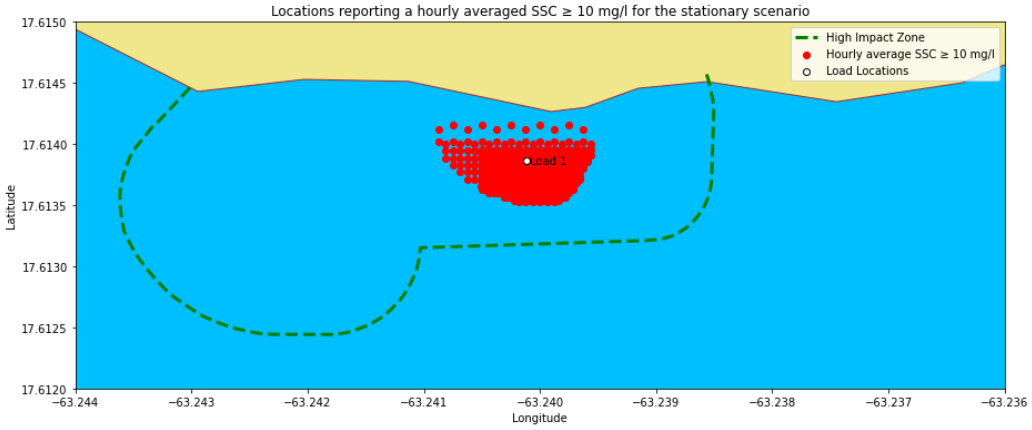

Figure 6.8: Overview of the locations in the project where an average hourly SSC of 10 mg/l or higher was reported during the simulations for the stationary source

The concentration of the sediment plumes further from the harbour is observed by means of a spatial scatter plot. Figure 6.9 shows the dispersion of the plume over time for the source term generated at a single location. Figure 6.9a on the top-left shows the SSC moments after halting the dredging operation. The other figures are all snapshots 1 hour apart after the dredging operation was halted for the day.

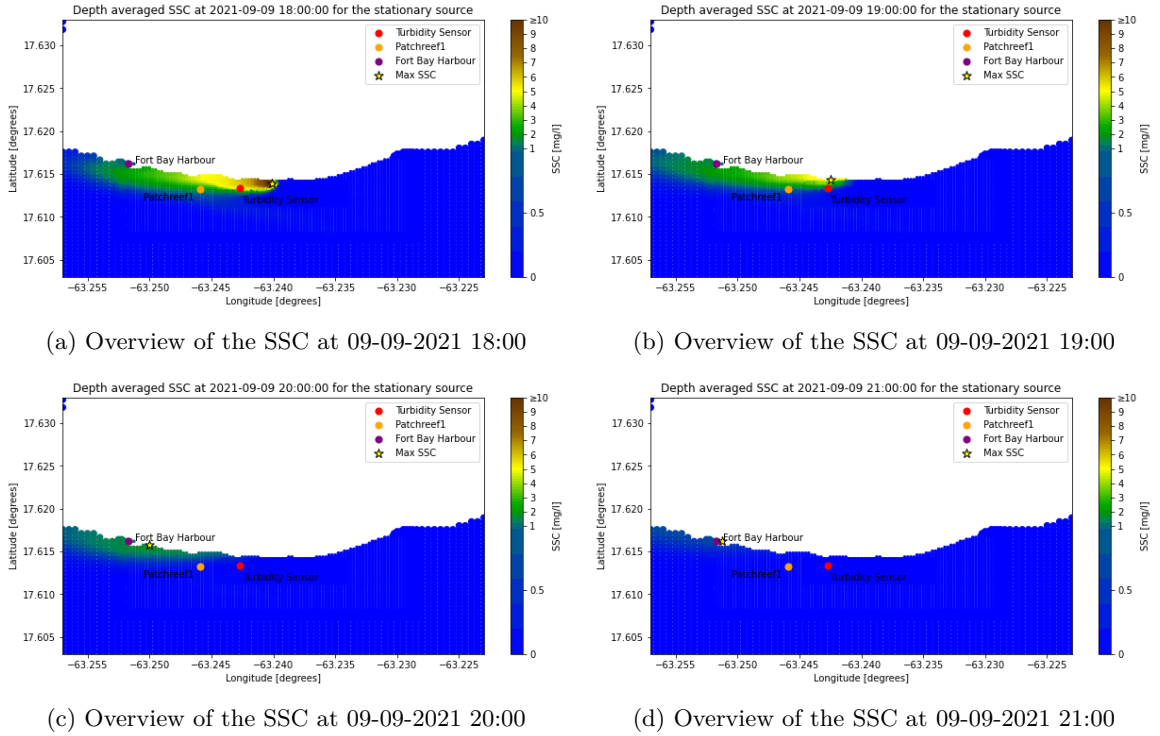

(a) Overview of the SSC at 09-09-2021 18:00

(b) Overview of the SSC at 09-09-2021 19:00

(c) Overview of the SSC at 09-09-2021 20:00

(d) Overview of the SSC at 09-09-2021 21:00

Figure 6.9: Figure indicating the dispersion of the sediment plumes after halting the stationary dredging operation at 09-09-2021 during normal flow conditions

The dispersion of the sediment plume, as illustrated in Figure 6.9, captures a snapshot taken at the end of the dredging operation on 09-09-2021, during normal flow conditions. The results are representative of the situation directly after the dredging operation is halted at 18:00 each day when no current reversal occurs. Important to note is that the figures only serve as a visual aid to indicate the dispersion pattern of the plume and provide a quantitative understanding of the approximate SSC. Due to the increased size of some data points for improved visibility, no values should be extracted directly from these figures.

The highest concentrations are reported near the source, while the plume disperses towards the west, remaining close to the shore. This aligns with the interpretation of the results presented in Figure 6.5. Appendix E.3 contains velocity vector plots of the area during at 09-09-2021, indicating the flow directions in the area. The locations of the turbidity sensor, patchreef1 and Fort Bay harbour have been added as a visual reference. The maximum concentration reported one hour after halting the dredging operation is 1.2 mg/l, located in the high impact zone. At 20:00 the maximum concentration has dropped to 0.35 mg/l and is reported in between the project area and Fort Bay. The SSC at Fort Bay consistently remains below 0.6 mg/l. Past Fort Bay, the concentration of the plume rapidly decreases. At the patch reef, the reported concentrations are below 0.7 mg/l, indicating a lower impact compared to Fort Bay. As the plume is concentrated nearshore, the plume does not reach the area in which the patch reef is located. The results further suggest that three hours after halting the dredging operation, reported concentrations are consistently below 0.2 mg/l at all locations.

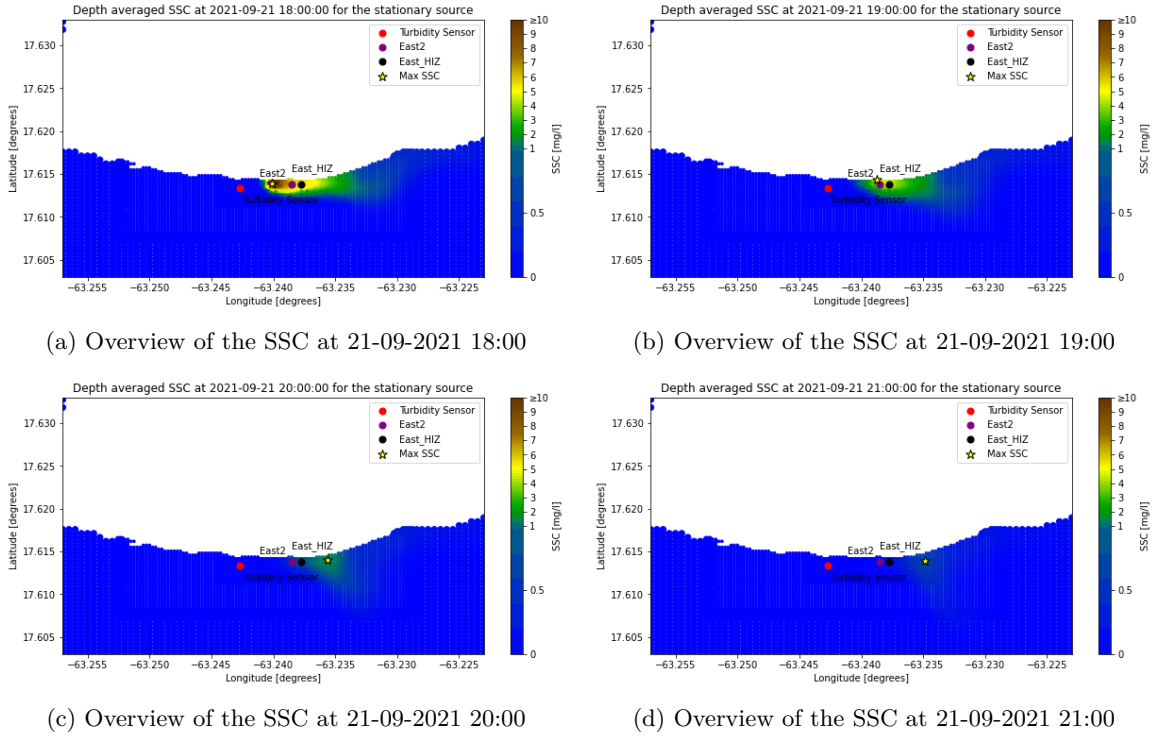

(a) Overview of the SSC at 21-09-2021 18:00

(b) Overview of the SSC at 21-09-2021 19:00

(c) Overview of the SSC at 21-09-2021 20:00

(d) Overview of the SSC at 21-09-2021 21:00

Figure 6.10: Schematization of the dispersion of the sediment plumes after halting the stationary dredging operation on 21-09-2021

Figure 6.10 illustrates the behaviour of the plume moments after halting the dredging operation on 21-09-2021. As discussed, a current reversal occurs at this moment, causing the plume to flow eastwards. The situation is similar to the westward plume as the highest concentrations are still reported near the source, while the plume remains relatively close to the shore. The plume does not stretch as far east as is the case for the westward location. The southwards direction of the plume at 21-09-2021 20:00 is caused by an ocean swirl, South-East of the Black Rocks harbour at this moment. Appendix E.3 contains velocity vector plots of the area during the current reversal, indicating the flow directions in the area.

At the start the SSC at observation point East-HIZ is 1.6 mg/l, while one hour after halting the dredging operation, the concentration at East-HIZ has dropped to 0.85 mg/l. The maximum reported concentration one hour after dredging has stopped is 1 mg/l. Two hours after dredging, the plume has dispersed further east and has a maximum concentration of 0.3 mg/l. At 21:00 the concentration is below 0.15 mg/l across the entire domain.

6.2.2 Relocating source scenario

For the model including a relocating source, the results are presented and analysed in a similar way as for the stationary source. The results for the depth averaged SSC are reported in Figure 6.11. The graphs illustrating the concentrations at the load locations can be found in Appendix E.2.

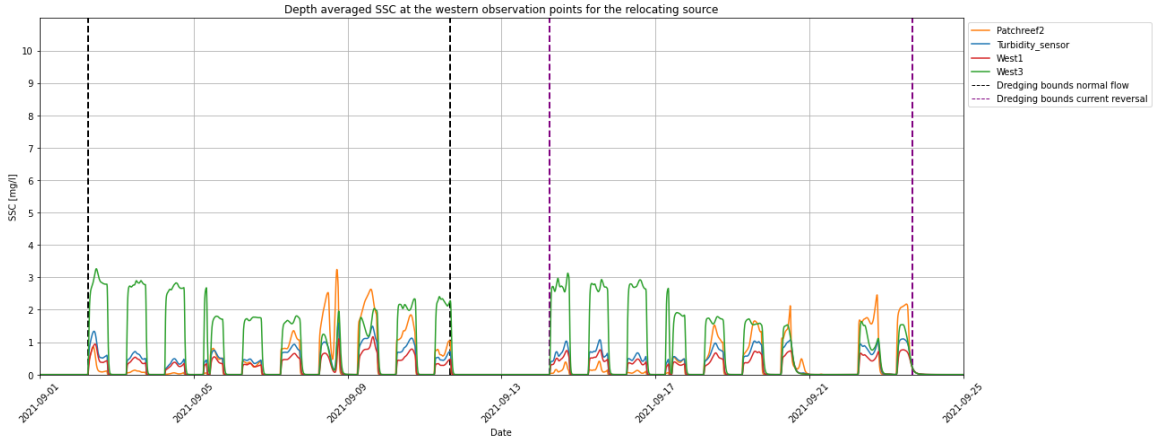

(a) Modelled depth averaged SSC for the specified observation stations west of the harbour

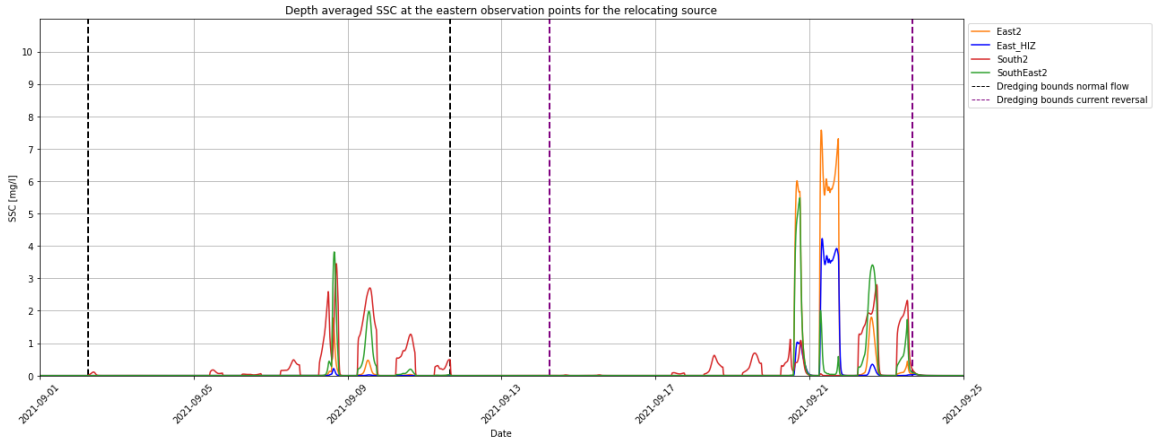

(b) Modelled depth averaged SSC for the specified observation stations east of the harbour

Figure 6.11: Modelled depth averaged SSC values at the observation points west (a) and east (b) of the harbour. The results shown are for the dredging scenario in which the source term was released at three separate location.

The results visualise the impact of different source term quantities and release locations. Similar to the stationary source, a clear difference between the eastern and western observation points is observed. The highest average concentrations are again found on the western side of the harbour. At observation point West3, similar average values of around 2.2 mg/l and 1.6 mg/l have been reported for respectively the first and second run. The distribution over time varies, as dredging started at the most western load location, indicating a higher concentration at West3 during this stage due to its proximity. At observation point West1, no significant differences have been reported compared to the stationary source. At the turbidity sensor, similar values are observed. The peak concentration reaches 1.5 mg/l, while the average value at this location remains below 1 mg/l. At Patchreef2, lower concentrations are reported during the first two phases of the dredging operation. Only when dredging at the location of Load 3 occurs during the current reversal at the bed, the concentration increases.

At the eastern observation points, differences in the concentration at SouthEast2 can be observed during the current reversal in the first run. The peak concentrations for the first simulation are reported both at SouthEast2 and South2 with a concentration of around 3.5 mg/l. At observation point SouthEast2, the concentration doubles compared to the previous scenario, while the concentrations at South2 are consistently higher at the end of the first run due to the higher source term. Concentrations at East2 and East-HIZ are negligible for the first run.
For the current reversal, similar patterns are observed as for the stationary scenario in general. However, the peak concentrations are twice as high for the relocating scenario, caused by the high source term on the eastern location at this moment. At East2 the peak concentration reaches 7.5 mg/l, while during dredging the average concentration is 6 mg/l during this period. Due to the closer proximity of the source to the eastern observation points and the higher source term, increased peak concentrations at East2 and SouthEast2 are observed just before and after the main current reversal period. Concentrations at each eastern observation point are negligible before dredging at the eastern load has started.

Now the concentrations in the top and bottom layers are analysed and compared for the relocating scenario. First the results at the western observation points illustrated in Figure 6.12 are discussed.

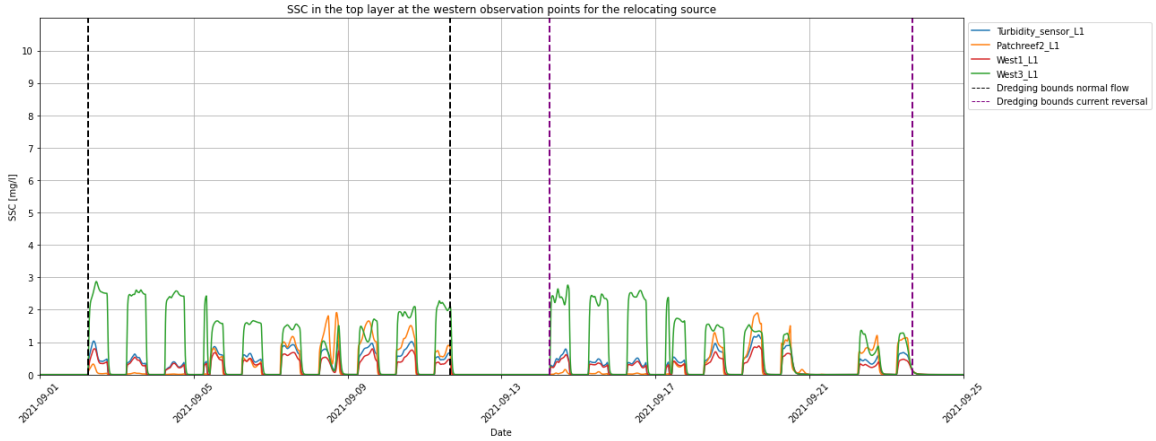

(a) SSC at the top layer for the specified observation stations west of the harbour

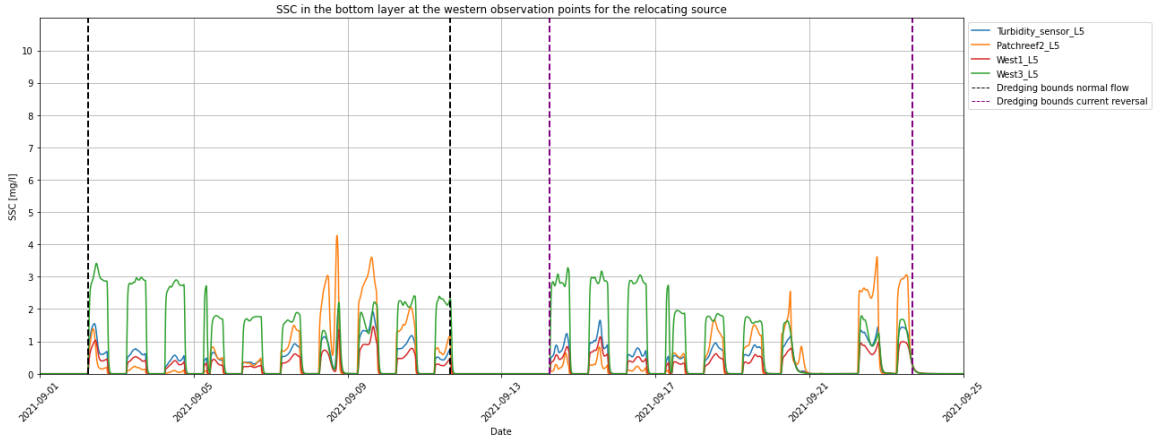

(b) SSC at the bottom layer for the specified observation stations west of the harbour

Figure 6.12: Modelled SSC at the top (a) and bottom (b) layer at the western observation points. The results shown are for the relocating dredging scenario in which a varying source term was released at three different locations.

The results again indicate similar patterns in both layers as for the depth-averaged SSC. Higher concentrations are observed in the bottom layer compared to the top layer, indicating a difference of approximately 0.5 mg/l. More significant differences between the top and bottom layers can be observed at observation point Patchreef2. On 09-09-2021 and at the end of the second simulation, peak concentrations are twice as high in the bottom layers as in the surface layer. At the other observation points, no significant disparities between the two layers can be noticed.

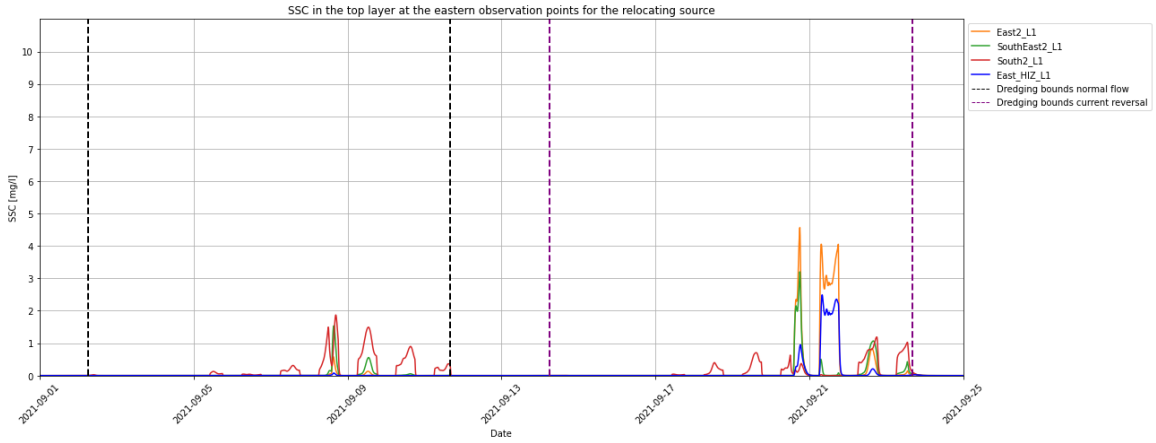

(a) SSC at the top layer for the specified observation stations east of the harbour

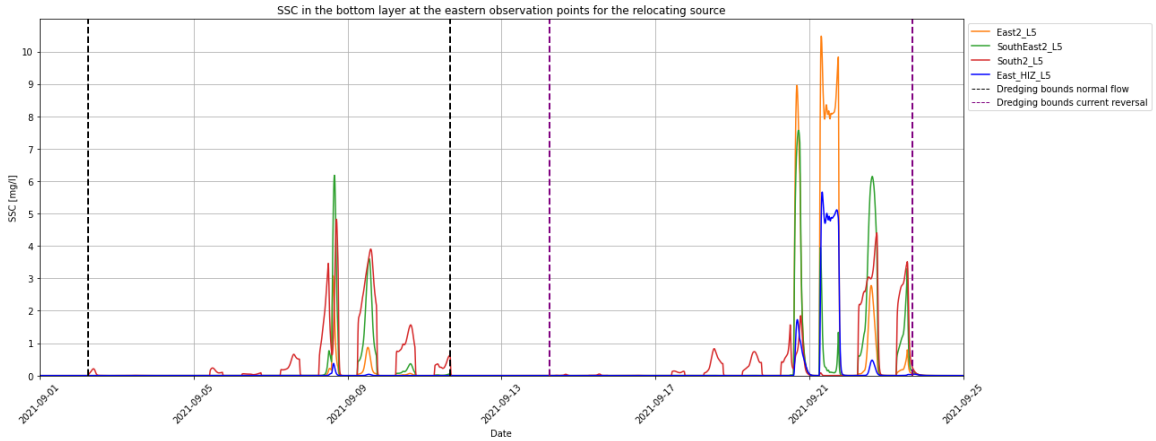

(b) SSC at the bottom layer for the specified observation stations east of the harbour

Figure 6.13: Modelled SSC at the top (a) and bottom (b) layer at the eastern observation points. The results shown are for the relocating dredging scenario in which a varying source term was released at three different locations.

For the relocating scenario, more significant differences have been observed at the eastern observation points due to a combination of the relocating source and changing quantity. As observed for the depth-averaged SSC, the concentration at SouthEast2 is significantly higher compared to the stationary source. In the first simulation, the concentration at the bed is more than three times higher than the concentration at the surface for observation SouthEast2. At South2, the SSC near the bed is twice as high as at the surface layer.
During the main current reversal in the second simulation, the concentrations reported at East2 reach a peak concentration at the bed of 10 mg/l and an average SSC of 8 mg/l, while at East-HIZ this is 5 mg/l. At both observation points, the SSC in the bottom layer is 2.5 times higher than the surface layer. At the shorter time intervals containing a current reversal, the concentrations at South2, SouthEast2 and East2 are even three times higher at the bed. The high concentrations at

these locations can be directly linked to the proximity of the third load location on the eastern side of the harbour. As the sediment particles released in the lower layers likely not have settled when they reach the observation points, the observed concentration differences are higher than when the source is present at other locations.

An overview of the locations where the hourly averaged SSC exceeded 10 mg/l during the relocating source scenario is given in Figure 6.14. As the source quantity and location changed throughout the dredging operation, a wider affected area in the basin can be observed. Due to the higher quantity of the eastern source and its closer proximity to the edge of the high impact zone, a larger number of locations at which the threshold is exceeded can be noticed. Nevertheless, no exceedance of the thresholds is observed at the edge or outside the high impact zone for the average hourly values. Figures illustrating the locations at which the daily and weekly thresholds are exceeded for the relocating source are reported in Appendix E.2.

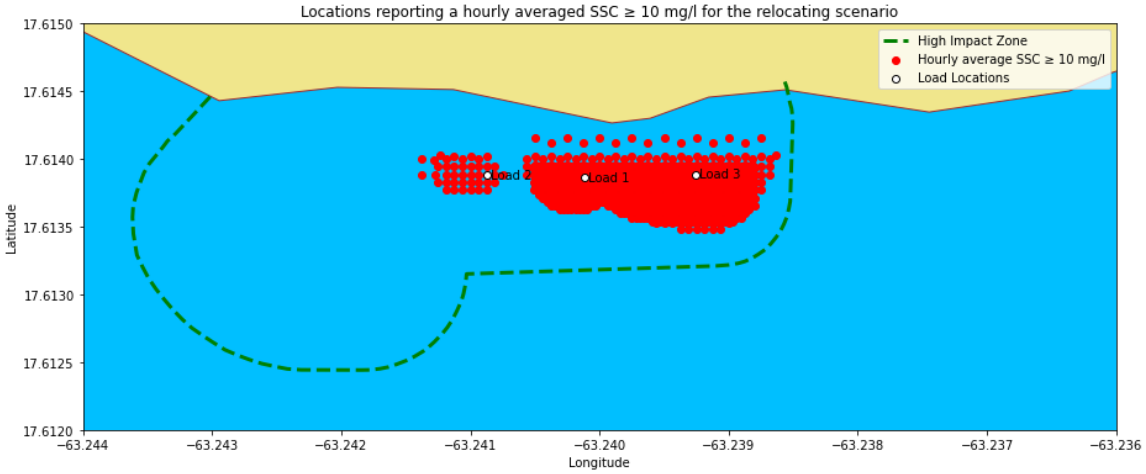

Figure 6.14: Overview of the locations in the project where an hourly average SSC of 10 mg/l or higher was reported for the relocating source

Figure 6.15 illustrates the dispersion of the plume over time for the source term at the location of Load 3 on the eastern side of the harbour. The timestamps align with those of the stationary source during the first run, showing snapshots taken one hour apart after the dredging operation was halted for the day.

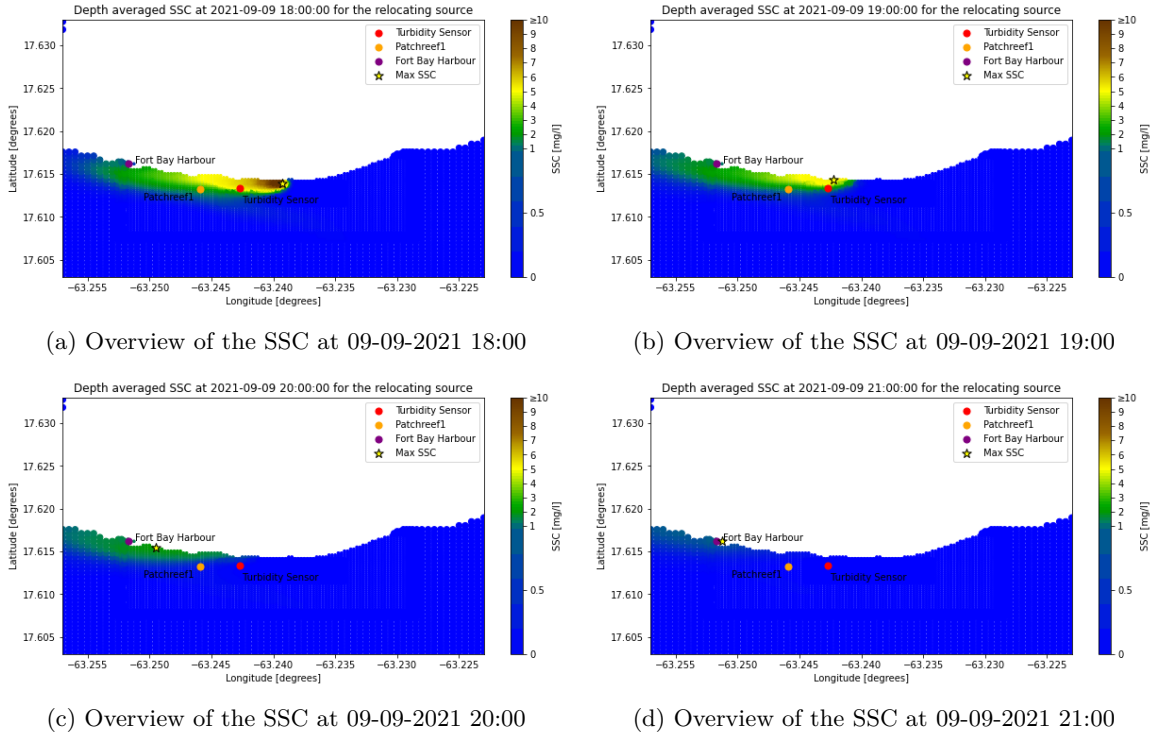

(a) Overview of the SSC at 09-09-2021 18:00

(b) Overview of the SSC at 09-09-2021 19:00

(c) Overview of the SSC at 09-09-2021 20:00

(d) Overview of the SSC at 09-09-2021 21:00

Figure 6.15: Schematization of the dispersion of the sediment plumes after halting the relocating dredging operation on 09-09-2021

The dispersion of the sediment plume for the source term at location Load 3, on the east side of the basin, shows a similar pattern compared to the stationary source. The figures again only serve as a visual aid to indicate the dispersion pattern of the plume.

The highest concentrations are reported near the source, which is situated further east for the relocating scenario at this moment. While exhibiting a similar pattern, the initial concentration nearshore at the project location is higher than during the stationary source. The elevated SSC is caused by the increased source term value. One hour after dredging has stopped, the maximum concentration is found in the harbour at 1.5 mg/l, the same concentration as reported for the stationary scenario at this time-step. At 20:00 the maximum reported concentration is again 0.4 mg/l, while at 21:00, the maximum concentration is 0.2 mg/l.

The concentration of the plume further from the source is similar to the stationary source. At Fort Bay, the concentration does not exceed 0.6 mg/l, while the concentration at the patch reef remains consistently below 0.6 mg/l. In this scenario, the sediment flux at the load location is slightly higher, however, the shift of the source location towards the east seems to counteract these factors, resulting in a similar sediment concentration. Consequently, no issues regarding the suspended sediment concentration at the patch reef and near the existing Fort Bay harbour are expected in this scenario.

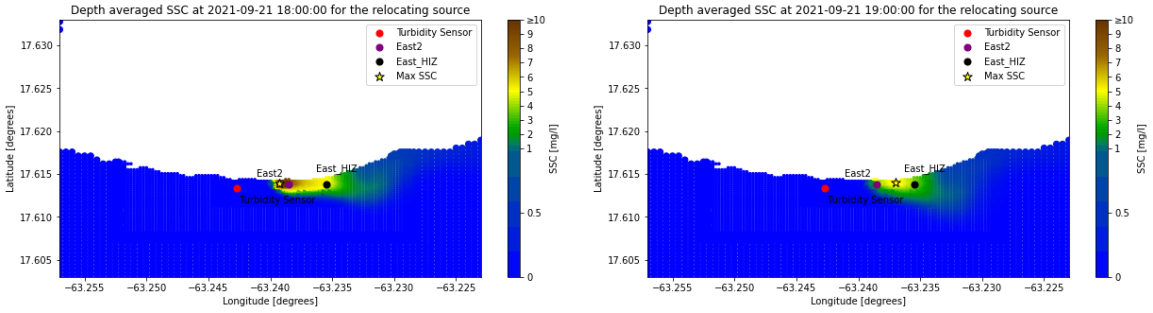

(a) Overview of the SSC at 21-09-2021 18:00

(b) Overview of the SSC at 21-09-2021 19:00

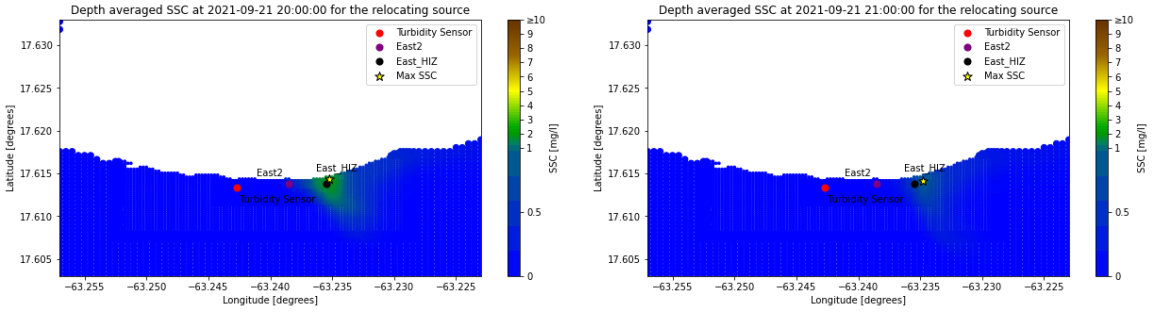

(c) Overview of the SSC at 21-09-2021 20:00

(d) Overview of the SSC at 21-09-2021 21:00

Figure 6.16: Schematization of the dispersion of the sediment plumes after halting the dredging operation for the relocating scenario on 21-09-2021

Figure 6.16 presents the results for the plume behaviour moments after dredging has stopped on 21-09-2021 for the relocating scenario. A similar pattern is observed as for the stationary scenario during the current reversal. The source is present at the eastern load location at this moment, resulting in an SSC of 3.7 mg/l initially at observation point East-HIZ. One hour after dredging has stopped, the concentration at East-HIZ has dropped to 0.87 mg/l, while the maximum reported concentration is 1 mg/l. Two hours after dredging the maximum concentration is 0.35 mg/l, while at 21:00, this is 0.17 mg/l. While the source location and quantity differ compared to the stationary source, causing a higher initial concentration at East-HIZ, similar results are observed in the hours after dredging is halted.

6.3 Comparison of the model results

The following sections will compare the model results, focusing on the effects of the different scenarios, such as the source quantity and location. An analysis is conducted to identify the likely cause(s) of the difference in SSC reported at the different observation points, aiming to obtain insight which scenario provides the most suitable approach in simulating the dredging operation for a BHD. Subsequently, the results of the two models created for this report are analysed based on the turbidity thresholds given in Section 2.5.

6.3.1 Analysis of stationary and relocating source models

In order to link the disparities in results to the difference in model approach, an overview outlining the distinctive aspects between the models is required. Both scenarios share the same processes based on hydrodynamics, water quality processes and temporal distribution of the source terms. The difference in the models is created by changing the quantity and spatial distribution of the source term throughout the harbour. Both of these aspects can affect the concentration in the far-field. The depth-averaged SSC, concentration across different depth layers and plume dispersion results are compared to correlate the differences in results to the variance in source term over the models.

First, the depth-averaged results are compared. The results showed no significant difference in the average SSC values between both simulations for the western observation points. In the vicinity of the turbidity sensor, the average concentration was approximately 1 mg/l for both scenarios, while at West3, on average similar values are reported as well. The plume dispersion displayed similar behaviour as both plumes moved towards the west during the first simulation while remaining close to the shore.

Due to the relocating source, the temporal distribution of the peak concentrations differs for the observation points. The peak concentrations vary for both scenarios as the relocating model does not maintain an equal source quantity at each location. The reported concentration at observation point West3 was 0.7 mg/l higher for the relocating scenario compared to the stationary source term at the start of both runs. This discrepancy aligns with the expectations, considering the closer proximity of the load location to the observation point during that particular moment. As the backhoe relocates throughout the basin during the operation, modelling this aspect of the dredging operation provides a more representative insight in the SSC over time. The higher peak concentrations at Patchreef2 and SouthEast2 for the first simulation are related to this difference between the models.

When comparing the results at the eastern observation points for the second simulation, during which a current reversal occurs, larger differences in the peak concentration are observed. The significantly higher peak concentrations at East2, SouthEast2 and East-HIZ for the relocating source during the reversal can be attributed to the closer proximity and higher quantity of the source to these observation points. This indicates that in order to accurately capture the concentrations over a short time interval, such as during the current reversal, a representative depiction of the source location and quantity is important.

For both scenarios, higher concentrations are observed near the bed compared to the surface layer. This difference is more pronounced during the tidal-induced current reversal periods. These occur on 09-09-2021 and just before and after the main current reversal. As the current direction at the bed shifts eastward, while remaining westward at the surface, higher concentration are reported at the bed. Sediment particles not only settle for a longer period of time at the same location during the start of the reversal period, but particles in the surface layers that have dispersed past the observation point are pulled back towards the observation point, while settling towards the bed, increasing the SSC near the seabed.
Higher peak concentrations are reported for the relocating source, again linked to differences in source location and quantity. This effect is clearly visible in the reported concentrations at East2 and East-HIZ during the main current reversal.

The comparison of the plume dispersion figures indicate that no difference is observed in both modelling approaches when comparing the settling time after dredging is halted. This result was expected, as no variation in fraction size or settling velocity was utilized.

Given that the scenario with an alternating source term is considered to be more representative, this approach is preferred for modelling the variation in concentration over time. The importance of modelling the spatial variation of the source becomes clear when comparing the dispersion of the plumes during current reversals. This suggests that while a stationary source may not pose problems regarding exceedance of turbidity thresholds, this can change for a moving source when considering peak concentrations at different locations.

From the analysis on the differences in results for the two models, it can be concluded that using a stationary source offers a reasonably accurate representation of the average SSC during dredging. However, for a more detailed overview on the peak concentrations at various observation points over time, applying a spatially varying source yields a more representative depiction of the peak concentrations. The use of a relocating source becomes important when the need to monitor specific coral patches located around the project area arises. If in this case study an important colony of corals is situated just outside the high-impact zone on the eastern side, the use of a stationary source would have resulted in a significantly lower intensity compared to the relocating source. It is worth to note that the scenario including an alternating source term requires a more comprehensive analysis of the area, particularly in terms of the difference in fines content.

6.3.2 Assessment of turbidity thresholds

Finally, an assessment on the turbidity thresholds is made for both situations and scenarios modelled. This offers valuable insight into the potential impact of the dredging operation on the water quality in the project area. When interpreting the results, the uncertainties and simplifications in the methods and data used in this study must be taken into account, as these factors may affect the accuracy of the results. The uncertainties in the methods used are further elaborated upon in Chapter 7.

The depth-averaged SSC's are reported for the most representative observation points located on the edge of the high impact zone, including the turbidity sensor. While the turbidity thresholds are originally designated for the turbidity sensor location, it was decided to observe the thresholds at the other locations around the high-impact zone as well, since the highest concentrations were not found at the location of the turbidity sensor. To provide a comprehensive overview of the locations around the high impact zone where the thresholds are exceeded or not, the decision was made to incorporate these other observation points as well.

The values for the turbidity thresholds are averaged over the entire duration of the dredging operation, from the moment dredging starts until dredging is completed. The thresholds established for this project are repeated below:

- The average hourly value per day cannot exceed a value of 10 NTU
- The average value per day cannot exceed a value of 3 NTU
- The average value per week cannot exceed a value of 2 NTU

It was decided that a 1 to 1 ratio for the conversion from NTU to mg/l was used. The depth-averaged concentrations for the averages during the first simulation run from 02-09-2021 to 11-09-2021 are reported in Table 6.1. The reported values are the maximum reported averages throughout the operation.

Scenario	Location	Max hourly average value [mg/l]	Max average per day [mg/l]	Max average per week [mg/l]	Maximum SSC per timestep [mg/l]
Stationary	Turbidity sensor	1.57	0.58	0.43	1.66
	West3	2.58	1.5	1.12	2.62
	South2	3.23	0.91	0.38	3.5
	SouthEast2	0.84	0.13	0.03	0.89
Relocating	Turbidity sensor	1.48	0.58	0.43	1.59
	West3	3.25	1.9	1.23	3.26
	South2	3.15	0.97	0.53	3.45
	SouthEast2	3.58	0.45	0.2	3.8

Table 6.1: Analysis on the SSC averages reported at the various observation points for the first simulation from 02-09-2021 to 11-09-2021

The results obtained from both the stationary and relocating scenario indicate no exceedance of any of the three thresholds at the observation points for the first simulation. Throughout the entire duration of the operation the concentrations remain within the established limits, even for the maximum reported SSC values. The highest average hourly value per day for the stationary source is 3.23 mg/l at location South2, while for the relocating source 3.58 mg/l is reported at SouthEast2. The maximum concentrations were reported at these observation points as well. The highest average values per day and per week are reported at location West3 for both scenarios. This confirms the conclusion drawn between the two different scenarios, as the peak concentrations are reported at different locations, while the average concentrations over a longer time period show better agreement. At the turbidity sensor, the highest average hourly values were reported at 1.57 and 1.48 mg/l for the stationary and relocating source respectively. The average daily and weekly values are identical at 0.58 and 0.43 mg/l.

The results for the second simulation running from 14-09-2021 to 23-09-2021, which includes the main current reversal, are reported in Table 6.2.

Scenario	Location	Max hourly average value [mg/l]	Max average per day [mg/l]	Max average per week [mg/l]	Maximum SSC per timestep [mg/l]
Stationary	Turbidity sensor	1.26	0.51	0.39	1.30
	West3	2.47	1.48	1.00	2.51
	South2	2.67	0.70	0.41	3.11
	SouthEast2	2.54	0.46	0.20	2.61
	East2	3.16	1.46	0.58	3.26
Relocating	Turbidity sensor	1.10	0.49	0.33	1.10
	West3	3.09	1.85	1.05	3.13
	South2	2.68	0.97	0.58	2.80
	SouthEast2	5.31	0.95	0.50	5.5
	East2	7.39	3.13	1.38	7.57

Table 6.2: Analysis on the SSC averages reported at the various observation points for the simulation, including a current reversal, from 14-09-2021 to 23-09-2021

For the assessment of the turbidity threshold during the second simulation, the concentrations at observation point East2 have been included, as for this run, the concentrations were not negligible anymore. For the stationary source, no thresholds are exceeded at any of the observation points. For the relocating source, only the daily average at observation point East2 is exceeded, as a value of 3.13 mg/l is reported, while the maximum allowed SSC per day is set at 3 mg/l. The highest daily

average at East2 was reported during the main current reversal on 21-09-2021. The hourly average concentrations during the relocating scenario are twice as high at East2 and SouthEast2 compared to the stationary source, but the thresholds are not exceeded. For the daily and weekly averages, a large difference between the concentrations reported at, mainly, East2 and SouthEast2 for the stationary and relocating source is observed. The reported average SSC for the relocating source is double the concentrations of the stationary source. This indicates that, especially for special events as a current reversal, a suitable representation of the source location and quantity is important. This problem was not observed for the first simulation, as most observation points were located much further from the source locations compared to the proximity of the eastern load to East2 and SouthEast2.

The effects of the turbidity stresses on the corals can be assessed if the thresholds for turbidity and the results are related to the intensity-duration relation by Erftemeijer et al. (2012) in Figure 2.25. While the figure does not indicate numerical values for the intensity of the stress event, an estimate can be made on the impact of the thresholds. It is assumed that the weekly average threshold of 2 NTU is related to very low to low impact, the daily average of 3 NTU to low impact and the hourly average of 10 NTU to moderate to high impact. If the thresholds are not exceeded, no harmfull effects on the coral is expected. As the threshold was only slightly exceeded on the eastern side during the current reversal, the effect on the coral at this location is expected to be in the region between no effect and sub-lethal effects. For all other locations, no exceedance was reported and therefore no effect on the coral colonies is expected.

A number of factors regarding the modelling choices and hydrodynamic conditions during the dredging operation might have influenced the results. The verification step for the hydrodynamics model, discussed in Section 6.1, indicated that tidal-induced current reversals at the bed are not consistently represented by the model. As the highest hourly and daily concentrations in the first run are reported at each observation point, except for West3, on 08-09-2021 and 09-09-2021, it becomes clear that these tidal-induced current reversals are significant factors in the results. As the highest hourly and daily averages are observed during one of these moments, no exceedance of the thresholds is expected if the current reversals were continuously simulated in the model throughout the dredging operation. Even if the reported daily concentrations were to occur on each day throughout the dredging operation, resulting in similar weekly averages as for the daily averages, the concentration at every observation point (except East2) remains below the threshold of 2 mg/l. Therefore, during normal flow conditions no problems regarding exceedance of the turbidity thresholds are expected, not accounting for the uncertainties in the methods and limitations of the model. If the situation arises where a current reversal over the whole depth occurs during dredging, the location of the BHD becomes important. The modelled scenario for the relocating source can be regarded as a worst-case scenario since dredging occurs on the east side of the basin during the current reversal. If the backhoe is located on the western side of the harbour, lower concentrations are expected at location East2. To ensure no thresholds are exceeded during a current reversal event, monitoring of the concentrations on the eastern side of the harbour will be required as well, such that dredging can be halted on time.

The assessment of the turbidity thresholds and the analysis of the results over the depth highlight two issues regarding the location and measuring principle of the turbidity sensor. First of all, the current placement of the turbidity sensor to the west restricts its ability to monitor the concentrations on the eastern side of the harbour. To address this limitation and to prevent the need of immediately halting the dredging operation during a current reversal, a second turbidity sensor can be installed on the eastern side of the harbour during dredging. Another option is to stop dredging at the moment of a current reversal to prevent the additional costs of an extra turbidity sensor and the need of monitoring a second location. A cost-benefit analysis by the contractor on placing a second sensor or halting dredging momentarily can determine the most viable option to choose. Secondly, as the turbidity sensor measures the concentration 2 metres below the surface, only the SSC in the surface layer is observed. Given that the concentrations in the top layer consistently register lower

values than those near the bed, an underestimation of the depth-averaged SSC is expected to be recorded by the turbidity sensor using this approach.

Finally, from the assessment on the turbidity thresholds and the figures showing the exceedance locations in Appendices E.1 and E.2, the extent of the current high-impact zone can be discussed. In the simulated scenarios, the thresholds have only been exceeded on the eastern side for the daily averaged SSC. Therefore, it was recommended to monitor the concentrations on this side of the harbour as well. If possible, the eastern border of the high-impact zone can be extended more towards the east.
At the western side, no exceedance of the thresholds was observed and it can be argued that the extent of the zone on the west can be reduced. As the focus in this study was only on the far-field plume, dynamic plume effects could still be of influence in the vicinity of the load locations. Additionally, as only three source locations were modelled, the effects from dredging at the location of the approach channel have not specifically been simulated. While from the current results it seems that the zone can be adjusted, the source for dredging at the approach channel will be located further South-West than currently modelled sources. This causes too much uncertainty to draw a conclusion in reducing the extent of the high-impact zone.

7 Discussion

This chapter aims to discuss the uncertainties in the methods, processes and data used in this study. First, a reflection on the differences in modelling approach between the created models for this study and the already existing EIA model is provided. The uncertainties are identified next and a reflection on their influence on the model results is given. Furthermore, the limitations and simplifications of the data and processes on the results are discussed. Insight in these factors helps to clarify the implications of the choices made on the reliability and validity of this study.

7.1 Comparative analysis of the modelling approaches between created and EIA models

In this section, the difference in modelling approach between the EIA model and the model developed for this study are explored. The focus is on providing insight in the different methodologies, since a direct comparison of the results between the two models is not feasible due to a variety of different factors, such as different goals and limitations. The goal, modelling approach and limitations of the EIA model are discussed first, followed by a comparison between the two modelling approaches and the applicability of the different models.

The model developed for the EIA has been the first attempt to simulate the expected SSC and informs on the extent of the high-impact zone for the dredging operation in the Black Rocks harbour. However, due to time constraints, data gaps and a different goal for the model some important processes for simulating a representative dredging operation were excluded. Surveys collecting additional data on the sediment characteristics and the multi-beam survey had not yet been conducted. Additionally, the design for the breakwater (rubble mound or caissons) was not yet decided upon. The choice was made to model the rubble mound breakwater, in which dredging only starts after completion of the breakwater, while in this study the breakwater is not build yet. A list highlighting the differences in modelling approach is provided below:

- A constant source term was applied for the entire model. For analysis of the turbidity thresholds only the SSC values during the day between 08:00 and 18:00 are taken into account. However, the constant source will influence these results.
- A production rate of 40 m3/h was assumed, resulting in a total dredging time of 12 weeks.
- No tidal and wind forcing was incorporated separately for the hydrodynamics model (only currents from the Hycom database), and was run in 2D without accounting for different layers over the depth. This results in no variation of the flow over the depth.
- Due to the absence of depth layers, no distinction is made for the source term release over the depth.
- A minimum grid resolution of 15 m was used, which is five times larger than the minimum grid size used in this study.
- Fractions of fines of 33% and 13% were used for the eastern and western part of the dredging volume respectively .
- A source term factor of 0.1 for dredging was applied, which is significantly higher than the maximum value of 0.04 used in this report.
- The resulting source terms were 0.55 kg/s for 20.000 m3 (east) and 0.22 kg/s for 10.000 m3 (west), indicating lower source terms on average and a lower total dredging volume.
- Dredging was assumed to start after completion of the breakwater, resulting in different flow velocities and directions in the vicinity of the harbour.

The model developed for the EIA offered valuable insights to obtain a general overview of the expected concentrations and the predominant direction for the plume dispersion, aiding in the determination of the high impact zone used in this study. However, a different approach is required to obtain deeper insights in the potential exceedance of the turbidity thresholds during dredging. One limitation of the EIA model was the absence of important hydrodynamic processes, such as tidal forcing and the influence of wind forcing on the current direction and velocity magnitude of the top layer. Additionally, the absence of depth layers, due to a 2D modelling approach, resulted in the varying direction and magnitude of the currents over the depth not being simulated correctly. As simulated in the models developed for this study, modelling of these processes allow for modelling of the effects of higher current velocities in the top layer and varying SSC over the depth due to the configuration of the source term in the model and the inclusion of current reversals over the depth.

The differences between the used fraction of fines arise in the approach of simulating a worst case scenario for the EIA and the limited available data. While a large fraction of fines for the dredging volume was chosen, the different choices made on the dredging processes, for example use of a significantly lower production rate, resulted in similar source terms as decided upon in this study. Since more data was available for this study, the possibility of 33% fines present in 20,000 m3 was already proven to be highly unlikely.

In addition to the different approach in determination of the source terms, the EIA model employed a constant source term throughout the entire project duration. While only the SSC during the day was observed, the influence of the continuous source will be visible in the reported concentrations, since no period in the model is present when the source term is absent. The approach used in this study to halt the source term at night and during relocation provides a more representative representation of the temporal distribution of the source term.

Finally, the lower grid resolution and the presence of the breakwater are additional factors that limit the applicability in determining the exceedance of the turbidity thresholds. The presence of the breakwater prohibits free flow in the model, while the caisson breakwater can only be build after completion of the dredging operation. The minimum grid size of 15 m may cause lower observations on the SSC as the source is immediately spread across a significantly larger area compared to the case for a 3.5 m grid.

It can be concluded that the EIA model provided a good approach for their own purpose in a first identification on the extents of the high impact zone, but the additions of wind- and tide forcing, a higher grid resolution, more in depth data analysis and the use of a 3D model made the model developed for this study a more representative simulation of the dredging operation. Therefore, a higher accuracy can be provided in the prediction of the SSC's during dredging.

7.2 Uncertainties of the used methods on the model results

In this section, the uncertainties associated with the methods used for this study and their impact on the model results are discussed. This includes the applied methods in the modelling approach and analysis of data. Some of the uncertainties treated relate both to the methods used and the processes and data included. These discussion points will be included in the methods section.

Dredging processes
Several uncertainties arise from the decisions made regarding the exclusion of dredging processes. It was decided that back-filling of the caissons and the removal of boulders are excluded from the dredging operation regarding the duration of the dredging cycle. Due to the unknown method the effects of back-filling the caissons were excluded. Consequently, all dredged sediment was dumped at the disposal site in this study. The exclusion of back-filling caissons and boulder removal may introduce downtime during dredging, as emptying barges and removing boulders between dredging temporarily halt the operation. These interruptions result in downtime regarding the sediment flux and extends the dredging operation over a longer period. The inclusion of these processes would have resulted in a similar effect as was visible for relocation of the backhoe, potentially reducing the peak concentrations around these moments of downtime.

Other choices made regarding the work method, including the bucket volume, number of barges and sailing speed of the barges impact the duration of the dredging operation as well. A larger bucket volume reduces loading time, but increases the source quantity for each filled barges, while the number of barges affects the waiting time of the backhoe. It can be argued that the chosen sailing speed of 8 and 10 knots is relatively high. A lower sailing velocity results in a longer sailing time and consequently in possible downtime for the BHD. While the operation will take longer, the downtime does reduce the SSC. The absence of downtime in the model is a general limitation, as the persistency analysis indicated that downtime is likely to occur during the operation. While the results suggest that downtime is not a requirement to meet these thresholds, the inclusion of downtime would provide a more representative simulation. Moreover, a prediction on the expected downtime following the persistency analysis would be more accurate if wave data from multiple years was analysed. Although the two-year dataset provides a general overview, it does not contribute enough to estimate the downtime expected during 9 days of dredging.

Source term selection & quantification
The potential spillage of fines resulting from back-filling of caissons, leakage during sailing and dumping is not accounted for due to the decision to exclude the source from the dredging operation. Due to uncertainties in the work method and the limited time available, the choice was made to exclude these processes as they were deemed to be less significant, while dumping at the disposal site was determined to be out of scope. While, the included source terms are expected to have the biggest influence on the SSC, a complete overview on the effects of the dredging operation would require the inclusion of dumping, leakage during sailing, overflow and bucket drip during emptying of the barges. Uncertainty in the source term rates for the bucket drip and crushing and removal of boulders can affect the accuracy of the results, due to possible overestimation of the source rates. While for the bucket drip an upper limit was taken, an estimate was taken for the fines released from boulder crushing, likely overestimating the source fraction. As upper limits were used, the expected concentrations when applying different source term rates can only turn out lower than simulated for this study.

The relocating source in this study consisted of three different dredging locations. While it can be argued that this scenario should have been split in more locations, the relatively small dredging volume justified the choice to only include three different dredging locations due to the limited length of 80 metres between the source locations. Another uncertainty arises in the number of relocation moments. Only two were modelled, however, in reality more frequent relocations occur. Since during relocation a reduction of the peak concentrations was observed, including more moments of relocation in the simulation reduces the peak concentrations at the time of relocating.

As a limited number of sediment samples were available, an average of the most representative samples was used to determine the fines content for the source term calculations. This method was considered to be the best available method due to heterogeneity of the soil and limited number of samples. If more samples had been available, directly using samples from the load locations could have provided a more accurate representation of the source terms.

The developed model represented the suspended sediment by only two fractions, excluding the smallest fractions, which remain suspended for longer periods. This might results in higher sediment concentrations in plumes further from the source. Due to the absence of data on sediment fractions smaller than 63 μm, no accurate representation could be given of the smaller fractions using the available PSD curves. Extrapolating the PSD's is highly uncertain, suggesting the need to assess data obtained from coasts with similar characteristics in the Caribbean. The available data on the smaller fractions can be used to substantiate the chosen distribution of fines over the sediment flux. Additionally, more than two fractions can be included, which gives a better representation of the far field concentration as fractions smaller than 30 μm are then included as well.
Moreover, the possibility of underestimation of the smallest fractions is likely if the percentage of carbonate content, which may erode into very small particles, in the samples is taken into account. Percentages of 10 to 20% were observed in the soil samples, leading to a possible large representation of the carbonates for the finer particles.

Model configuration & results

A number of uncertainties arise from the used methods for the model configuration. First of all, the absence of grid refinement over the vertical limits accuracy in representing flow variations in the top layer influenced by wind forcing. Refining the grid in the top layers could improve the depiction of this process, but to not make the model too complex, no refinement was included. Consequently, the accuracy of the flow in the top layers may be limited. Additionally, exclusion of the grid refinement on the northern side of the island causes uncertainty in correctly capturing the effects of swells diffracting around the island. As the model currently cannot be validated at locations other than the ADCP, the correct representation of these ocean circulations in the model remain uncertain and should be kept in mind when addressing the dispersion pattern of the plumes.

For the water quality model, the chosen method for the settling velocity and the distribution of the source term over the depth are points of uncertainty. Despite using a formula by van Rijn (1993), generally applicable for turbulent flow and is expected to provide a good representation of the settling velocity for the particles, further insight in different formulations better applicable for the local conditions and the small diameter of the modelled particles will increase the reliability of the model results. In this study, the bucket drip was distributed equally over the depth. However, sediment is also spilled when the bucket is lifted above the water level, potentially leading to more sediment spillage in the top part of the water column. However, it can also be argued that most of the sediment in the overtopped bucket has already spilled by the time the bucket is above the water level, resulting in an equal sediment entry in each layer. The distribution of the sediment flux over the depth affects the concentration of the sediment plumes in the far-field, as sediment in the top layer takes longer to settle and can therefore disperse further. Further research on this particular aspect of the dredging operation will enhance the accuracy of the simulation of the dredging cycle.

Finally, the interpretation of the model results using point data to observe the SSC at the monitoring locations can lead to inaccuracies. As the bathymetry data is interpolated on the grid, disparities between the depth and geometry near the grid cell and at the real life location can occur. This can in turn affect the local flow velocities, current patterns and SSC in the grid cell, due to a difference in pressure gradients and shallower or deeper depths, which directly influence the local hydrodynamic processes. Observing the results regarding SSC at the surrounding grid cells and comparing the data allows to identify possible significant differences in the results.

7.3 Uncertainties of the included processes & data

The uncertainties associated with the included processes and data on the model results are discussed next. Starting with the data collected following the area study in Chapter 2 is analysed. These datasets form the foundation of the model and, therefore, directly influence the accuracy of the model results. Regarding the bathymetric data, a detailed overview on the project area was obtained by means of a multi-beam survey. As nearshore data was only available for the project area and the area surrounding the Fort Bay harbour, inaccuracies outside the project area can present in the form of incorrect representation of the current direction and formation of eddies when modelling the hydrodynamic processes.

Another limitation affecting the model results arises from the exclusion of turbidity caused by run-off from land after heavy rainfall events. High erosion rates on the island lead to significant amounts of boulders and sediment to be swept towards the ocean following heavy rainfall events. Figure 7.1 illustrates the aftermath of such an event, which cause both large boulders to end up on the roads and high concentrations of suspended sediment in the harbour.

(a) Boulders remains on the road after heavy rainfall

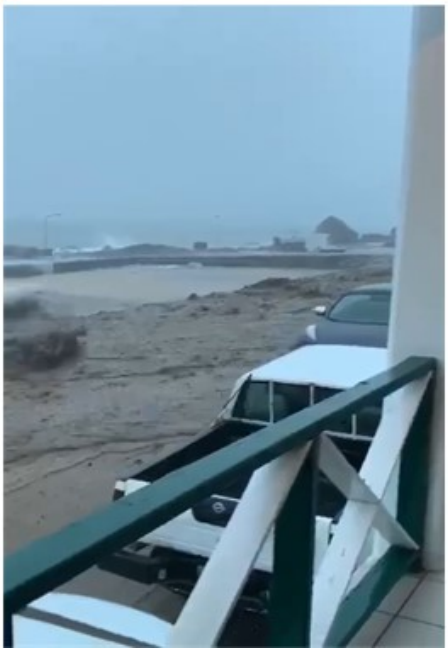

(b) Snapshot of run-off into Fort Bay harbour during heavy rain

Figure 7.1: Overview of the impact from erosion following heavy rainfall

This run-off can lead to a rapid increase in turbidity, potentially reaching the turbidity thresholds faster and leading to more downtime due to halting the dredging operation. As currently data from hydrology models is unavailable for the SSC in the run-off, the effects cannot be incorporated into the models for this report. This limits the accuracy of model results, especially if during the modelling time frame such a peak precipitation event occurs.
The turbidity caused by dredging can be put into perspective when observing these extreme events. The SSC in the harbour is expected to be significantly higher during such events, compared to the effects following the dredging operation.

To limit the complexity of the model, several processes were excluded, which may lead to an incomplete representation of the effects following the dredging operation. For instance, salinity and temperature, which influence the water density and in turn cause density-induced currents impacting the flow velocity, mixing of the water column and circulation patterns, were not included.
Secondly, wave forcing and wave-induced resuspension of the suspended sediment are excluded for this case study, despite the crucial role waves play in mixing of the water column and transport of the sediment plumes. Additionally, resuspension of the settled sediment and its impact on nearshore regions is not accounted for, which may lead to higher concentrations of suspended sediment nearshore over time, although the increase in concentration is expected to be limited. As the resuspended fines are expected to remain close to shore, no problems for the sensitive receptors located further from shore are expected. For each project the influence and importance of waves on the sediment concentration must be assessed separately. Including all of the processes mentioned would lead to a significant increase in calculation time. Therefore, choices should always be made on the significance of the influence of different factors. Finally, the influence of the water temperature on the kinematic viscosity was not considered for the settling velocity. As warmer temperatures decrease the kinematic viscosity, increased settling velocities can be expected for the warm temperatures of Caribbean oceans, resulting in lower concentrations in the far-field.

7.4 Limitations on the methods & data

A number of limitations regarding the used methods and available data are discussed, which restrict the possibilities on the model approach. Firstly, the available data for validation of the model was limited to one period during the hurricane season. Consequently, the model had to be run assuming that the dredging operation would occur during this season, which is unlikely. As a result, different hydrodynamic conditions are simulated in the model than those expected during the actual dredging operation. During the hurricane season wind speeds are generally higher, leading to higher flow velocities and faster dispersion of the sediment plumes. Furthermore, validation of the model was conducted at a single location, limiting the model's accuracy as the hydrodynamics in other areas in the model cannot be validated. To address this limitation, additional measuring campaigns during the favourable months for the dredging operation between February and April should be conducted at multiple locations.

The available data from the soil investigations used to estimate the fines content in Chapter 4 presents another limitation. The limited number of representative borehole samples available for the estimation of the fines content in the dredging volume reduces the accuracy of the estimated source term. The heterogeneity of the soil introduces extra uncertainty, as multiple pockets containing large amounts of fine sediment could be present in the dredging volume. However, overestimation on the fines content in the area remains a possibility as well. The questions remains to what extent the accuracy of the results would improve if more sediment samples are available. Furthermore, the available background turbidity data is limited, with only 6 months of data available, while the sensor has difficulty registering values below 0.5 NTU. As a result, useful data on the background turbidity is absent. The constant turbidity measured will be subtracted from the values reported by the turbidity sensor during dredging, potentially extending the dredging duration before thresholds are exceeded. As more data becomes available on the background turbidity, it can be used as an initial condition in the model or subtracted from the results for the SSC.

The hydrodynamic model created in this study poses a limitation regarding the tidal-induced current reversals at the bed, as these are not consistently captured resulting in different flow patterns at the bed compared to the ADCP data. While the current reversal at the bed is captured on a number of occurrences, providing some insight in the effects on the concentration, the exact influence on the peak concentrations and weekly averages remain unknown. Finally, the model does not account for the effects at the disposal site, which could potentially lead to negative impacts on coral reefs nearshore. It is essential to model this process to obtain a complete and representative overview of the full effects of the dredging operation.

8 Conclusion & recommendations

In this final chapter, the insights gathered in this study are provided by a comprehensive conclusion, reflecting on each sub-research question. This provides a summary of all key findings, leading up to the answer of the main research question. Additionally, a number of recommendations for future research are given based on the conclusion.

8.1 Conclusion

The aim of this research is to develop a representative approach to simulate the turbidity effects of dredging activities by backhoe dredgers in the vicinity of Caribbean islands. The main research question "**How can the turbidity impact of dredging activities by a backhoe in the Black Rocks area be simulated using a representative approach, while accounting for both local physical characteristics and dredging specific processes**" is addressed by investigation of a number of sub-research questions in this study. The sub-research questions are answered by analysing the system and configuring relevant processes into a numerical model. Each sub-question is addressed individually, ultimately contributing to provide an answer on the main research question.

1: *What relevant local hydrodynamic conditions and sediment characteristics should be considered when simulating the effects of the dredging operation?*

The influence of the local physical processes on the turbidity stresses and dispersion of the sediment plumes must be understood to consider their importance of inclusion in the simulation. Firstly, regarding the hydrodynamic processes, the wave climate must be studied to obtain a better understanding of the working conditions during dredging. Large wave heights and long wave periods, caused by swells, reduce the workability of the BHD if these exceed the operational limits of the equipment. Downtime can especially be expected during the hurricane season in the Caribbean between June and November. Additionally, mixing by waves and breaking waves can result in wave-induced resuspension. This process was deemed to have a less significant influence, especially on coral colonies located in deeper water from the 5 to 6 metre depth contour onwards, which is outside the breaking zone. Secondly, insight in the current patterns and flow velocities over the depth is essential to determine sediment plume dispersion and distribution of the SSC over the depth. Tidal and wind influences can result in variation of flow velocities and direction over the depth. The occurrence of rare hydrodynamic conditions, such as current reversals, should be captured to obtain a complete overview of the varying flow conditions. For a representative simulation, it is recommended to make use of a 3D model to accurately simulate the flow dynamics over the depth, while simulating varying flow conditions. The effects from peak precipitation events resulting in high turbidity levels caused by run-off, a recurring phenomenon on Saba and other Caribbean islands, should be considered as it significantly increases the background turbidity, potentially resulting in downtime to oblige to the turbidity thresholds.

Accurate data of local sediment samples should be collected and analysed to determine the fines content in the soil, with special attention on spatial variability in the fines content and distribution. This is an important step for the estimation of the source terms. Knowledge on the distribution of the particle size and density is crucial for an accurate determination on the settling velocity, which influences the SSC in the far-field. Including these processes allows for a representative approach in simulating the turbidity stresses caused by dredging. An accurate estimate of the turbidity stresses allows for timely proactive measures to prevent negative effects on the corals in the vicinity.

2: *What is the used work method for the dredging operation and which dredging processes should be incorporated in the model?*

In this study, the focus was on the passive plumes caused by dredging using a BHD to analyse the concentration and dispersion of sediment plumes in the far-field. The method considerations in this study have been based on dredging activities by a BHD. Regarding the work method, the equipment should be chosen based on cost consideration, the quantity and characteristics of the dredging volume and hydrodynamic conditions regarding operational limits for workability. A persistency analysis on historic data can be used to predict periods of downtime, which aids in determining an accurate estimate for the duration.

Processes such as filling, emptying and sailing of the barges should be included to allow for a representative estimate on the temporal distribution of the source terms in the model. It was determined that no distinction has to be made for the individual bucket lifting cycles as this has limited to no effect on the far-field concentration. Therefore, applying a constant source during continuous dredging activities is considered to be a suitable representation, while the source is absent between longer time intervals such as during relocation and halting of dredging activities.

3: *What are the relevant source terms and how should they temporally and spatially be distributed to represent the dredging operation?*

The main source term contributing to the release of fines considered is associated with the bucket drip from the BHD. While additional sources, such as overflow and leakage of barges, bucket drip during emptying of barges, dumping and release of fines during crushing and removal of boulders are present, these sources are believed to contribute significantly less and where therefore not considered for the case study in this report. However, if an accurate estimate on the contribution of these sources can be made, including them allows for a more representative simulation.

The lateral distribution of source terms was found by Tuinhof (2014) to influence the far-field concentrations. It is therefore recommended to apply a spatially varying source, with source terms present at multiple locations to simulate the relocation of the BHD, allowing for a more representative approach. The source terms can be quantified by first estimating the total amount of available fines using the approach for estimating source terms by Becker et al. (2015). If the fines content in the dredging volume varies spatially, a representative estimate on the local fines content should first be made for each source term by analysing sediment samples taken at different locations. For a correct representation of the various particle diameters, the calculated sources must not only be assigned to the fraction of 63 μm considered for the threshold of fines, but also to the smaller fractions. The smaller particles influence the far-field concentrations due to their slower settling velocity, resulting in a higher SSC further away from the source. If no data is available on the distribution of fractions smaller than 63 μm, the PSD curves can be extrapolated or PSD curves from similar locations in the area can be used if available.

4: *What is the most suitable modelling approach and how should the source terms and local hydrodynamic conditions be configured and implemented for an accurate simulation of the dredging operation?*

While different options for modelling software are available as CFD models and more global models as Delft3D, MIKE21 and FINEL, it is recommended to use the latter options. These type of models are sufficient to model the level of detail for the hydrodynamic processes required, while also providing computational efficiency. The case study in this report was simulated using Delft3D, utilizing the D-Flow and D-Water Quality modules to simulate the hydrodynamics and plume dispersion respectively. The grid resolution must be chosen accordingly to accurately represent the SSC by the initial sediment flux, in this case the bucket drip. If the grid cell size is too large, the initial source is dilluted, simulating a lower concentration. To capture the variations in flow velocity and direction

over the depth, a 3D model is recommended including a number of depth-layers. The relevant hydrodynamic processes, discussed for sub-question 1, should be included as boundary conditions for an accurate reflection of the local processes. For this case study, tidal and wind-forcing were deemed important processes to include to simulate the fluctuations in flow velocity and direction over the depth. Waves, salinity and temperature were excluded from the model, but the influence of each of these processes has to be evaluated for each project separately.

Suitable formulations for calculating the settling velocities of particles must be used, based on the local hydrodynamic conditions and sediment characteristics. In coastal environments, formulations applicable for turbulent flow are recommended. The source term originating from the bucket drip of a BHD should not be implemented in only one depth-layer of the model, but distributed equally over the depth to represent the gradual loss of fines while moving through the water column. Finally, to allow for spin-up of the hydrodynamic model, the source terms should not be included directly at the start.

5: What is the potential intensity and duration of the turbidity stresses at the monitoring locations and on the environment resulting from the simulated dredging operation?

The results of the water quality model, run for the Black Rocks harbour case, indicated that during normal flow conditions, the main dispersion direction of the plume is towards the west, while remaining close to the coast. The maximum concentration on the western edge of the high-impact zone did not exceed 4 mg/l for both the stationary and relocating source scenarios. The concentration recorded on the east were negligible during normal flow conditions. During tidal-induced current reversals, a significant increase in disparity between the SSC near the bed and at the surface layer was observed, with higher values near the bed. Modelling of a main current reversal exhibited significantly higher values near eastern observation points, especially for the relocating source, mainly caused by the increased source quantity and closer proximity.

Turbidity thresholds set for the project were not exceeded at any time during the dredging operation simulated under normal flow conditions. However, for the second simulation, an exceedance of the daily averaged threshold was reported for an observation point located on the east during the current reversal for the relocating scenario. This was not reported for the stationary source, indicating the influence of source location and quantity, especially during varying flow conditions. As the exceedance was observed at an eastern observation point, monitoring of the SSC not only on the western side, but also on the eastern side of the harbour is advised.

6: What additions to the current available methods can be suggested to improve the representation of the dredging processes?

A number of additions have been introduced to the already existing methods for estimating source terms and modelling far-field plume dispersion by Tuinhof (2014) and Becker et al. (2015). These additions aid in a more representative approach for simulating turbidity stresses from backhoe related dredging activities. Firstly, an overview identifying the relevant local physical processes must be created, aiming to improve the representation of the local conditions in the model. Insight into the temporal distribution following the work method was incorporated to suitably simulate the loss of fines over time. Consideration was given to simulating the relocation of the backhoe for a representative spatial distribution, which was not specifically stated for BHD's in the existing methods. An addition to the step for the determination of the fines content in the soil was provided to take into account the possibility of spatially varying fines content and its effect on the various sources. Morever, a methodical step stressing the need of incorporating multiple sediment fractions for an accurate simulation of the far-field concentrations was included.

Finally, a number of specific modelling considerations were implemented. These included the use of a 3D model to simulate the varying flow conditions and the inclusion of tidal and wind forcing.

Additionally, the importance of using a suitable formulation to calculate the settling velocity was stressed, as the numerical value obtained can vary significantly depending on the method used. Lastly, distributing the source term for the bucket drip equally over the depth was recommended as the most suitable approach.

How can the turbidity impact of dredging activities by a backhoe in the Black Rocks area be simulated using a representative approach, while accounting for both local physical characteristics and dredging specific processes

From the additions to the methods suggested in this report, an updated approach to simulate the turbidity stresses, specifically by a BHD, is proposed:

1. Identify and select the relevant local physical processes
2. Analyse the work method and determine temporal distribution of source terms
3. Identify the relevant source terms and distribute them spatially over the area
4. Assess and estimate the spatial variability of fines content for the source locations
5. Quantify the source terms, using the local fines content and distribute accordingly over the sediment fractions
6. Configure the relevant physical processes and source terms appropriately in the numerical model

The suggested method, applied for the Black Rocks harbour case, demonstrated that that for both a stationary and relocating source term, an accurate depiction of the average SSC values over longer time periods as days and weeks is simulated, while the relocating source tends to estimate peak concentrations more accurately, as the source location and quantity is represented more precisely. Therefore, to obtain an estimate of the turbidity effects over longer time periods, the labour intensive approach of a highly detailed model would not be recommended. However, if precise predictions of the peak concentrations are required over short time periods or during events as a current reversal, a more detailed approach would be beneficial for a more accurate representation on the effects of the dredging process.

8.2 Recommendations

To enhance the suitability of the method to represent the turbidity effects and to improve the accuracy of the results for the case study, recommendations are provided. First suggestions to for further improvement of the method to simulate turbidity effects by a BHD are given. Finally, based on the described steps and model results in this report, recommendations are given to improve the accuracy of the results on the turbidity effects of the Black Rocks harbour project.

A number of recommendations to further improve the suitability of the approach to simulate the turbidity stresses by a backhoe can be given number, focusing on a number of specific aspects. First of all, research into the required level of detail for the spatial distribution of the source terms, simulating relocation of the backhoe, is required to state the increase in accuracy. In this study, the three source locations were distributed 80 metres apart, which resulted in a variance in the observed SSC accross the domain compared to the stationary source. By testing the effects of applying more than three source terms and adjusting the distance between the sources, insight in the added accuracy on the results is obtained.

Additionally, the effect of refining a number of model related aspects on the accuracy of the model results can be researched. Insight in the effect of refinement of the grid over the vertical, allowing for a more detailed representation of the effects of surface stresses by wind and the tidal influence near

the bed on the current velocity and direction, can be obtained by testing a number of grid resolutions for similar hydrodynamic conditions. Similarly, the ideal grid size to represent the source input from the bucket drip can be tested by performing a sensitivity analysis on the grid size. Accurate measurements on the SSC in the far-field, along with accurate data on fines content and equipment used, are essential for performing a correct analysis.

Finally, a number of recommendations to improve the results on the turbidity effects for the Black Rocks dredging operation can be given. To obtain a complete overview on the effects of the dredging operation, the effects from dumping at the disposal site should be modelled. The sources resulting from emptying of the barges and consequently filling the caissons should be included as well to capture the full extent of the fines released during dredging. Additionally, by incorporating an increased number of sediment fractions by studying PSD curves from similar project sites in the Caribbean a more accurate representation of the particle distribution in the sediment plumes and consequently the far-field concentration can be simulated.

It is recommended to run the new models during the period between December and May in which dredging is recommended. As tropical storms are less frequent, flow velocities might be significantly lower, which influences the dispersion of the plumes. On the other hand, calm periods occur during the hurricane season as well (see Figure 2.6), such that the conditions modelled for the case study can be regarded as representative year-round. To validate these statements, additional data from the ADCP is required and must be collected first. By analysing the results for these flow conditions, a complete overview of the expected turbidity stresses throughout the year is obtained. When running the new models, it is advised to use nested models, in which boundary conditions from large scale models are provided to the localised model in the project area. This will ensure that regional effects on wind and tidal driven currents, influenced by the Saba bank and other islands, are incorporated correctly. Finally, if for the newly suggested model set-up a source is modelled near the approach channel, a well substantiated conclusion can be drawn on the recommended size of the high impact zone, based on the results from multiple scenarios.

If during the dredging operation in the Black Rocks harbour data is collected at multiple locations on the SSC, the model results from this study and refined models can be verified and the accuracy of the suggested method to simulate the dredging operation can be assessed.

References

Landscapes and Landforms of the Lesser Antilles. Springer International Publishing, 2017. ISBN 9783319557878. doi: 10.1007/978-3-319-55787-8. URL http://dx.doi.org/10.1007/978-3-319-55787-8.

Mahfuzuddin Ahmed, Gloria Magnayon Umali, Chiew Kieok Chong, Mary Franz Rull, and Marissa C. Garcia. Valuing recreational and conservation benefits of coral reefs—the case of bolinao, philippines. *Ocean &amp Coastal Management*, 50(1-2):103–118, January 2007. doi: 10.1016/j.ocecoaman.2006.08.010. URL https://doi.org/10.1016/j.ocecoaman.2006.08.010.

J.H. Becker. Dredge plumes: Ecological risk assessment. Master's thesis, TU Delft, Faculty of Civil Engineering and Geosciences, Hydraulic Engineering, 2011.

Johannes Becker, Erik van Eekelen, Joost van Wiechen, William de Lange, Thijs Damsma, Tijmen Smolders, and Mark van Koningsveld. Estimating source terms for far field dredge plume modelling. *Journal of Environmental Management*, 149:282–293, February 2015. doi: 10.1016/j.jenvman.2014.10.022. URL https://doi.org/10.1016/j.jenvman.2014.10.022.

R N Bray, editor. *Environmental aspects of dredging*. CRC Press, London, England, June 2008.

Joe Breman. *Ocean Globe*. Environmental Systems Research Institute, Redlands, CA, April 2010.

Paula Cartwright, Jordan Iles, Carlo Mattone, Mark O'Callaghan, and Nathan Waltham. Turbidity (ntu) to suspended sediment concentration (ssc) conversion protocol: Technical report. Technical report, James Cook University, 2022.

Alan Cuthbertson, Ping Dong, Stuart King, and Peter Davies. Hindered settling velocity of cohesive/non-cohesive sediment mixtures. *Coastal Engineering*, 55(12):1197–1208, December 2008. doi: 10.1016/j.coastaleng.2008.05.001. URL https://doi.org/10.1016/j.coastaleng.2008.05.001.

P.J.T. Dankers. The behaviour of fines released due to dredging: A literature review. Technical report, TU Delft, Section Hydraulic Engineering, 2002.

Deltares. *D-Flow Flexible Mesh User Manual*, October 2023a. URL https://content.oss.deltares.nl/delft3dfm2d3d/D-Flow_FM_User_Manual.pdf.

Deltares. *D-Morphology User Manual*, October 2023b. URL https://content.oss.deltares.nl/delft3d/manuals/Delft3D-WAVE_User_Manual.

Deltares. *D-Water Quality User Manual*, October 2023c. URL https://content.oss.deltares.nl/delft3dfm2d3d/D-Water_Quality_User_Manual.pdf.

E.J.C. Dupuits. Stochastic effects of dredge plumes: Development and application of a risk-based approach to assess ecological effects of dredge plumes on sensitive receivers. Master's thesis, 2012.

Christopher A. Ellison, Brett E. Savage, and Gregory D. Johnson. *Suspended-sediment concentrations, loads, total suspended solids, turbidity, and particle-size fractions for selected rivers in Minnesota, 2007 through 2011*. 2014. doi: 10.3133/sir20135205. URL http://dx.doi.org/10.3133/sir20135205.

Paul L.A. Erftemeijer, Bernhard Riegl, Bert W. Hoeksema, and Peter A. Todd. Environmental impacts of dredging and other sediment disturbances on corals: A review. *Marine Pollution Bulletin*, 64(9):1737–1765, September 2012. doi: 10.1016/j.marpolbul.2012.05.008. URL https://doi.org/10.1016/j.marpolbul.2012.05.008.

Nathan Hawley. Settling velocity distribution of natural aggregates. *Journal of Geophysical Research*, 87(C12):9489, 1982. doi: 10.1029/jc087ic12p09489. URL https://doi.org/10.1029/jc087ic12p09489.

W. F. Henley, M. A. Patterson, R. J. Neves, and A. Dennis Lemly. Effects of sedimentation and turbidity on lotic food webs: A concise review for natural resource managers. *Reviews in Fisheries Science*, 8(2):125–139, April 2000. doi: 10.1080/10641260091129198. URL https://doi.org/10.1080/10641260091129198.

Shahadat Hossain, Bradley D. Eyre, and Lester J. McKee. Impacts of dredging on dry season suspended sediment concentration in the brisbane river estuary, queensland, australia. *Estuarine, Coastal and Shelf Science*, 61(3):539–545, November 2004. ISSN 0272-7714. doi: 10.1016/j.ecss.2004.06.017. URL http://dx.doi.org/10.1016/j.ecss.2004.06.017.

Terence P. Hughes, David Ayre, and Joseph H. Connell. The evolutionary ecology of corals. *Trends in Ecology &amp Evolution*, 7(9):292–295, September 1992. doi: 10.1016/0169-5347(92)90225-z. URL https://doi.org/10.1016/0169-5347(92)90225-z.

Ross Jones, Pia Bessell-Browne, Rebecca Fisher, Wojciech Klonowski, and Matthew Slivkoff. Assessing the impacts of sediments from dredging on corals. *Marine Pollution Bulletin*, 102(1):9–29, January 2016. doi: 10.1016/j.marpolbul.2015.10.049. URL https://doi.org/10.1016/j.marpolbul.2015.10.049.

P. Laboyrie, Mark van Koningsveld, Stefan Aarninkhof, M. Van Parys, M. Lee, A Jensen, Csiti A., and R. Kolman, editors. *Dredging for Sustainable Infrastructure*. CEDA, 2018. ISBN 978-90-9031318-4.

Jan M Lindsay. *Volcanic hazard atlas of the lesser Antilles*. Seismic Research, 2005.

Christopher McArthur, Roland Ferry, and John Proni. Development of guidelines for dredged material disposal based on abiotic determinants of coral reef community structure. In *Dredging '02*. American Society of Civil Engineers, October 2003. doi: 10.1061/40680(2003)115. URL https://doi.org/10.1061/40680(2003)115.

Erik H. Meesters, , Leontine E. Becking, Matthijs van der Geest, , , and and. Achteruitgang koraalriffen caribisch nederland: oorzaken en mogelijke oplossingen voor koraalherstel. Technical report, 2019. URL https://doi.org/10.18174/496168.

VICKI BUCHSBAUM PEARSE and LEONARD MUSCATINE. ROLE OF SYMBIOTIC ALGAE (ZOOXANTHELLAE) IN CORAL CALCIFICATION. *The Biological Bulletin*, 141(2):350–363, October 1971. doi: 10.2307/1540123. URL https://doi.org/10.2307/1540123.

P. Ridd, G. Day, S. Thomas, J. Harradence, D. Fox, J. Bunt, O. Renagi, and C. Jago. Measurement of sediment deposition rates using an optical backscatter sensor. *Estuarine, Coastal and Shelf Science*, 52(2):155–163, February 2001. doi: 10.1006/ecss.2000.0635. URL https://doi.org/10.1006/ecss.2000.0635.

Claire L. Ross, Andrew Warnes, Steeve Comeau, Christopher E. Cornwall, Michael V. W. Cuttler, Melissa Naugle, Malcolm T. McCulloch, and Verena Schoepf. Coral calcification mechanisms in a warming ocean and the interactive effects of temperature and light. *Communications Earth &amp Environment*, 3(1), March 2022. doi: 10.1038/s43247-022-00396-8. URL https://doi.org/10.1038/s43247-022-00396-8.

Mark D. Spalding, Corinna Ravilious, and Edmund P. Green. World atlas of coral reefs. 2001.

H.L. Toh. Suspended sediment and light attenuation characteristics in singapore waters. Master's thesis, TU Delft, Faculty of Civil Engineering and Geosciences, Hydraulic Engineering, 2012.

T.J. Tuinhof. Modelling far-field dredge plume dispersion. Master's thesis, TU Delft, Faculty of Civil Engineering and Geosciences, Hydraulic Engineering, 2014.

C. van der Vlugt. Status and trends of coral reef health indicators on saba (caribbean netherlands). Master's thesis, 2016.

L.C. van Rijn. *Principles of Sediment Transport in Rivers, Estuaries and Coastal Seas*. Number dl. 2 in Principles of Sediment Transport in Rivers, Estuaries, and Coastal Seas. Aqua Publications, 1993. ISBN 9789080035621. URL https://books.google.com/books?id=gGIYAQAAIAAJ.

Amelia S. Wenger and Mark I. McCormick. Determining trigger values of suspended sediment for behavioral changes in a coral reef fish. *Marine Pollution Bulletin*, 70(1–2):73–80, May 2013. ISSN 0025-326X. doi: 10.1016/j.marpolbul.2013.02.014. URL http://dx.doi.org/10.1016/j.marpolbul.2013.02.014.

J. C. Winterwerp. Near-field behavior of dredging spill in shallow water. *Journal of Waterway, Port, Coastal, and Ocean Engineering*, 128(2):96–98, March 2002. doi: 10.1061/(asce)0733-950x(2002)128:2(96). URL https://doi.org/10.1061/(asce)0733-950x(2002)128:2(96).

Haley Zanga, Audrey Boraski, Alana Olendorf, Marisa Benjamin, Haley Fantasia, Simone McEwan, Jaime Marsh, Melissa Wydra, Will Trautmann, Emily Michaeles, Maddi Ouellette, Andrew Fuhs, Allie Tolles, Suki Graham, Mary Swain, Devon Audibert, Sarah Larsen, Emma Verville, Tim Brodeur, Jason Charbonneau, Christian Paparazzo, Bryce Chounard, Malisa Rai, Jennifer Rosado, Morgan Tupper, , and Jessica Comeau. *A STUDENT'S GUIDE TO TROPICAL MARINE BIOLOGY*. Libretexts, Keene, 2023.

A.C. Ziegler. Issues related to use of turbidity measurements as a surrogate for suspended sediment, 2002.

A Area study elaboration

A.1 Bathymetry

This section elaborates on the available bathymetric datasets around Saba, additionally providing a comparison between the results obtained by the single-beam and multi-beam survey in the Black Rocks area.
The results of the single-beam survey in the Black Rocks area can be seen in Figure A.1. The resolution of the single-beam is noticeably lower than the multi-beam survey.

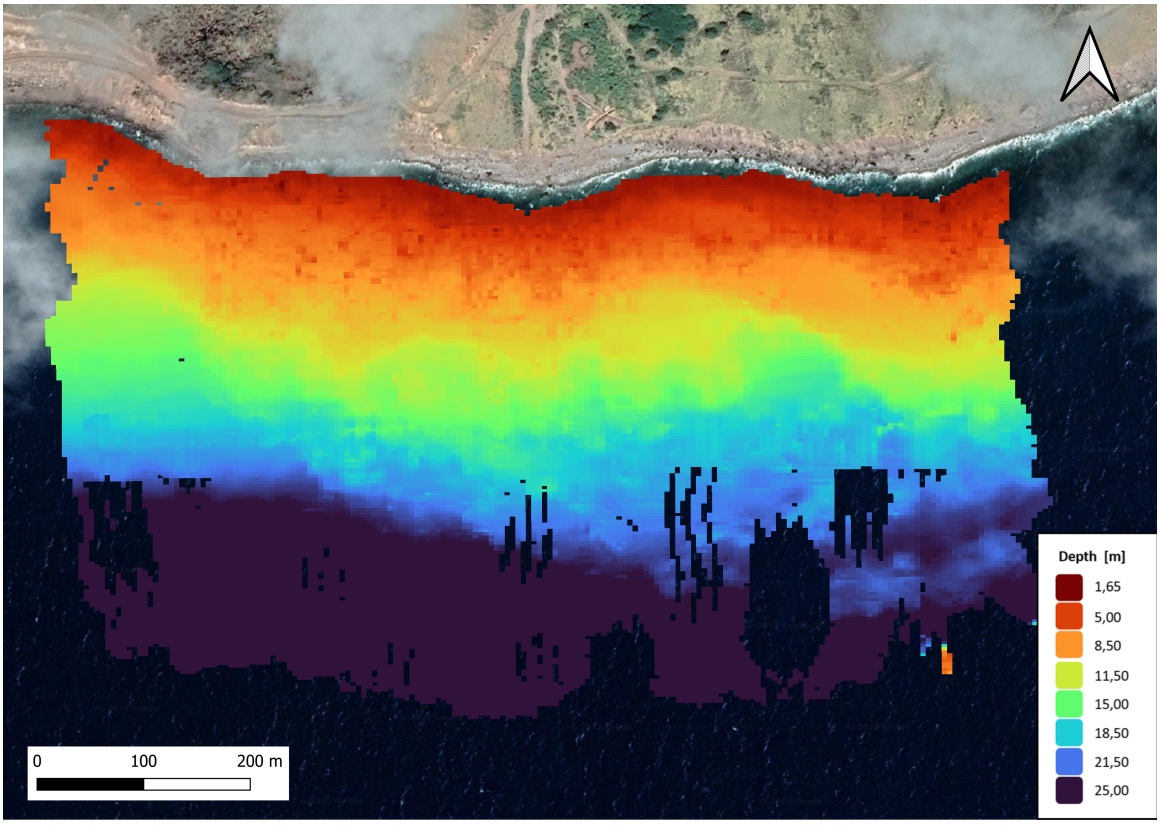

Figure A.1: Results from the single-beam bathymetry survey in the Black Rocks area

The difference between the single and multi-beam survey is shown in Figure A.2. Two different profiles of the seabed from the two surveys are compared. The red line shows the multi-beam survey and the blue line the profile obtained from the single-beam survey. The multi-beam survey shows a more detailed depiction than the single-beam. Some of the large boulders in the area can be seen in multi-beam profile. For the single-beam survey the results can be seen as a depth averaged profile of the multi-beam survey. Not only are the boulders less distinguishable, but the nearshore measurements around the 3 to 6 m depth contour appear to show a consistent difference of 0.5 to 1 m deeper water compared to the multi-beam survey.

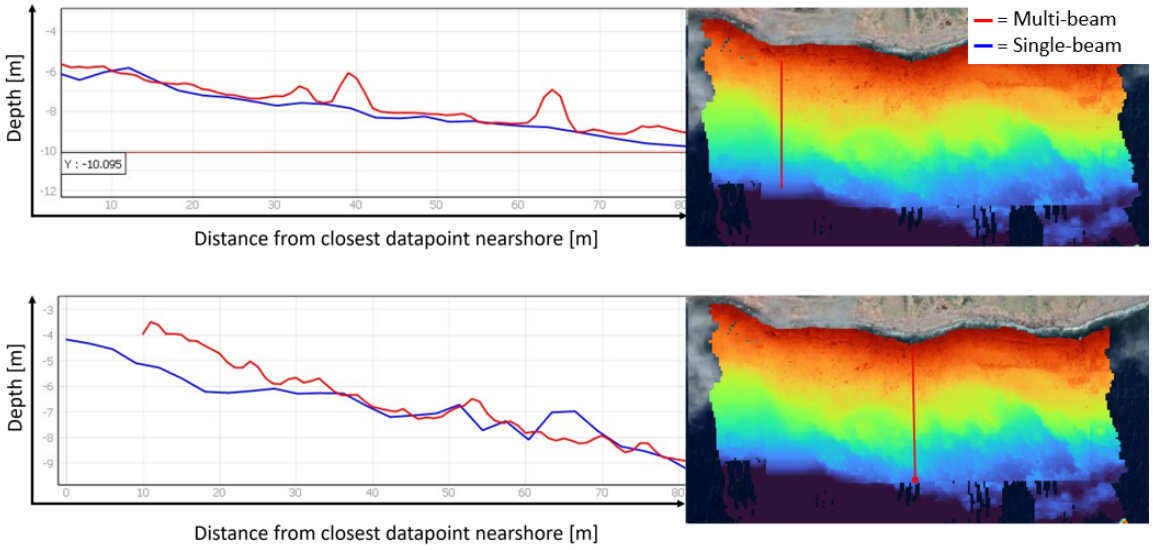

Figure A.2: Comparison between the single and multi-beam survey at two different transects in the Black Rocks area

For the existing harbour Fort Bay the results of the bathymetry survey performed can be seen in Figure A.3. When comparing both surveys, it can be noticed that the depth increase at Fort Bay is significantly faster than at the Black Rocks area. The change in steepness of the foreshore is already visible on the eastern side of the Fort Bay survey, where the depth increase is more gradual than directly in front of the harbour.

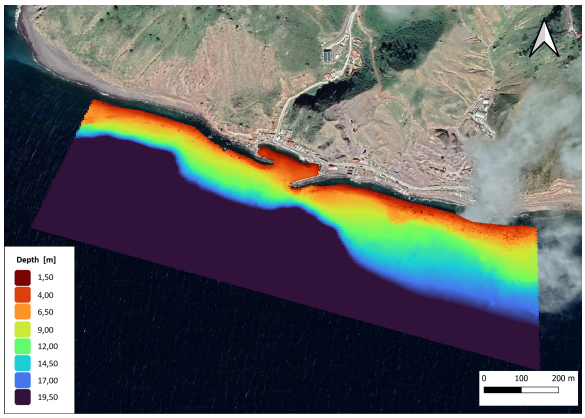

Figure A.3: Overview of the single-beam survey results at Fort Bay

B Coral theory

The presence of corals in the area is the main driver for creating a representative model on the effects of the dredging operation. This section delves into the characteristics of corals and the various coral stressors, which pose threats to the coral colonies. By gaining a better understanding of these factors, the need of safeguarding the corals from high sediment concentrations is emphasized.

B.1 Characteristics of corals

Corals are not only visually attractive for divers, but also serve as a shelter and feeding place for countless aquatic species and in some cases even serves as a natural breakwater for coastal protection (Ahmed et al., 2007). Most coral branches people see are made up of thousands of single corals which are called polyps. These corals are modular organisms, meaning that they are made up of several individual, but identical pieces (Hughes et al., 1992). Within these polyps live tiny unicellular algae called zooxanthellae. The coral and zooxanthellae live in symbiosis, meaning that at least one of the two organisms benefit of the presence of the other. (PEARSE and MUSCATINE, 1971) Zooxanthellae are photosynthetic organisms meaning they can use the energy from sunlight to provide nutrients for the coral species the zooxanthellae is hosting on while it also has benefit from the waste products of corals (Spalding et al., 2001). Protection to these algae is also provided by the coral as it provides shelter for the zooxanthellae (PEARSE and MUSCATINE, 1971). The zooxanthellae produce pigment, which is visible as they inhabit the clear tissue of the polyps (Zanga et al., 2023). Coral can regulate the number of zooxanthellae cells and the amount of chlorophyll in them (Zanga et al., 2023). The beautiful colours, which characterize corals are obtained from the pigment produced by the zooxanthellae.
Many corals have the ability to live in colonies, which allows them to create a joint skeleton (Spalding et al., 2001). An example of such coral species are reef-building (hermatypic) corals, which are hard corals that create a skeleton from calcium carbonate (limestone) in warm, shallow water, which typically grow only millimeters every year (Spalding et al., 2001). Zooxanthellae can influence this calcification process by removing phosphates and converting carbon dioxide indirectly into carbonate (PEARSE and MUSCATINE, 1971).
Soft corals do not form a limestone skeleton, but grow as a result of budding. Polyps bud off from each other, forming new polyps and consequently forming a larger colony (Hughes et al., 1992).

An example of a coral species, which can be found around Saba, is the Acropora Palmata, which can be seen in Figure B.1.

Figure B.1: Colony of Acropora Palmata in the Black Rocks area

B.2 Coral stressors

Coral health is influenced by a wide range of different factors. It can be affected by both natural and anthropogenic (man-made) threats. The focus on this project is, due to the dredging activities, to identify the different man-made threats and to assess the possible damage these can have on the corals. Some natural threats will be listed as well. In case of coral starvation during or after completing the project the possibility of damage to the corals caused by dredging can be ruled out if the natural threats are known as well.

Two of the main threats to the coral as a result of dredging are sedimentation and light attenuation in the water column. Sedimentation of corals can occur when (part) of the sediment plume settles on the coral itself. The coral responds by attempting to remove the sediment which has settled by pushing it off towards the edges. Once the sedimentation is too high (partial) mortality of the coral can happen if sediment is not removed by a storm (Jones et al., 2016). The sediment plume also affects the amount of light able to penetrate through the water as it causes light attenuation. The light limitation caused by the suspended sediment and sedimentation of the corals negatively influences the zooxanthellae due to a decline in photosynthetic productivity (Erftemeijer et al., 2012). A decreasing number of zooxanthellae can result in coral bleaching and even starvation due to receiving less nutrients from the zooxanthellae. Fishing nets or anchors from ships can destroy part of the coral colonies by dragging them across the seabed. This should be prevented as much as possible in areas containing coral species.
Pollution as well as global warming form great risks to the corals. Pollution by run-off from land can add nutrients to the water, which may cause an immense growth of algae (Meesters et al., 2019). This process, called euthrophication, may cause smothering of the corals by algae. Rising CO2 levels cause warmer and more acidified oceans. Ocean acidification forms a threat to corals as it is expected to cause a decrease in calcification rates (Ross et al., 2022). Another consequence of the warmer water is the expelling of zooxanthellae from the coral, which may result again in coral bleaching. A similar phenomenon happens when the coral is under stress, which may cause the release of zooxanthellae (Zanga et al., 2023).
Among the natural threats harming corals are the different diseases affecting different species such as white and black band disease (Dupuits, 2012). As mentioned by Meesters et al. (2019) other stressors include overfishing and invasive species. Additionally, overgrazing by goats causes erosion rates to be high, contributing to high turbidity levels in the water after heavy rainfall (Meesters et al., 2019).

C Persistency analysis

This section presents a persistency analysis for the dredging operation in order to assess the duration during which the dredging operation can proceed without exceeding the wave height limits for the chosen BHD. The analysis covers the significant wave height, maximum wave height and peak wave period as these factors determine the workable days for the BHD. The persistency analysis provides an overview on the expected duration in which the MetOcean conditions stay within the criteria set for a safe and efficient continuation of the dredging operation. Historical data collected from wave buoys deployed in the area is used to assess the number of workable days during these periods. The analysis is crucial when calculating the complete duration of the dredging cycle, as insight is given to optimise the dredging operations. The outcome assist in scheduling the operation during periods with a higher persistency of favourable conditions, minimizing potential downtime due to adverse environmental conditions.

Starting the analysis, a decision must be made on the workability limits for factors regarding wave height and period. These limits are first of all imposed to guarantee the safety of the personnel and the equipment. Operating in rough conditions significantly increases the risk of accidents and damage to or loss of expensive equipment. Another important reason is that these rough conditions can cause instability of the pontoon. This instability not only affects the precision of the dredging operation during sediment excavation, but also complicates the process of disposing the sediment in the barges. This can lead to loss of sediment, raising the suspended sediment concentration in the water column. This situation is unfavourable as it accelerates exceedance of the turbidity thresholds. It is decided to use a Backhoe with a bucket volume of 10 m3 and a draught of approximately 2 m as stated in Section 3. Equipment of this size is expected to remain operable within maximum significant wave heights of 0.9 m, maximum wave heights of 1.5 m and peak wave period of 10 s.

To perform the analysis, historical data needs to be collected. For the project area, wave data is available during the period of August 2020 to October 2023, with some minor data gaps. The data for all the parameters considered is given in separate figures for its respective measuring period. The first dataset ranges from 24-08-2020 to 06-08-2021. For the other two years the data collection periods are 30-08-2021 to 23-06-2022 and 13-10-2022 to 13-10-2023. It must be noted that for the first two time periods, a different wave buoy was used than for the 2023 measuring campaign. The red horizontal lines represent the value that was set as the limit for each parameter. The data collected for the measurement periods can be seen in Figures C.1, C.2 and C.3 below.

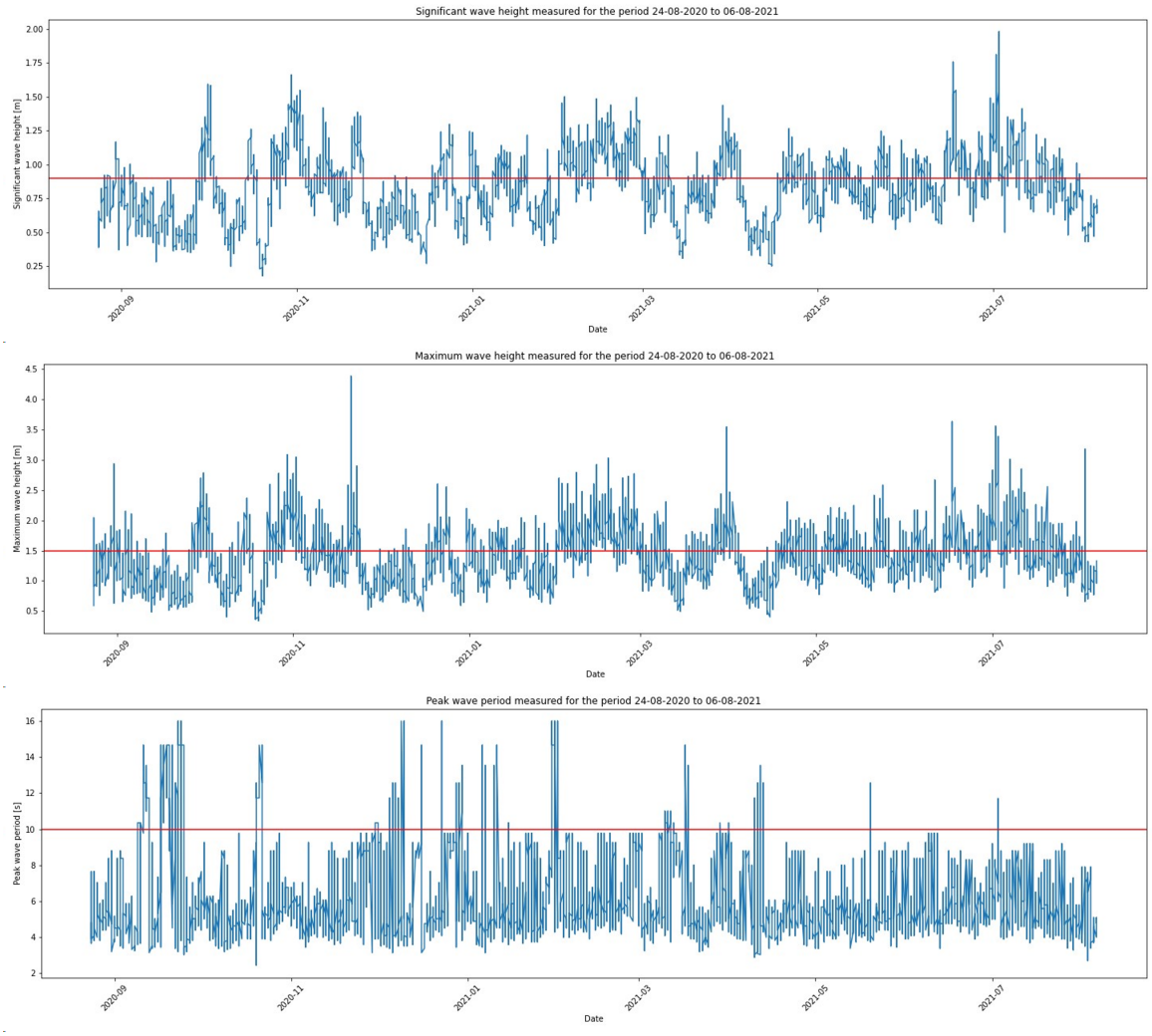

Figure C.1: Overview of the wave buoy measurements at Black Rocks on Hs, Hmax and Tp during the period 24-08-2020 to 06-08-2021

Figure C.2: Overview of the wave buoy measurements at Black Rocks on Hs, Hmax and Tp during the period 30-08-2021 to 23-06-2022

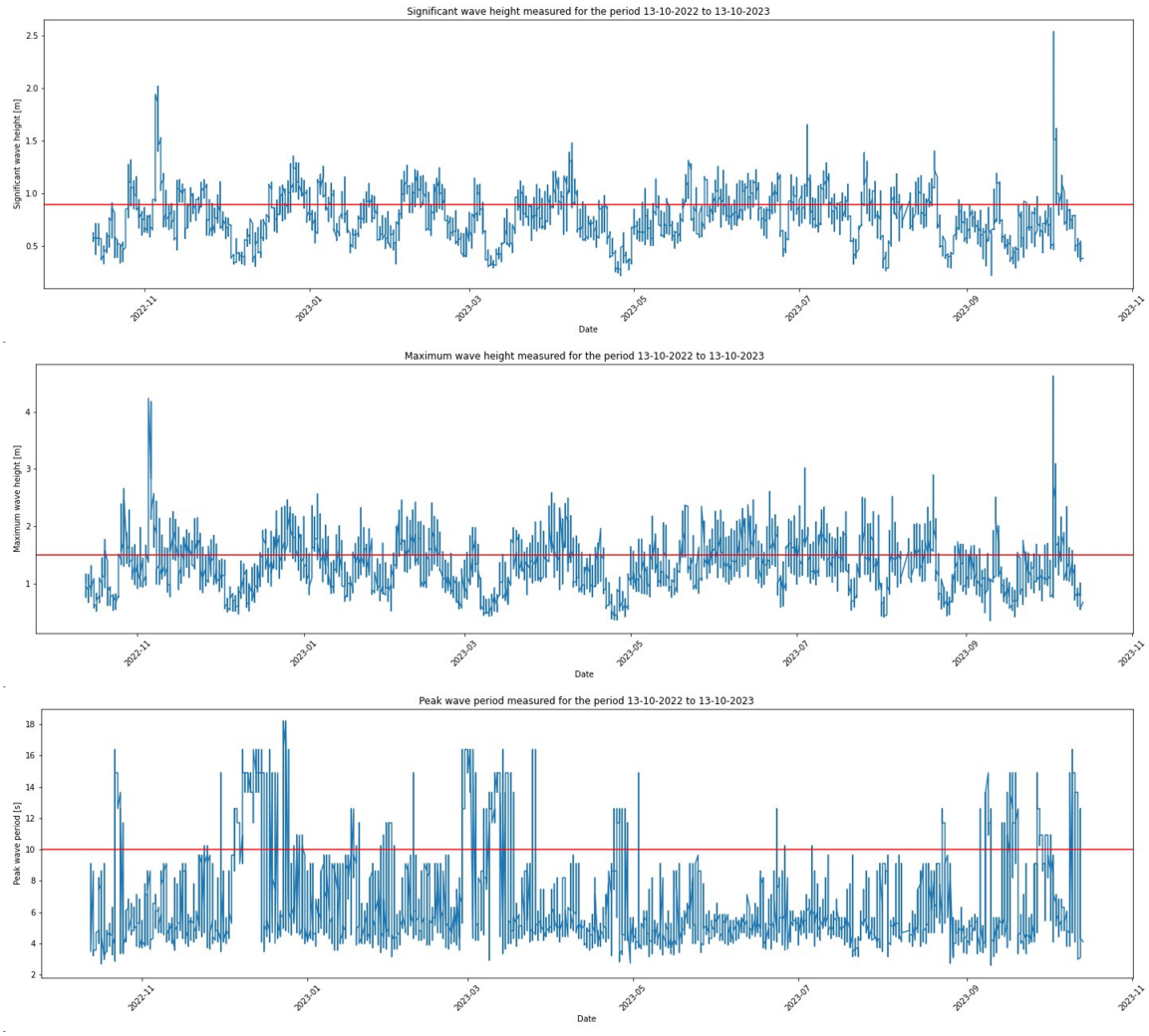

Figure C.3: Overview of the wave buoy measurements at Black Rocks on Hs, Hmax and Tp during the period 13-10-2022 to 13-10-2023

From the figures, a clear difference in the data can be seen for the year 2022 compared to 2021 and 2023. During the period between September and November, it appears that tropical storms and hurricanes may have caused exceptionally high waves and peak periods for an extended period. The reliability of the 2022 dataset must be analysed carefully before a decision on its use is made.
In addition to the created plots, the dataset is subjected to an analysis in which the number of days is counted during which the defined limits for each parameter were not exceeded between 5:00 and 19:00. This time frame is chosen to take the dredging window per day and the time during which sailing to and from the location takes place into account. This provides an overview on the number of workable days over the year. In Table C.1 the results of the persistency analysis are presented.

Year	Parameter	Days in dataset	Number of days
2023	Hs	342	169
2023	Hmax	342	119
2023	Tp	342	268
2022	Hs	291	88
2022	Hmax	291	56
2022	Tp	291	166
2021	Hs	348	149
2021	Hmax	348	97
2021	Tp	348	303

Table C.1: Results of the persistency analysis for the workability of the BHD according to the set parameter limits

From the persistency analysis it can be seen that the years 2021 and 2023 provide fairly similar results, while for 2022 only half the available working days compared to 2021 and 2023 are counted. While at the start of the second measuring period some tropical storms moved past the area, logically resulting in larger wave heights and wave periods, a pattern of high wave heights and wave periods can be seen throughout the year long measuring period. It appears that the measured data for 2022 is consistently too high. The choice is therefore made to not include the second measuring period in the decisions made for the expected downtime for the dredging cycle. The data for 2021 and 2023 will still be used.

D Sediment characteristics

This section contains the figures showing the PSD's from the different soil investigations and provides an overview of the complete list of samples taken during both surveys.

D.1 Particle size distributions

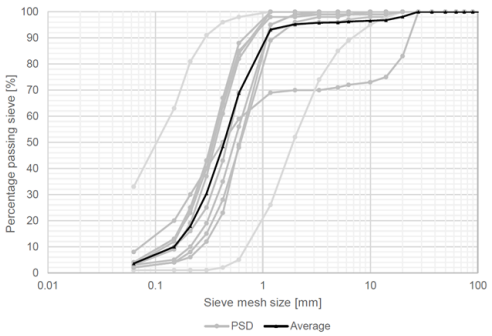

Figure D.1: Overview of different PSD's from the 2020 soil investigation on land and sea including the average PSD

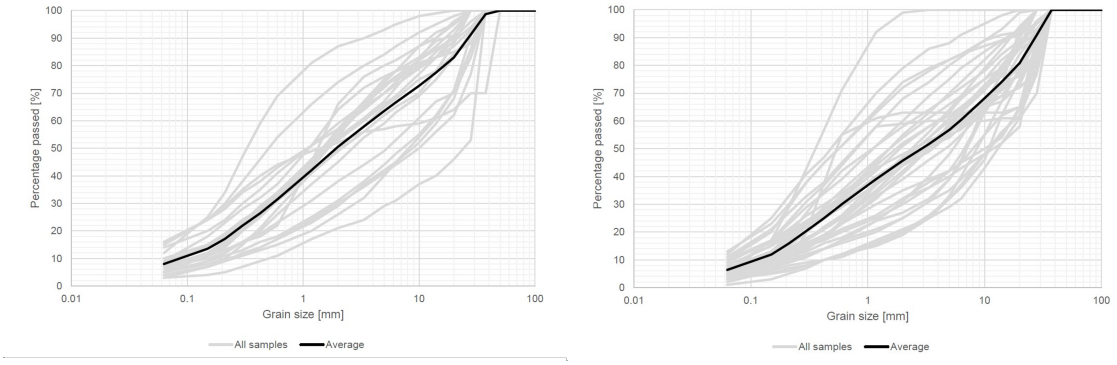

Figure D.2: Overview of the PSD's from the 2023 soil investigation including the average PSD. The left figure shows the offshore PSD's and right the onshore PSD's

D.2 Overview of fines content in the borehole samples

Borehole	**Depth relative to SD [m]**	**Fines content [%]**
B1	+10.39 - +8.69	8
B3	4.07 - 4.87	33
B7	6.00 - 6.45	4
B7	10.00 - 11.00	4
B8	7.50 - 9.50	3
B9	6.60 - 6.75	3
B9	9.30 - 10.50	2
B10	10.40 - 12.40	3
B12	8.30 - 8.80	1
B12	12.30 - 13.30	3
B16	10.50 - 15.20	2

Table D.1: Overview of the fines content in the boreholes samples taken in the 2020 geotechnical survey in the Black Rocks area

Borehole	**Depth [m]**	**Fines content [%]**
BH1	3.44 - 3.89	6
BH1	4.94 - 5.39	12
BH1	6.44 - 6.89	9
BH1	7.94 - 8.39	10
BH2	5.02 - 5.47	8
BH2	8.02 - 8.47	6
BH3	(+) 2.17 - (+) 1.82	4
BH3	(+) 0.67 - (+) 0.22	5
BH3	0.83 - 1.28	5
BH3	3.83 - 4.28	4
BH3	5.33 - 5.78	7
BH5	1.90 - 2.35	6
BH5	4.90 - 5.35	7
BH5	6.40 - 6.85	7
BH6	3.88 - 4.33	6
BH6	5.38 - 5.83	8
BH6	8.38 - 8.83	11
BH6	9.88 - 10.33	10
BH11	8.78 - 9.23	5
BH11	10.28 - 10.73	10
BH11	11.78 - 12.23	16
BH14	10.73 - 11.18	4
BH18	7.07 - 7.52	3
BH18	8.57 - 9.02	7
BH18	10.07 - 10.52	7
BH18	11.57 - 12.02	5

Table D.2: Overview of the fines content in the boreholes samples taken in the 2023 geotechnical survey in the Black Rocks area

E Additional model results

This section provides additional figures on the hydrodynamic and water quality model results. For both scenarios the SSC at the load locations is given, as well as figures indicating the exceedance locations for the daily and weekly thresholds for both scenarios. Additionally, velocity vector plots are presented to provide insight in the behaviour of the plume dispersion in the Figures presented in Chapter 6.

E.1 Stationary source results

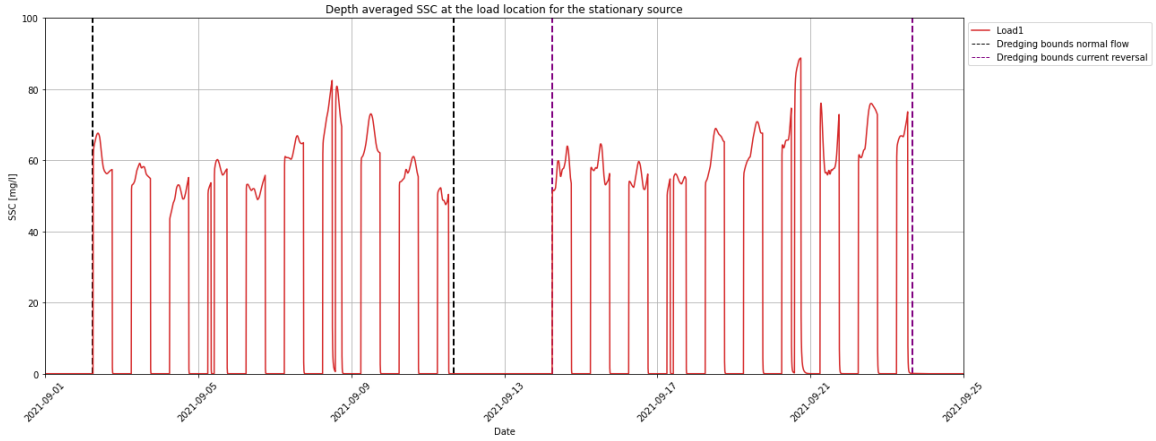

Figure E.1: Depth average SSC at the load location for the stationary source term

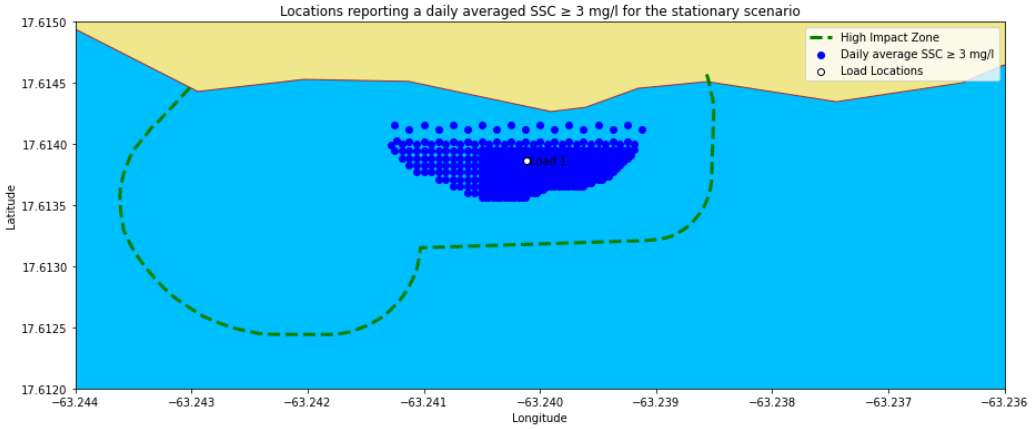

Figure E.2: Overview of the locations in the project where an average daily SSC of 3 mg/l or higher was reported during the simulations for the stationary source

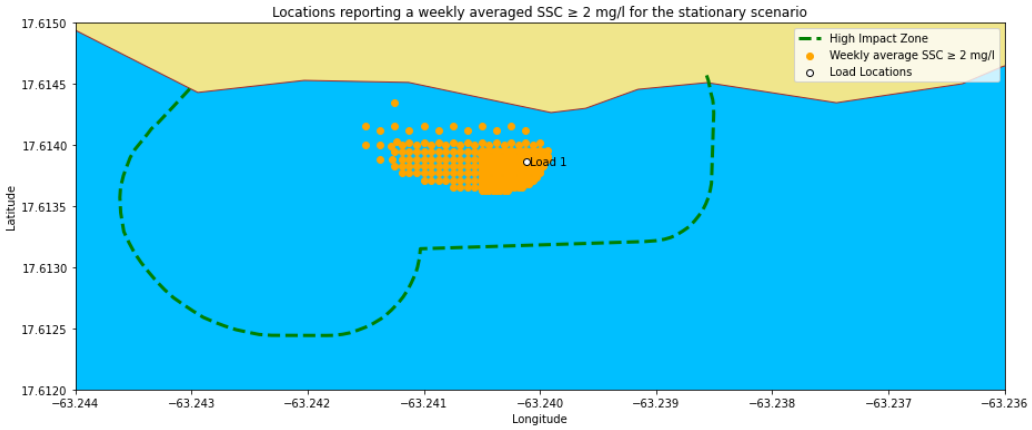

Figure E.3: Overview of the locations in the project where an average weekly SSC of 2 mg/l or higher was reported during the simulations for the stationary source

E.2 Relocating source results

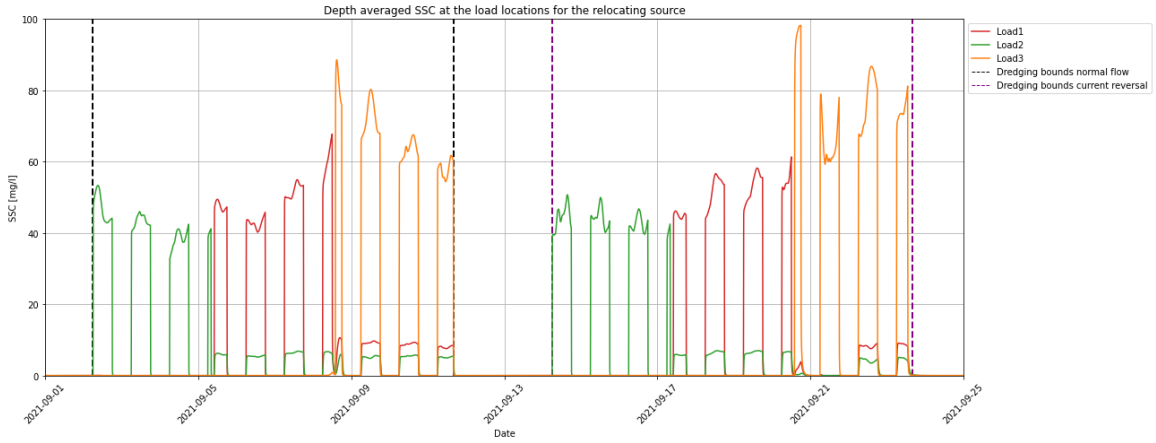

Figure E.4: Depth average SSC at the three different load locations for the changing source term

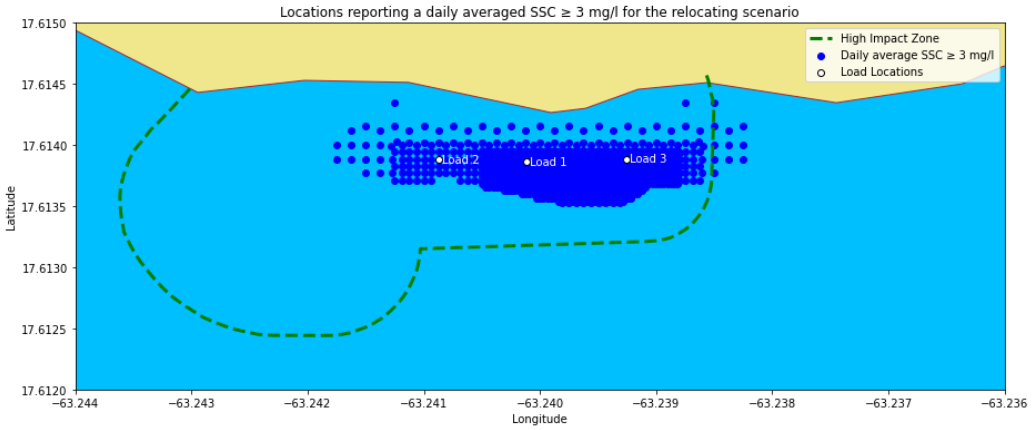

Figure E.5: Overview of the locations in the project where an average daily SSC of 3 mg/l or higher was reported during the simulations for the relocating source

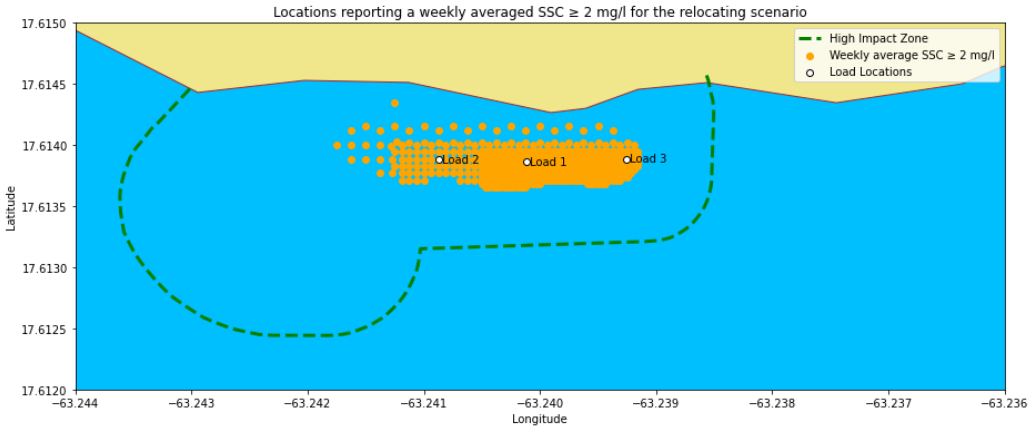

Figure E.6: Overview of the locations in the project where an average weekly SSC of 2 mg/l or higher was reported during the simulations for the relocating source

E.3 Velocity vector plots

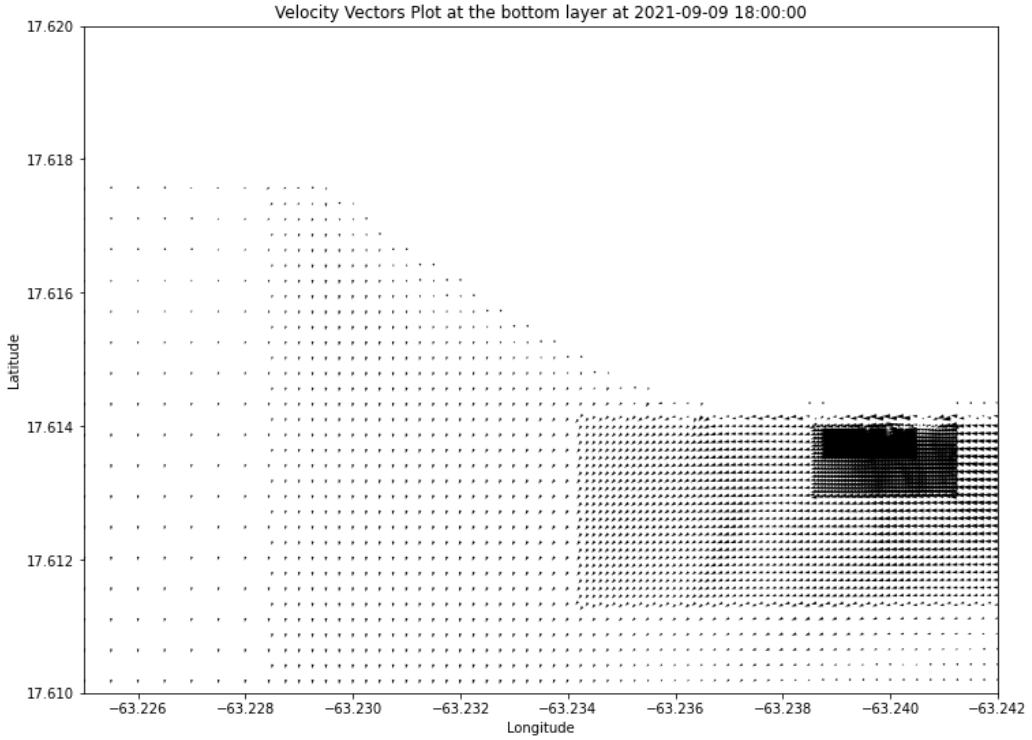

Figure E.7: Velocity vector plot of the western side of the Black Rocks area near the bed at 09-09-2021 18:00

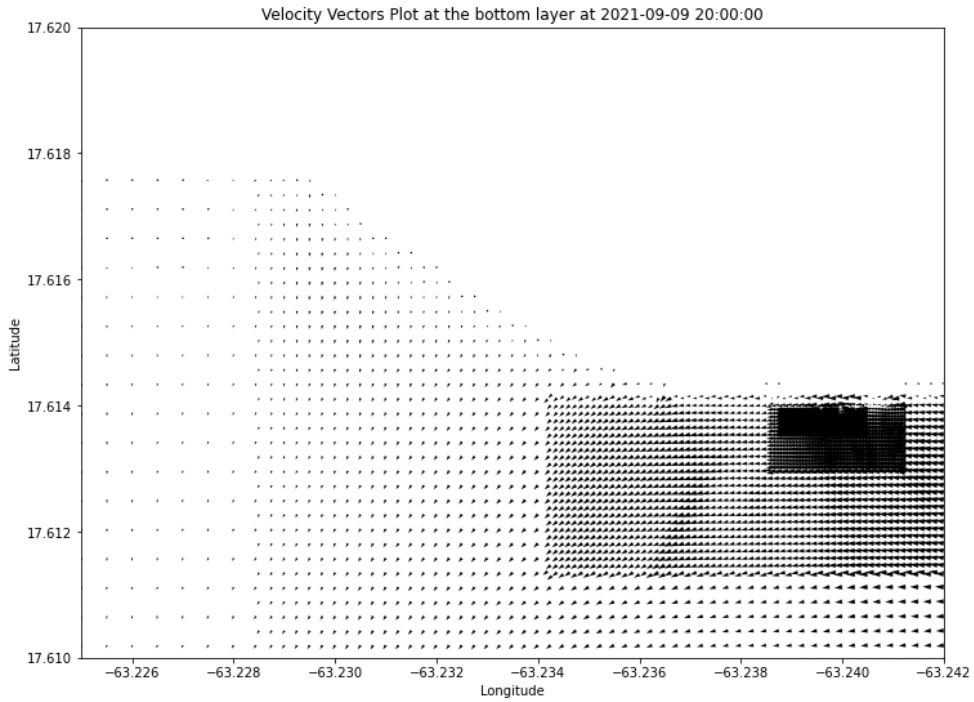

Figure E.8: Velocity vector plot of the western side of the Black Rocks area near the bed at 09-09-2021 20:00

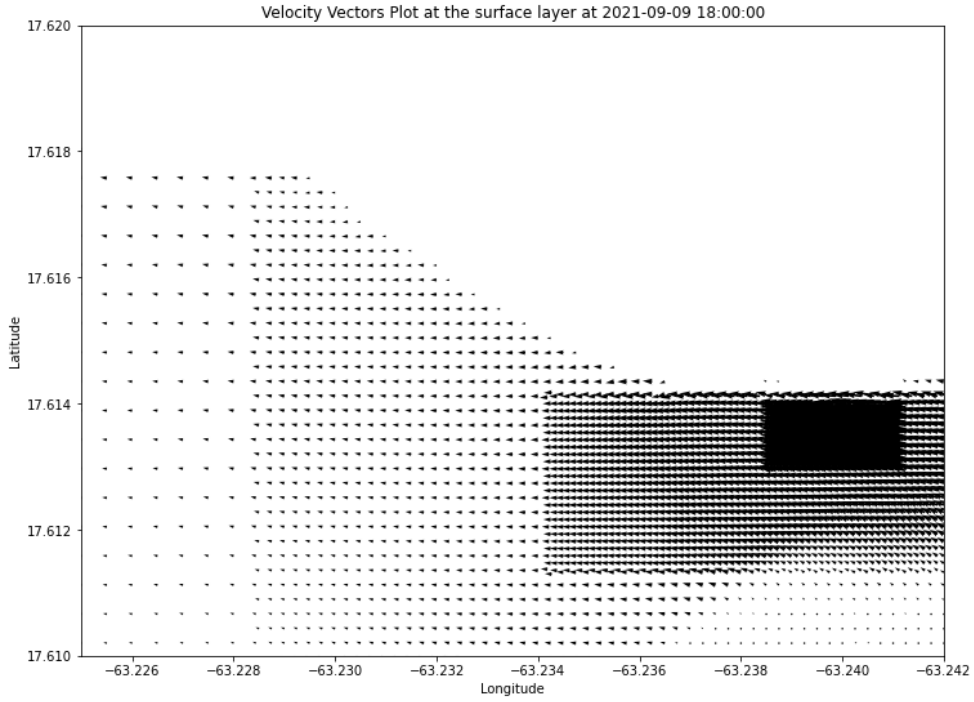

Figure E.9: Velocity vector plot of the western side of the Black Rocks area near the surface at 09-09-2021 18:00

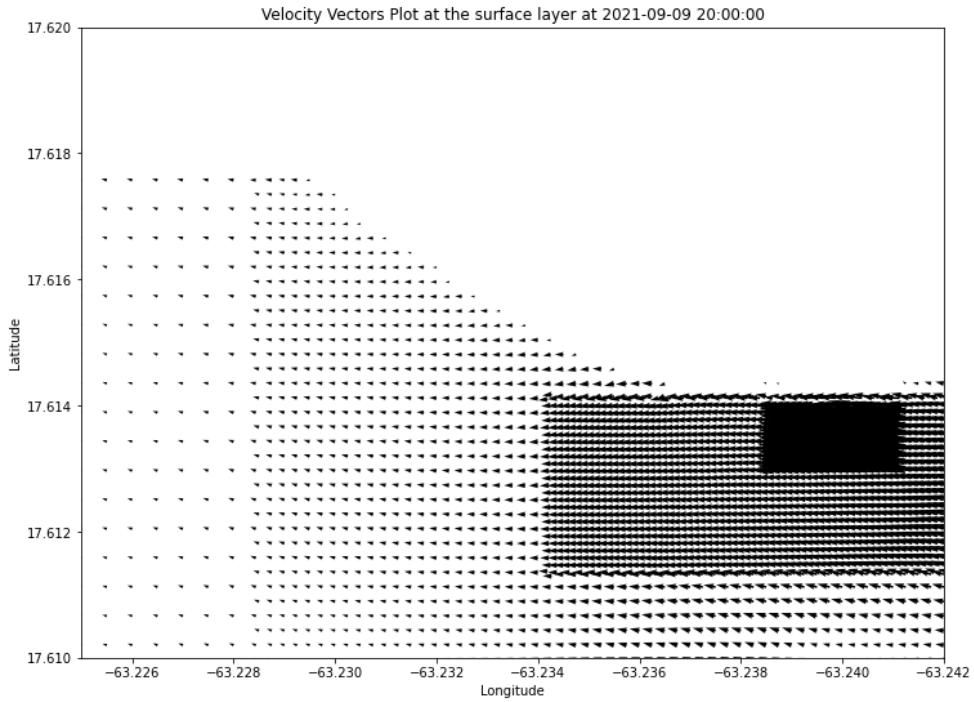

Figure E.10: Velocity vector plot of the western side of the Black Rocks area near the surface at 09-09-2021 20:00

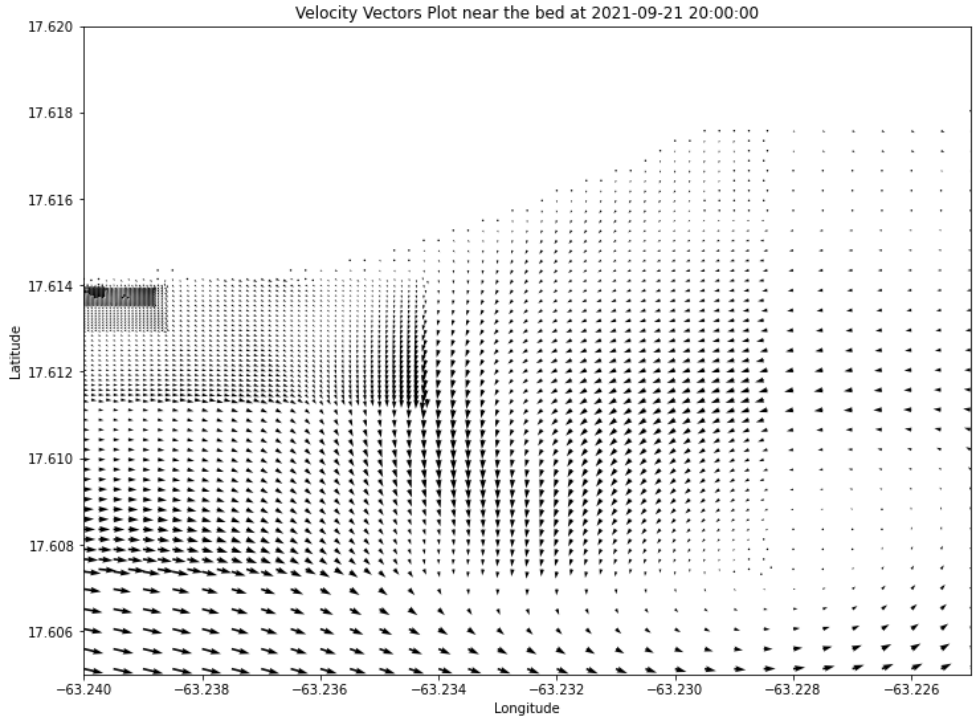

Figure E.11: Velocity vector plot of the eastern side of the Black Rocks area near the bed at 21-09-2021 20:00

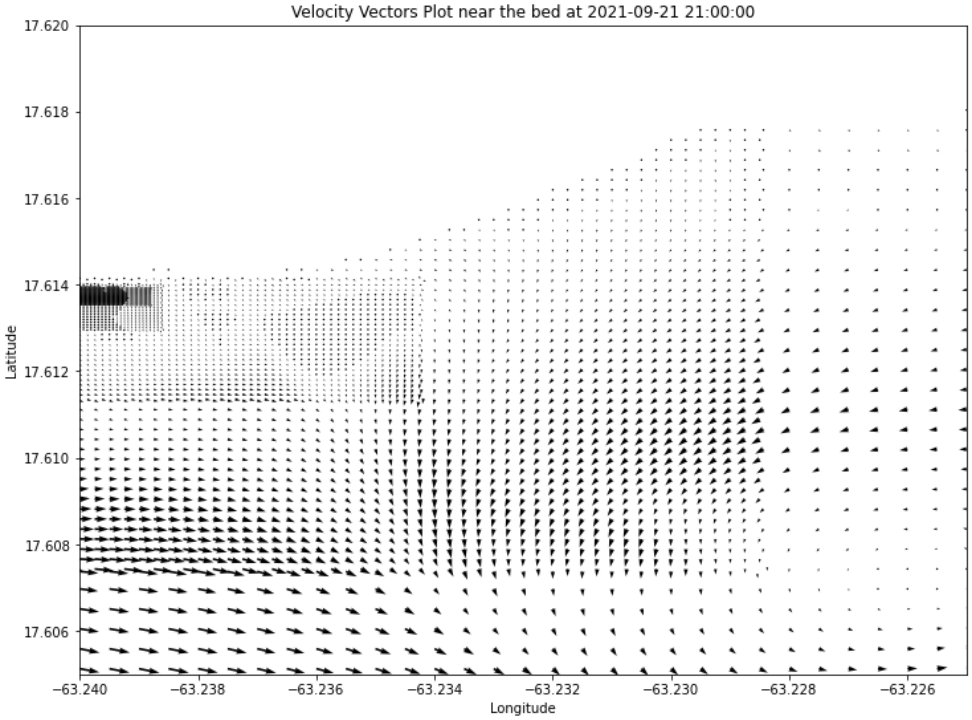

Figure E.12: Velocity vector plot of the eastern side of the Black Rocks area near the bed at 21-09-2021 21:00

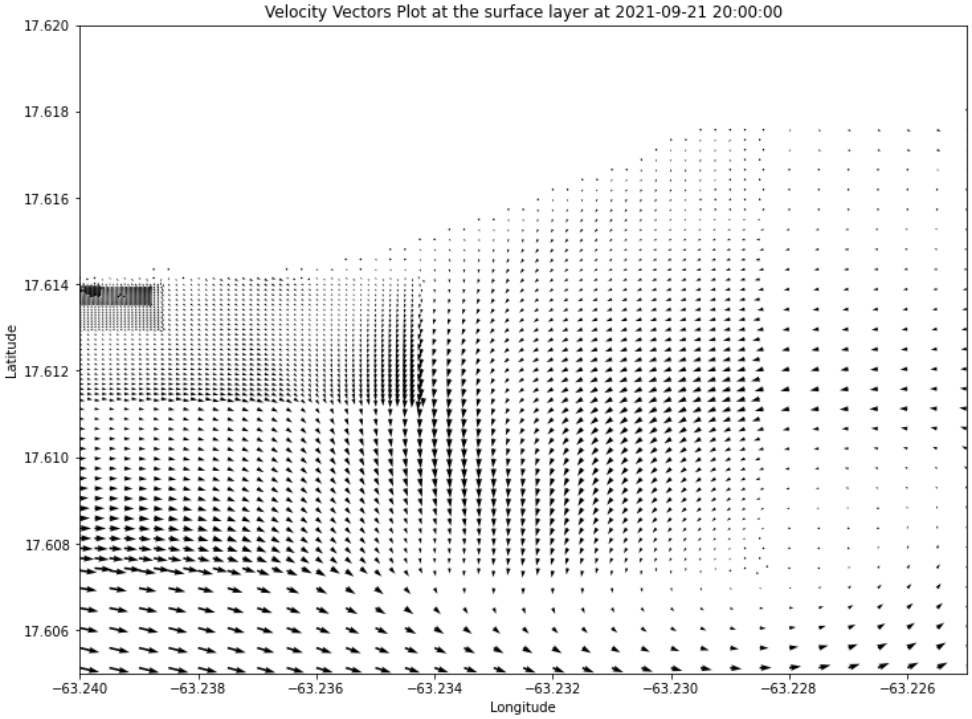

Figure E.13: Velocity vector plot of the eastern side of the Black Rocks area at the surface at 21-09-2021 20:00

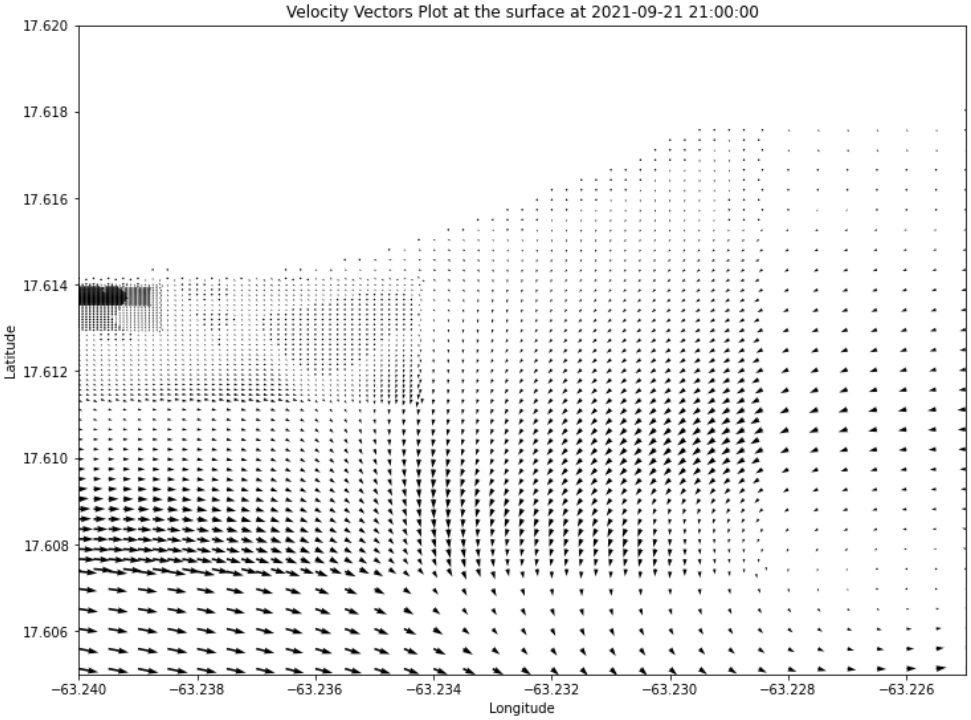

Figure E.14: Velocity vector plot of the eastern side of the Black Rocks area at the surface at 21-09-2021 21:00

List of Figures

List of Tables